

# Aesculap<sup>®</sup> MINOP<sup>®</sup> TREND

TRansnasal NeuroENDoscopy:  
A Practical Atlas

Robert Reisch, M.D., Ph.D.



In collaboration with

André Grotenhuis, M.D., Ph.D.

Evaldas Cesnulis, M.D.

Gábor Baksa, M.D.

Lajos Patonay, M.D.

Daniel Simmen, M.D., Ph.D.

Hans Rudolf Briner, M.D.

Hans-Christian Geiss, M.D., Ph.D.

Stefan Kindel

Aesculap Neurosurgery



---

Aesculap® MINOP® TREND

## TRansnasal NeuroENDoscopy

The TREND pituitary endoscope

A trend-setting equipment for TRanssphenoidal  
ENDoscopic exposure of the pituitary gland  
and surrounding structures

Robert Reisch, M.D., Ph.D.

In collaboration with

André Grotenhuis, M.D., Ph.D.

Evaldas Cesnulis, M.D.

Gábor Baksa, M.D.

Lajos Patonay, M.D.

Daniel Simmen, M.D., Ph.D.

Hans Rudolf Briner, M.D.

Hans-Christian Geiss, M.D., Ph.D.

Layout and Illustration

Stefan Kindel



Prof. Robert Reisch, M.D., Ph.D.  
Centre of Endoscopic and  
Minimally Invasive Neurosurgery  
Clinic Hirlanden Zurich  
Witelliker Strasse 40  
8032 Zurich, Switzerland  
Email: robert.reisch@hirlanden.ch



Prof. André Grotenhuis, M.D., Ph.D.  
Department of Neurosurgery  
Reinier Postlaan 4 Radboud  
Univ. Med. Ctr.  
Nijmegen 6525, Netherlands  
Email: j.grotenhuis@nch.umcn.nl



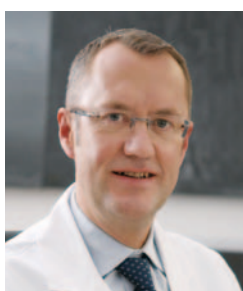
Evaldas Cesnulis, M.D.  
Centre of Endoscopic and  
Minimally Invasive Neurosurgery  
Clinic Hirlanden Zurich  
Witelliker Strasse 40  
8032 Zurich, Switzerland  
Email: evaldas.cesnulis@hirlanden.ch



Gábor Baksa, M.D.  
Anatomical Department  
Semmelweis University, Budapest  
Tűzoltó u. 58  
Budapest, Hungary  
Email: gabor\_baksa@hotmail.com



Lajos Patonay, M.D.  
Anatomical Department  
Semmelweis University, Budapest  
Tűzoltó u. 58  
Budapest, Hungary  
Email: patonay@ana.sote.hu



Prof. Daniel Simmen, M.D., Ph.D.  
Centre for Rhinology, Skull Base and  
Facial Plastic Surgery  
Clinic Hirlanden Zurich  
Witelliker Strasse 40  
8032 Zurich, Switzerland  
Email: simmen@orl-zentrum.com



Hans Rudolf Briner, M.D.  
Centre for Rhinology, Skull Base and  
Facial Plastic Surgery  
Clinic Hirlanden Zurich  
Witelliker Strasse 40  
8032 Zurich, Switzerland  
Email: briner@orl-zentrum.com



Hans-Christian Geiss, M.D., Ph.D.  
Centre for Metabolism and  
Endocrinology  
Clinic Hirlanden Zurich  
Witelliker Strasse 40  
8032, Zurich, Switzerland  
Email:  
hans-christian.geiss@hirlanden.ch



Stefan Kindel  
Graduate in Fine Arts  
artepalatina  
Hartmannstraße 1  
67487 Maikammer, Germany  
Email: stefan.kindel@artepalatina.de



## Transnasal Neuroendoscopy

### The endoscopic endonasal transsphenoidal binostril approach: Concept and surgical technique

*"Every step of the procedure must be conducted  
under the eye of the operator"*

*Harvey Cushing; The Pituitary Body and its Disorders, 1912*

Around the world, the majority of neurosurgeons use the traditional microsurgical approach in transsphenoidal surgery. The main advantage of this method is the neurosurgeons's familiarity with the microscope as a standard piece of equipment in neurosurgical procedures. However, there are two major drawbacks to the traditional microsurgical transsphenoidal technique: limited maneuverability of instruments and significantly reduced visual control of dissection due to the long and narrow surgical corridor created by the nasal speculum.

However, Harvey Cushing pointed out almost 100 years ago, direct visual control of precise, unimpeded manipulation is vital for neurosurgery.

It is precisely in the area of visualization and manipulation where transsphenoidal endoscopy offers an advantage: endoscopes offer increased light intensity and clear representation of patho-anatomical details in hidden parts of the deep surgical field. In addition, the fact that a nasal speculum surgical dissection is not impeded and the instruments are freely mobile.

This practical atlas describes basic endoscopic principles, relevant anatomy and surgical methods in transsphenoidal neurosurgery. Illustrative cases demonstrate four different adenomas of the pituitary gland, operated through four different endoscopic approaches. Our goal is to increase familiarity with these minimally invasive technologies, thus providing effective assistance in introducing endoscopes into daily routine treatment.

---

**Acknowledgements:**

Transsphenoidal endoscopy relies on teamwork. We express our gratitude to our friends and colleagues at the University Hospital Mainz, the University Hospital Zurich, the University Hospital Nijmegen and at the Hirslanden Clinic in Zurich. Special thanks go to Erik van Lindert, Zsolt Kulcsár, Daniel Rüfenacht, Isabel Wanke and Stephan Wetzel for the fruitful day-to-day cooperation. Intraoperative photographs courtesy of Judith Stadler, Andre Uster and Zoltán Kalmár; copy editing by Adrian C. Sewell.

## Introduction

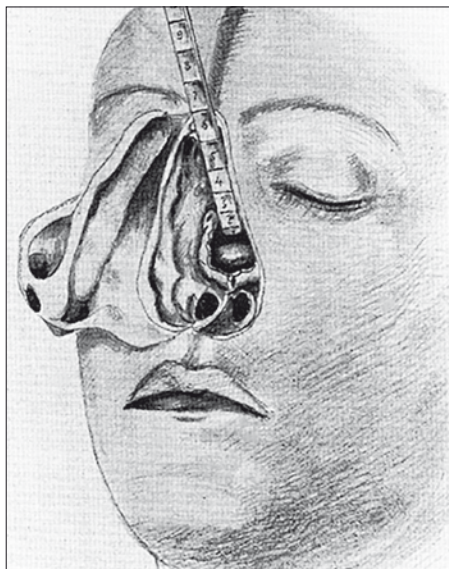


**Fig. 1** Hermann Schloffer's transnasal macro-surgical approach described in 1907. Note the traumatic exposure for removal of an extended pituitary adenoma. To overcome the limited visibility, Schloffer used a stick to measure the depth and to palpate the tumour tissue.

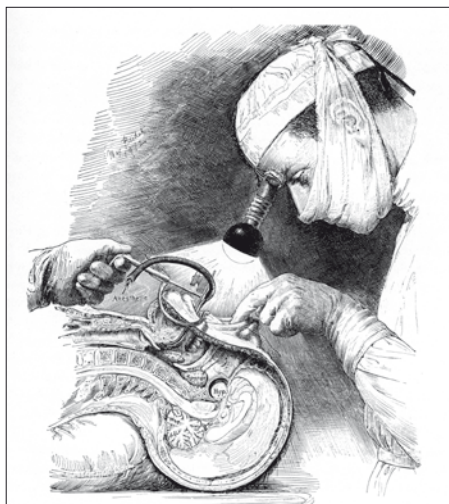


**Fig. 2** Harvey Cushing, operating via a sublabial-transnasal approach in 1923. Note the head-mounted lamp and use of specially designed instruments.

Transsphenoidal surgery for removal of a space-occupying pituitary tumor was first performed in 1907 by Hermann Schloffer in Innsbruck. Schloffer had to use a broad approach to expose the central skull base: after a perinasal skin incision and external rhinotomy, he removed the nasal septum, all turbinates and the ethmoid bone with the medial orbital wall on both sides (Fig.1).

Such extensive exposure was required in order to provide both illumination and space for the use of general surgical instruments. Today, it is quite impossible to imagine that Schloffer dissected almost blindly within the deep-seated field with very limited illumination and no magnification tools, using a simple stick for palpation of the tumor tissue. In 1910, Harvey Cushing, still operating in Baltimore, described a less traumatic technique using self-made instruments and a head-mounted lamp for his transsphenoidal macro-surgical approach (Fig.2). With this method, Cushing demonstrated a marked improvement in postoperative results, reporting on 231 operations with a 5.6% mortality rate. Concurrent with Cushing, Oscar Hirsch in Vienna pioneered the endonasal transsphenoidal approach to the sellar region, and, in fact, completed his first procedure on the same day, June 3<sup>rd</sup> 1910, that Cushing performed his first sublabial procedure. However, due to the restricted possibilities of the transsphenoidal approach, Cushing was never fully satisfied with it and, for most cases of pituitary tumors, he preferred the subfrontal approach. Norman Dott from Edinburgh, one of Cushing's students, was even more influential in pioneering and promoting the transsphenoidal surgery of pituitary adenomas than his teacher. He added to the limited available technology of his time by developing an illuminated nasal speculum and other nasal instruments to further augment the approach. In addition, the evolution of preoperative diagnostic tools, neurosurgical instruments and intraoperative illumination devices gave rise to a tremendous development in neurosurgical techniques, making such interventions less dangerous and less traumatic.

The real revolution in illumination of the surgical field was the introduction of operating microscopes in the 1960's and early 1970's. Dwight Parkinson, one of the pioneers of microneurosurgery, pinpointed the advantages of this new device: "... the neurosurgical section borrowed an operative microscope from the otolaryngology department. The microscope provided us with the enormous advantages of coaxial illumination, magnification, and simultaneous viewing for the surgeon and resident". The first neurosurgeon to use an operating microscope for transsphenoidal surgery was Jules Hardy in 1962. In the classic publication "Microsurgery, Applied to Neurosurgery", edited by M. Gazi Yasargil in 1969, Hardy reported on details of the technique having performed several operations with improved surgical effectiveness

and safety (Fig.3). Hardy championed the transsphenoidal approach for pituitary adenomas and described the "benignity of this method and quality of its results". In 1971, Hardy also declared the transsphenoidal microsurgical approach to be the standard treatment for pituitary tumours.

Recognition of the potentials of surgical microscopes led to a renaissance of the transsphenoidal approach in the late 1970's that has continued to this day.. However, it is interesting to note that, despite major advances in preoperative diagnostics, microneurosurgical techniques, microscopes and neuronavigation devices, transsphenoidal surgery has not demonstrated a marked improvement since Hardy's first description. The international gold standard remains transseptal exposure of the sphenoid sinus with either sublabial or septal incision of the mucosa.

One of the main advantages of the microscope is its familiarity to neurosurgeons as a standard piece of equipment used for the majority of neurosurgical procedures. The microscopic view is three-dimensional, which is of enormous importance during tumor resection, and the zoom and focus features are also beneficial.. The benefit of a microscope to the surgeon's comfort should not be underestimated! Nevertheless, there are two major drawbacks to the traditional microsurgical transsphenoidal approach: (1) limited maneuverability of instruments due to the long and narrow surgical corridor created by the nasal speculum and (2) limited visual control of dissection because of the reduced light intensity in the deep-seated operating field (Fig. 4A).

1) Due to the predefined surgical pathway given by the nasal speculum, the corridor of dissection cannot be changed during surgery; the narrow space between the blades of the speculum causes an almost coaxial view of the instruments and very little free movement within the deep-seated field. Note that the speculum acts much like a blinker for a horse, thus narrowing the angle of vision and manipulation.

2) The neurosurgeon must be able to see anatomical structures if he is to save them and must be able to recognise pathologies if he is to attack them. The second main difficulty of microsurgical transsphenoidal approaches is the loss of intraoperative light and sight through the long and narrow surgical pathway. The surgeon cannot see around corners, causing significantly reduced visual control. To bring light into the surgical field and control micro-instruments, modern endoscopes represent an effective replacement for surgical microscopes. The four main advantages of endoscopes are as follows: 1) increased light intensity, 2) an extended viewing angle with potential direct visualization of hidden parts of the field, 3) a clear depiction of details in close-up positions and 4) a thick focus field (Fig. 4B).

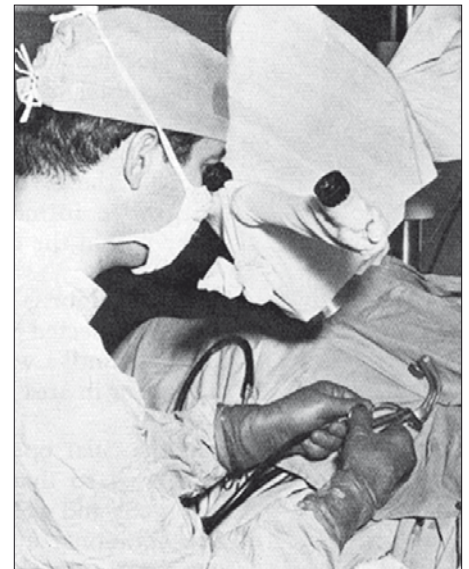
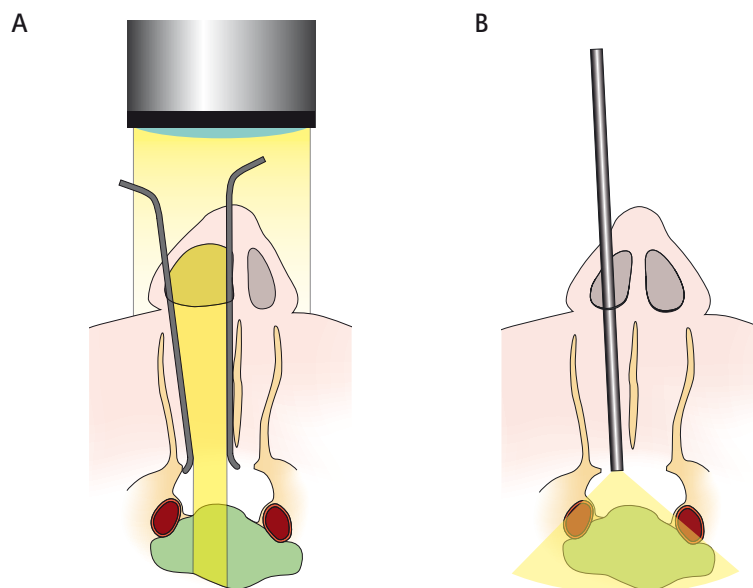


**Fig. 3** Jules Hardy undertaking transnasal surgery using a first-generation operating microscope and C-arm for appropriate intraoperative orientation. Despite the enormous development in preoperative diagnostics, microneurosurgical techniques, illumination devices and microscopes, transsphenoidal surgery has not shown a marked improvement since Hardy's first description in 1962.

**Fig. 4A** Diagram illustrating a transsphenoidal exposure using an operating microscope. Note the significant drawbacks with this technique. Due to the narrow and predefined surgical corridor provided by the nasal speculum, visual control of tumor removal in hidden parts of the surgical field is extremely limited.

**Fig. 4B** Endoscopic transsphenoidal exposure offers increased visibility. The improved light intensity, clear depiction of pathoanatomical details, and extended viewing angle ensure safe surgical dissection in the deep operating field and enable visually controlled tumor removal in hidden parts of the surgical field.



The absence of the nasal speculum and improved endoscopic visualization solve the main problem of the microsurgical technique, namely the limited control of tumor removal in blind corners of the surgical field. The view through the operating microscope allows a purely coaxial visualization: laterally located structures are concealed behind the nasal speculum, resulting in uncontrolled surgery. However, blind tumor removal involves a high risk of iatrogenic damage to neurovascular structures and a possible increase in tumor remnants. With the intraoperative use of endoscopes, these laterally located parts of the field are directly visible and therefore surgically approachable.

The first attempt to use an endoscope for transsphenoidal pituitary surgery dates back to 1963 when Gérard Guiot in Paris, supplemented the microsurgical exploration of the sellar region with an endoscope. He used an endoscope with a powerful external quartz rod illumination. This apparatus functioned as a focused light source and generated a well illuminated field. It is interesting to note that, after the initial efforts of Guiot, no further data regarding the use of an endoscope for transsphenoidal surgery were reported for more than 20 years. Michael Apuzzo from Los Angeles, introduced and promoted the "side-viewing telescope" in 1977, and Eckard Halves with Karl August Bushe in Würzburg, described the successful resection of sellar tumors using a microscope with the endoscope as an adjunct. Other surgeons realized the limited visualization in transcranial surgery: in 1974, Werner Prott from Würzburg performed diagnostic endoscopic cisternoscopy of the cerebellopontine angle, and Falk Oppel, who, at the time, was operating in Berlin, used an endoscope during microvascular trigeminal decompression



in 1981. In 1978, it was the renowned neurosurgeon Takanori Fukushima, at that time in Japan and later in Virginia, who described spinal endoscopy and cisternoscopy as well as endoscopy of the Meckel's cave, cisterna magna and cerebellopontine angle. All of the above can be regarded as the first forays into endoscope-assisted microneurosurgery, which, along with other neuroendoscopic techniques, experienced a revival in the 1990's.

The primary innovator of the endoscope-assisted technique was Axel Perneczky from Mainz, who published several key papers on this topic (Fig. 5). In 1993, Perneczky organized the first international congress on minimally invasive and endoscopic techniques in Wiesbaden, Germany (Fig. 6). At this meeting, several papers were presented: Andre Grotenhuis from Nijmegen reported on endoscope-assisted surgery of pituitary tumors and aneurysms, Engelbert Knosp from Vienna and Mamoru Taneda from Osaka on technical considerations of neuroendoscopy.

Although endoscope-assisted techniques were reported, the pure endoscopic transsphenoidal approach was not introduced and popularized until the early to mid 1990's. The pure endoscopic technique refers to surgery in which the endoscope is the only device used for visualization; the microscope is not used for any part of the procedure. After Roger Jankowsky and co-workers from Nancy first described this pure endoscopic technique in 1992, Drahambir Sethi and Prem Pillay from Singapore reported back on their initial experience with 40 patients in 1995 and in 1996, Hae-Dong Jho and Ricardo Carrau from the University of Pittsburgh Medical Centre reported on their experience with the first 50 patients.

The fruitful collaboration between neurosurgeon Jho and otorhinolaryngologist Carrau played an important role in development of the technique. To be exact, rhinological surgeons were historically more familiar with nasal endoscopic techniques. The first pioneer in endoscopy of the nasal cavity was Walter Messerklinger, founder of the technique of systematic endoscopic investigation of the nasal and paranasal cavities (Fig. 7). The school in Graz, with his student and later chairman Heinz Stammberger, developed the technique following essential advances in surgical instrumentation. Wolfgang Draf in Fulda also popularized the use of modern endoscopes for nasal and paranasal surgery. In the USA, Charles Gross of Charlottesville, and David Kennedy from the University of Pennsylvania, were pioneers of the technique and coined the term "functional endoscopic sinus surgery" (FESS).

More recently, due to major advances in otorhinolaryngological and neurosurgical endoscopy, Guiot's basic idea has been reconsidered using the method of pure endoscopy in transsphenoidal surgery and has gained widespread popularity. Following a similar evolution to microsurgical approaches, endoscopic techniques were initially restricted to dealing with

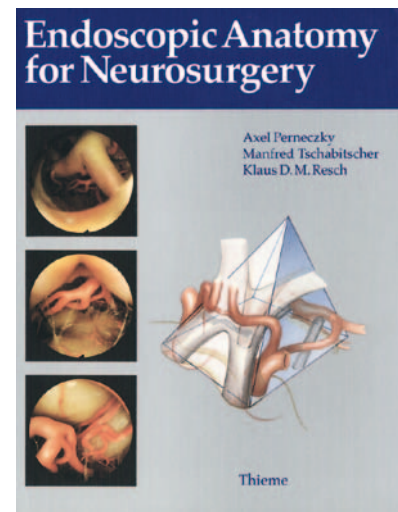


**Fig. 5** In 1993, Axel Perneczky, Manfred Tschabitscher and Klaus D. M. Resch published a comprehensive book on "Endoscopic Anatomy for Neurosurgery".

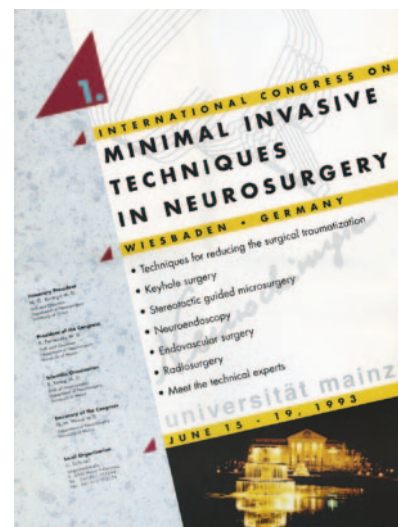


**Fig. 6** The First International Congress on Minimally Invasive Neurosurgery, organized by Axel Perneczky in 1993, presented several key papers on endoscopic skull base surgery.



**Fig. 7** *Walter Messerklinger, pioneer of functional endoscopic sinus surgery (FESS) during endoscopic transnasal inspection.*



**Fig. 8** *In this issue of the pioneering journal "Minimally Invasive Neurosurgery" from 1998, Paolo Cappabianca and co-workers reported initial experiences in endoscopic transnasal surgery.*

pituitary adenomas. Paolo Cappabianca and Enrico de Divitiis from Naples were also among the first to report on their experiences with the use of a pure endoscopic technique, introducing the term "functional endoscopic pituitary surgery" (FEPS). Their contribution cannot be stressed enough, as they described anatomical basics and surgical techniques and developed dedicated instrumentation for transnasal endoscopic use (Fig. 8).

Within the last few years, thanks to the introduction of technical adjuncts such as novel endoscopes, instruments and neuronavigation tools, endoscopic transsphenoidal surgery has been extended to the treatment of lesions outside the sella turcica, introducing the concept of "extended approaches" to the skull base. Several groups have dealt with these extended endoscopic approaches, which expose intracranial lesions via the endonasal transsphenoidal route. Giorgio Frank and Ernesto Pasquini from Bologna developed ethmoid-pterygoid-sphenoid exposure for the treatment of lateral situated lesions. Also in Italy, Davide Locatelli and Paolo Castelnovo from Pavia described perspectives and realities on approaches to the cranial base. The New York team with neurosurgeon Theodore Schwarz and otorhinolaryngologist Vijay Anand described successful removal of pure intradural lesions located in the pre- and post-chiasmal cisterns. Neurosurgeon Amin Kassam and otorhinolaryngologist Carl Snydermann described the removal of extended intracranial pathologies using an endoscopic endonasal technique, thus widening the concept of transsphenoidal surgery.

A particular surgical challenge is the transsphenoidal endoscopic removal of intradural lesions using extended approaches. Working groups in Naples, Bologna, Pavia and Pittsburgh have reported on increasing experience in this field, operating on meningiomas, craniopharyngiomas and other tumors. However, in our opinion, the minimal invasiveness of these approaches requires close scrutiny, especially if transcranial keyhole approaches offer less approach-related morbidity when dealing with comparable pathologies. Critical points are 1) approach-related trauma to the nasal cavity, 2) limited maneuverability of surgical instruments with decreased control of microsurgical dissection and 3) enormous problems with skull base reconstruction to avoid postoperative CSF leakage. Nevertheless, the most important contraindication to the extended endonasal approach is surgical experience. The learning curve, particularly in this region, is very steep and requires perfect anatomical knowledge, endoscopic experience and harmonic teamwork between neuro- and rhinosurgeons.

## Anatomical background

The key to minimizing damage within the surgical field is an anatomical understanding of the nasal and parasellar regions combined with specific endoscopic experience. A vital part of basic endoscopic training is to identify anatomical landmarks using special visualization and to use these landmarks for appropriate surgical orientation. Thus, the path to transnasal endoscopic surgery leads through an anatomical-endoscopic laboratory involving considerable training on cadavers. In addition to ensuring safe dissection during the first surgically treated cases, this training may help to shorten the initial steep learning curve.

### The nasal cavity and epipharynx

The entrance to the nasal cavity is a pear-shaped opening bordered by the nasal and maxillary frontal processes (Fig. 9). The piriform aperture is separated by the nasal septum, an osteocartilaginous and mucous formation with two mostly asymmetrical parts.

The nasal cavity itself is similar in configuration to the piriform aperture offering more space for surgical dissection in the basal part of the chamber (Fig. 10).



**Fig. 9** The bony anterior aperture of the nasal cavity. Note the bordering nasal and maxillary bones and the osseous nasal septum. In several cases, severe alterations of the septum can hinder intranasal exploration.

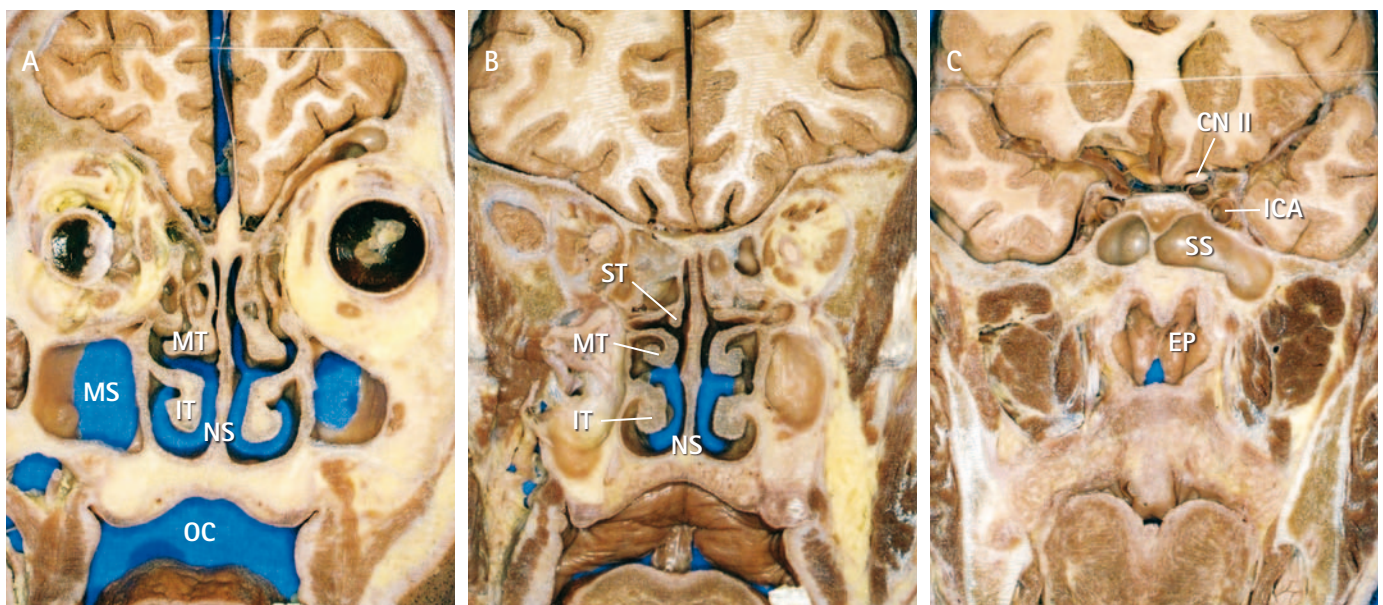


**Fig. 10** Coronar sections in a fixed specimen in the anterior (A), middle (B) and posterior (C) portion of the skull base from an anterior view. The nasal cavity itself is similar in configuration to the piriform aperture offering more space for surgical dissection in the basal part of the chamber. Note the nasal septum and the highly irregular and variegated lateral wall of the nasal cavity. The posterior section (C) shows the sphenoid sinus and epipharynx.



The floor of the nasal cavity comprises the maxillary palatine process and the horizontal palatine bone lamina; the medial wall is formed by the septum according to the perpendicular plate of the ethmoid, vomer and, near to the nostril, the quadrangular cartilage. The septum is bordered postero-superiorly by the body of the sphenoid, following along the free edge of the vomer, at the choana. The narrow superior wall of the nasal cavity corresponds to the cribriform plate of the ethmoid bone (Figs. 10, 11).

The lateral wall is the most complex, forming a highly irregular and varied anatomy. Six bones are involved, e.g. the maxillary, lacrimal, ethmoid, sphenoid and palatine bones and the inferior nasal turbinate (Figs. 10, 12). The anterior part is created by the compact and thick frontal process of the maxilla and by the nasal bone. The posterior part is similarly stable, formed by the sphenopalatine junction bordering the pterygopalatine fossa antero-medially. Here, in the upper part, is the sphenopalatine foramen, an important neurovascular connection of the pterygopalatine fossa to the nasal cavity (Fig.12).

**Fig. 11** Paramedian sagittal sections showing the nasal septum in osseous (A) and fixed (B) specimens.

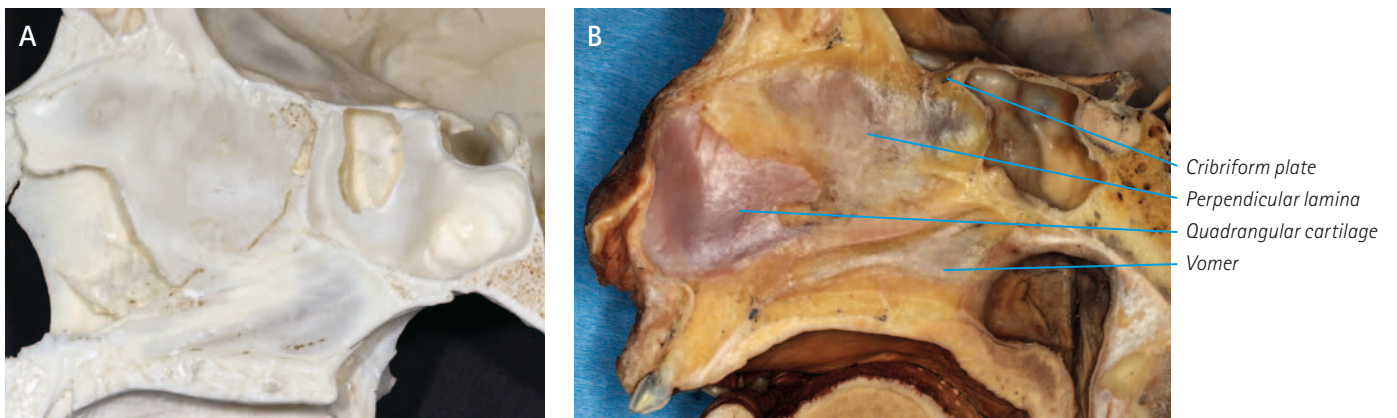
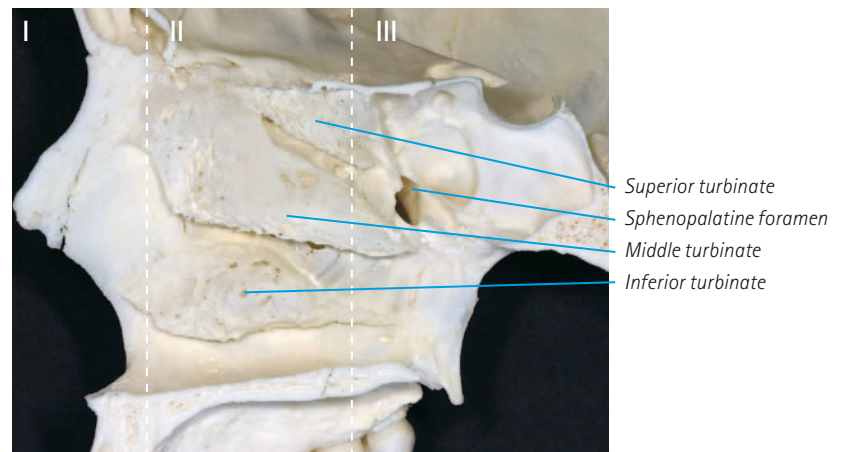


**Fig. 12** The bony lateral wall of the nasal cavity (right side). The anterior portion is created by the compact frontal process of the maxilla and by the nasal bone (I). Similarly stable is the posterior part, formed by the maxillopalatine junction (III). The central part of the lateral wall, created by the inferior turbinate and ethmoid bone, is thin and fragile (II).



The central part of the lateral wall is thin and fragile. The most important anatomical landmarks for endoscopic orientation are located here, namely the turbinates and the spaces lying below them: the upper, middle and lower nasal meati (Figs. 12, 14).

Situated in front of the anterior wall of the sphenoid sinus is the superior turbinate (Fig 14). Here, medial from the superior turbinate, is the natural opening of the sphenoid sinus, the sphenoid aperture. The sphenoid aperture may appear in a different size and form and in a different position in the anterior wall of the sphenoid sinus. A large number of studies have been conducted with the aim of determining average dimensions, but these values differ individually according to the development and dimensions of the sphenoid turbinates. These "mini-turbinates", also called conchae sphenoidales or Bertini-ossicules, develop from the anterior and inferior walls of the sphenoid sinus and close the anterior wall of the sphenoid sinus. If these small bones are poorly developed, one finds large, round apertures situated medially. If the Bertini-ossicules are hard, they tighten the area and the apertures are small and oval with the larger diameter placed horizontally and situated laterally (Fig. 13). The mucous membrane can also further tighten the bony aperture, thus making the identification of these apertures much more difficult.

The posterior ethmoidal cells enter the superior meatus, which is bordered anteriorly by the superior and middle conchae and posteriorly by the sphenoidal recess, under the superior concha (Fig. 15).

The middle concha is situated under the superior meatus. The middle turbinate is usually larger than the superior one. Its head is juxtaposed to the frontal process of the maxilla and it descends backwards in an oblique route with its tail tangent to the inferior edge of the sphenopalatine foramen. A characteristic prominence can be observed at the point where the head of the turbinate is inserted corresponding to the region of the agger nasi (Fig. 15).

Under the middle turbinate the highly variable middle meatus can be exposed. The uncinate process is situated in its anterior part. Originating at the agger nasi, the uncinate process ends imperceptibly close to the body of the inferior turbinate. This region, covered mostly by a thin mucosal membrane, is the most fragile part of the lateral nasal cavity. Above the uncinate process is a regular, curved, and superiorly concave area, the semilunar hiatus. The natural opening of the maxillary sinus into the nasal cavity is situated here: an important landmark for lateral and extended skull base approaches.

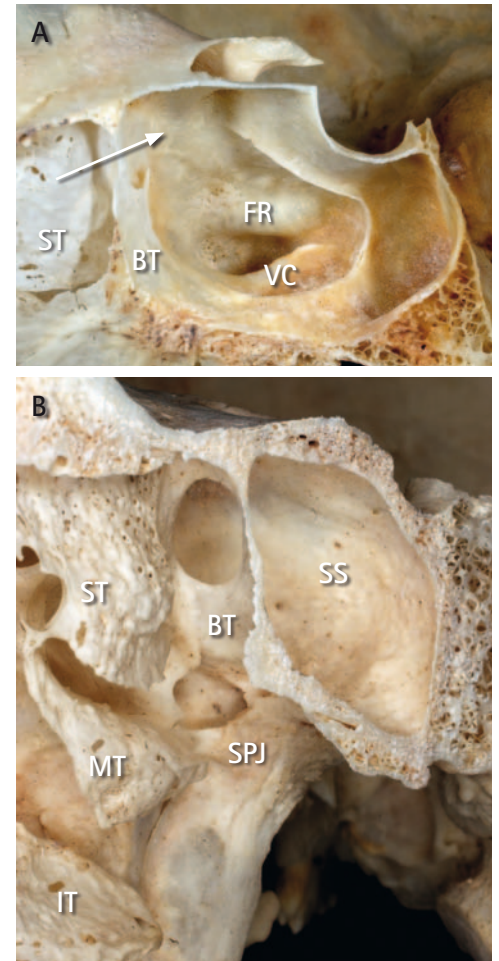


**Fig. 13** Lateral view of the sphenoid sinus in a midsagittal sectioned osseous specimen, demonstrating the relation of the sphenoid aperture (arrow) to the sphenoid planum and sellar floor (A). Note the superior turbinate and Bertini's "mini-turbinates" according to the anteroinferior sinus wall. The foramen rotundum and Vidian's pterygoid canal are situated on the right lateral wall of the sphenoid sinus. The anterior view (B) shows the relation of the sphenoid aperture to the superior turbinate.

**Fig. 14** The lateral wall of the left nasal cavity in a fixed specimen with the characteristic nasal turbinates. Note the main anatomical connections of the nasal cavity demonstrated by colored wires (red wire: sphenoid aperture; yellow and blue wires: posterior ethmoidal cells; white wire: maxillary sinus; green wire: nasolacrimal duct; orange wire: tuba auditiva).

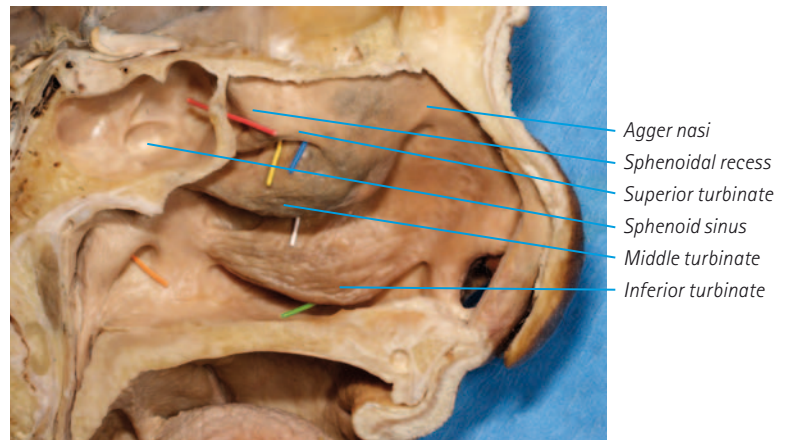


**Fig. 15** View of the superior and middle meatus after resection of the superior and middle turbinates. Note the posterior ethmoidal cells, agger nasi, and the semilunar hiatus between the ethmoid bulla and uncinate process. The inferior turbinate is voluminous and regular in shape showing a large anterior head followed by a long body that converges to form a thin tail.

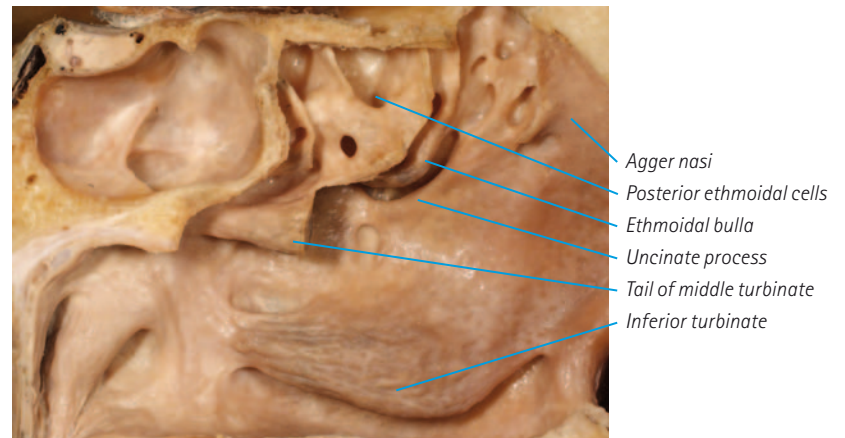
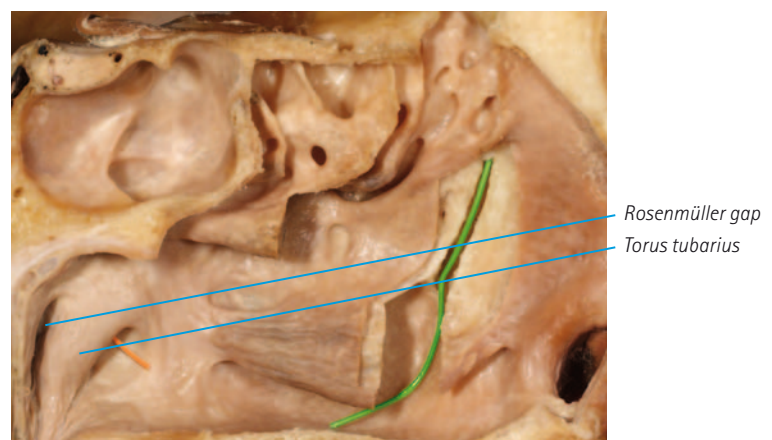


**Fig. 16** The nasolacrimal duct entering the inferior meatus is shown using a green wire after partial resection of the inferior turbinate. Note the important landmarks of the epipharynx, e.g. the torus tubarius and the tuba auditiva (orange wire). The Rosenmüller gap is situated between the torus and the posterior wall of the epipharynx.





Above the semilunar gap, the ethmoidal bulla can be observed although exhibiting a highly variable anatomy (Fig. 15). In the very posterior part of the meatus, located just laterally from the tail of the middle turbinate, the sphenopalatine foramen can be identified. This foramen is one of the most important neurosurgical landmarks for identification of the passing septal branch of the sphenopalatine artery.

The inferior turbinate is voluminous and regular in shape, showing a large anterior head followed by a long body converging to form a thin tail (Fig. 15). Below the anterior one third of the turbinate, the funnel-like nasolacrimal duct opens into the inferior meatus (Fig. 16). Dissecting along the inferior border of the nasal cavity through the inferior meatus, one can pass the posterior exit of the nasal cavity: the choana. The significant landmarks of the epipharynx can be observed here, e.g.: the Rosenmüller gap, torus tubarius and tuba auditiva.

The neurovascular supply of the nasal cavity is an important consideration with regard to the transsphenoidal exposure of the sphenoid sinus and sellar region. Basically, the nasal cavity is supplied by the maxillary artery and nerve which arise from the external carotid artery and trigeminal nerve, complemented by branches of the ophthalmic artery and nerve deriving from the internal carotid artery and trigeminal nerve, respectively. Of particular importance are the olfactory filaments supplying the mucosal covering of the superior conchae, superior meati and the sphenoethmoidal recess on both sides.

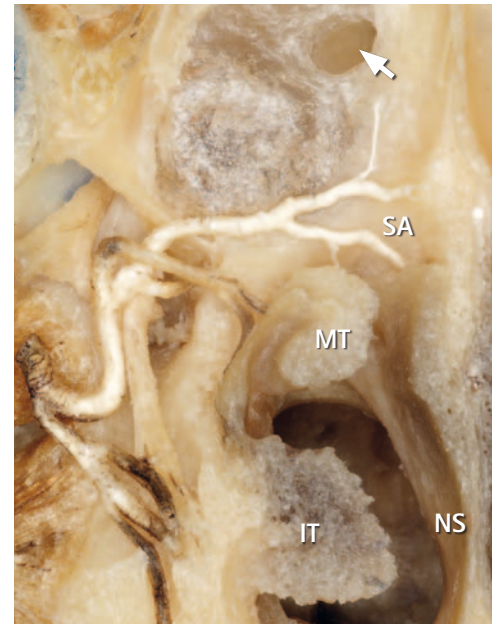
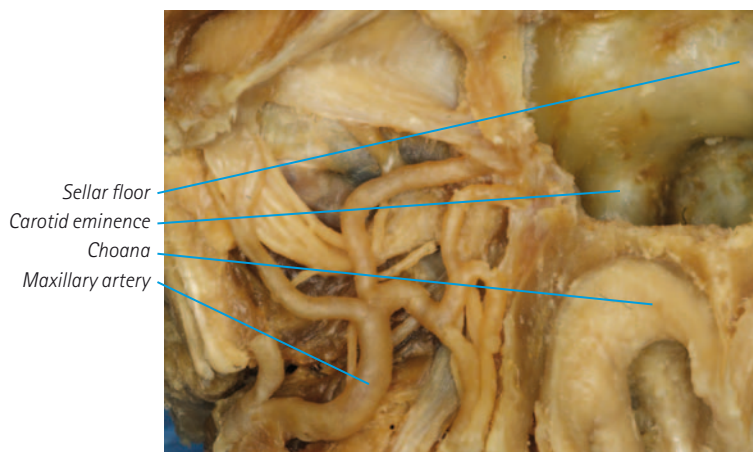


**Fig. 17** Anterior view of the right septal artery. The vessel passes the sphenopalatine foramen and ascends medially towards the lower part of the anterior wall of the sphenoid sinus. The bony anterior wall of the sphenoid sinus is partially removed allowing observation of the intact sphenoid mucosa; note the sphenoid aperture (arrow). Caution is advised when performing a direct endonasal endoscopic approach to the sphenoid sinus: when drilling the anterior wall, the septal artery can be damaged causing severe arterial bleeding.

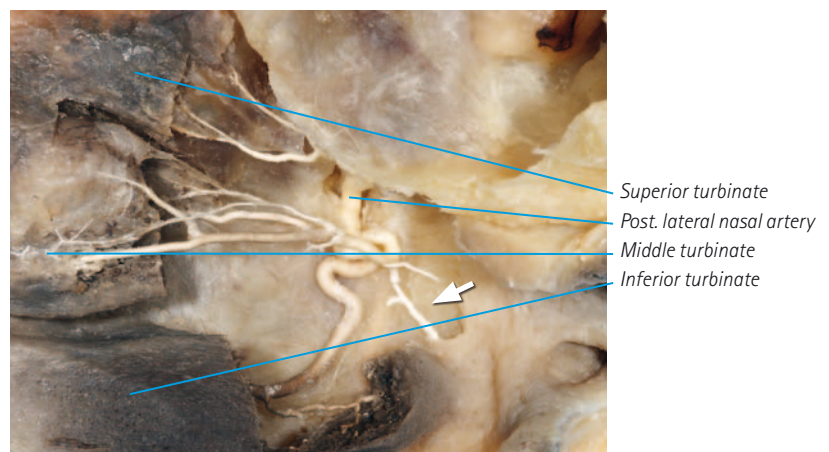
**Fig. 18** Anterior view of the right pterygopalatine fossa. Note the maxillary artery and its terminal branches that supply the lateral nasal cavity and central skull base.

The maxillary artery shows a short lateromedial course within the pterygopalatine fossa giving rise to small branches extending to the round and palatine canals and to the orbit. Still inside the fossa, a few millimetres from the sphenopalatine foramen and thus outside the nasal cavity, the maxillary artery divides into two terminal branches. The main vessels are the septal artery and posterior lateral nasal artery; some publications actually describe these two branches as a common vessel, called the sphenopalatine artery, which enters the nasal cavity through the sphenopalatine foramen (Fig. 17, 18).

As mentioned above, the septal artery passes the superior edge of the sphenopalatine foramen, passing the tail of the middle turbinate and ascends medially towards the anteroinferior part of the anterior wall of the sphenoidal sinus (Fig. 17). When performing a direct transnasal approach to the sphenoid, this course becomes extremely important: drilling of the anterior wall can damage the artery causing bleeding; however, this bleeding should not be confused with fatal damage to the ICA! If direct coagulation of the vessel is complicated, the sphenopalatine artery can be immediately localized in the posterior middle meatus, thus staunching the bleeding. On reaching the nasal septum, the septal artery branches off into the descending nasopalatine artery and to several small caliber ascending branches.

The posterior lateral nasal artery crosses the inferior edge of the sphenopalatine foramen and descends along the lateral wall of the nasal cavity. Main branches supply the middle and inferior turbinates. Some small ascending vessels run to the superior concha, building anastomoses with the posterior ethmoidal arteries. Posterior branches supply the choanal region (Fig. 19).

**Fig. 19** The posterior lateral nasal artery crosses the sphenopalatine foramen and descends along the lateral wall of the nasal cavity (right side). Main branches supply the middle and inferior turbinates, some small ascending vessels run to the superior concha, building anastomoses with the posterior ethmoidal arteries. Note the posterior branches supplying the choanal region (arrow).



## Sphenoid sinus

Located in the sphenoid body, the sphenoid sinus is the most posterior paranasal cavity, communicating to the sphenoethmoid recess through the sphenoid apertures (Figs. 10C, 11, 14–16, 20, 22, 23). Pneumatization of the sphenoid bone occurs after enchondral ossification of the sphenoid cartilages. In those places of the sphenoid bone where ossification is incomplete, small vertical, horizontal and sagittal plates remain which can be seen later as variable septa in the sphenoid sinus. Usually, a large, paramedian-sagittal septum separates the cavity into two major parts but does not form a strict barrier (Fig. 20).

Around the sphenoid sinus there are a number of essential anatomical structures which usually extend into the cavity through the bony wall. It is important to note that these structures are not at all variable. It is only their appearance that changes individually according to the degree of pneumatization!

In the midline axis, the sellar floor is the first anatomical landmark with common enlargement in pathological situations (Figs. 10C, 20, 22, 23). In a frontal direction is the planum sphenoidale; between the thin sella and the fragile planum the bone is thick due to the osseous tuberculum sellae. Caudal from the sella, the clivus appears formed by the sphenoid and, in extensive pneumatization, by the occipital bones.

The sphenoid part of the clivus is bordered laterally by the horizontal segments of the ICA. Inferolaterally, the ICA disappears into the petrous bone at the level of the foramen lacerum. Here, due to extensive pneumatization, the pterygoid canal can be identified consisting of the major and deep petrous nerves running lateral from the vessel. This canal, also called the Vidian channel, is an important landmark for localization of the ICA at the level of the foramen lacerum (Figs. 13A, 21, 23 F). In its further course, the ICA enters the cavernous sinus and shows a kinked path. The anterior knee appears in the sphenoid sinus as a prominent swelling. This anterior knee corresponds to the paraclinoid carotid segment located between the proximal and dural rings of the cavernous sinus (Figs. 22, 23). The optic nerve runs into the bony optic canal at the cranio-lateral end of the sphenoid cavity. Lateral from the anterior carotid knee, just below the optic nerve, is the prominent lateral optocarotid recess. However, for surgical orientation, the critical landmark is the medial recess pointing to the region between the anterior fossa, sellar floor, carotid artery and the optic nerve. Note that the medial optocarotid recess corresponds to a "negative intendation" of the middle clinoid process of the sphenoid bone, always located medially from

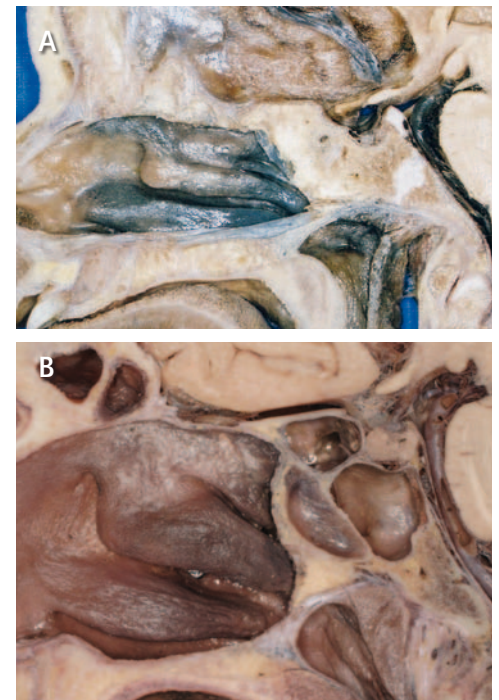


**Fig. 20** Median sagittal section in fixed cadaver of a 2-year-old boy (A) and an adult (B). Note the absent pneumatization of the sphenoid body and the spheno-occipital synchondrosis in the young child.

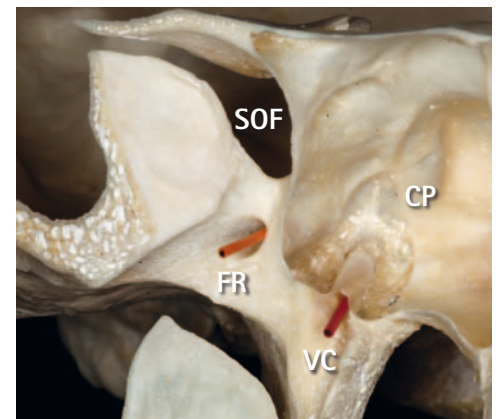
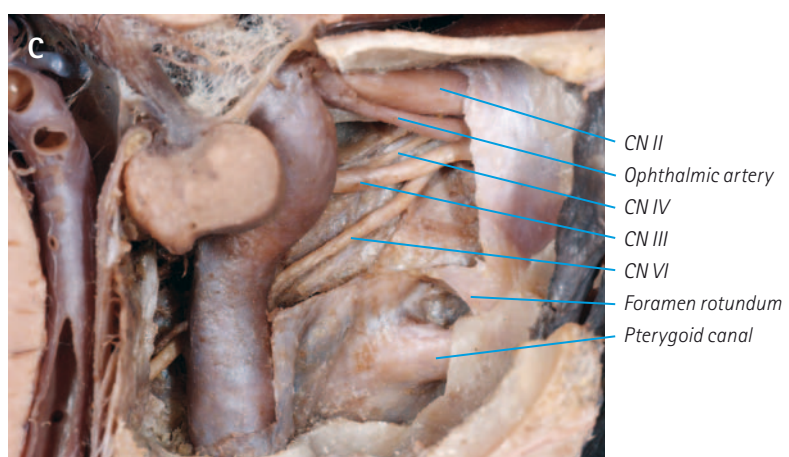
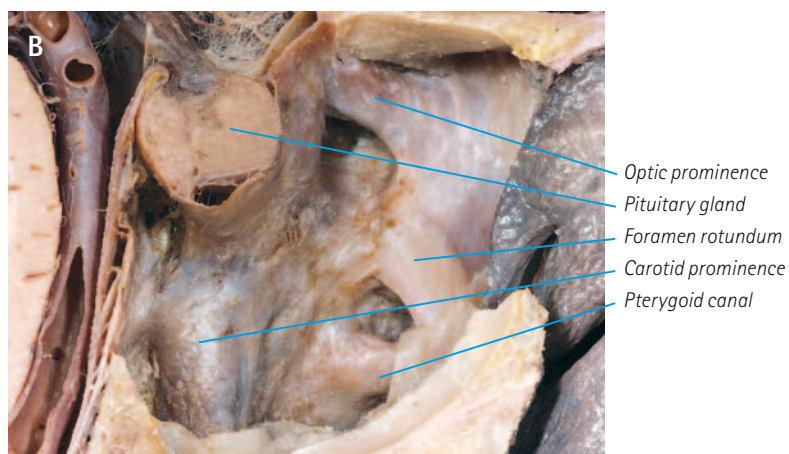
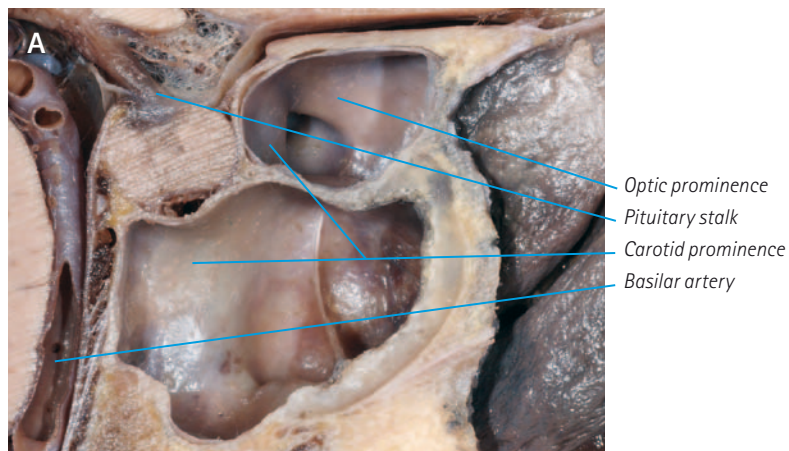


**Fig. 21** Anterior view of the right sphenopalatine junction in bony specimen. Note wires, placed into the foramen rotundum and Vidian's pterygoid canal as important landmarks leading to the lateral sphenoid sinus, and supraorbital fissure. This anterior view can be compared with the lateral appearance in Fig. 13 (different specimens).



**Fig. 22** *The sphenoid sinus in the median sagittal section of a fixed specimen. Figure A demonstrates the pituitary gland and stalk in relation to the sella turcica and sphenoid sinus. After removal, the bony lateral wall, characteristic prominences of the lateral wall become evident (B). Focusing deeper after dissection of the dural covering, neurovascular structures of the cavernous sinus can be observed (C).*



the ICA. In the lateral part of the sphenoid sinus, the channel-like foramen rotundum with the mandibular branch of the trigeminal nerve can usually be seen (Fig. 23).

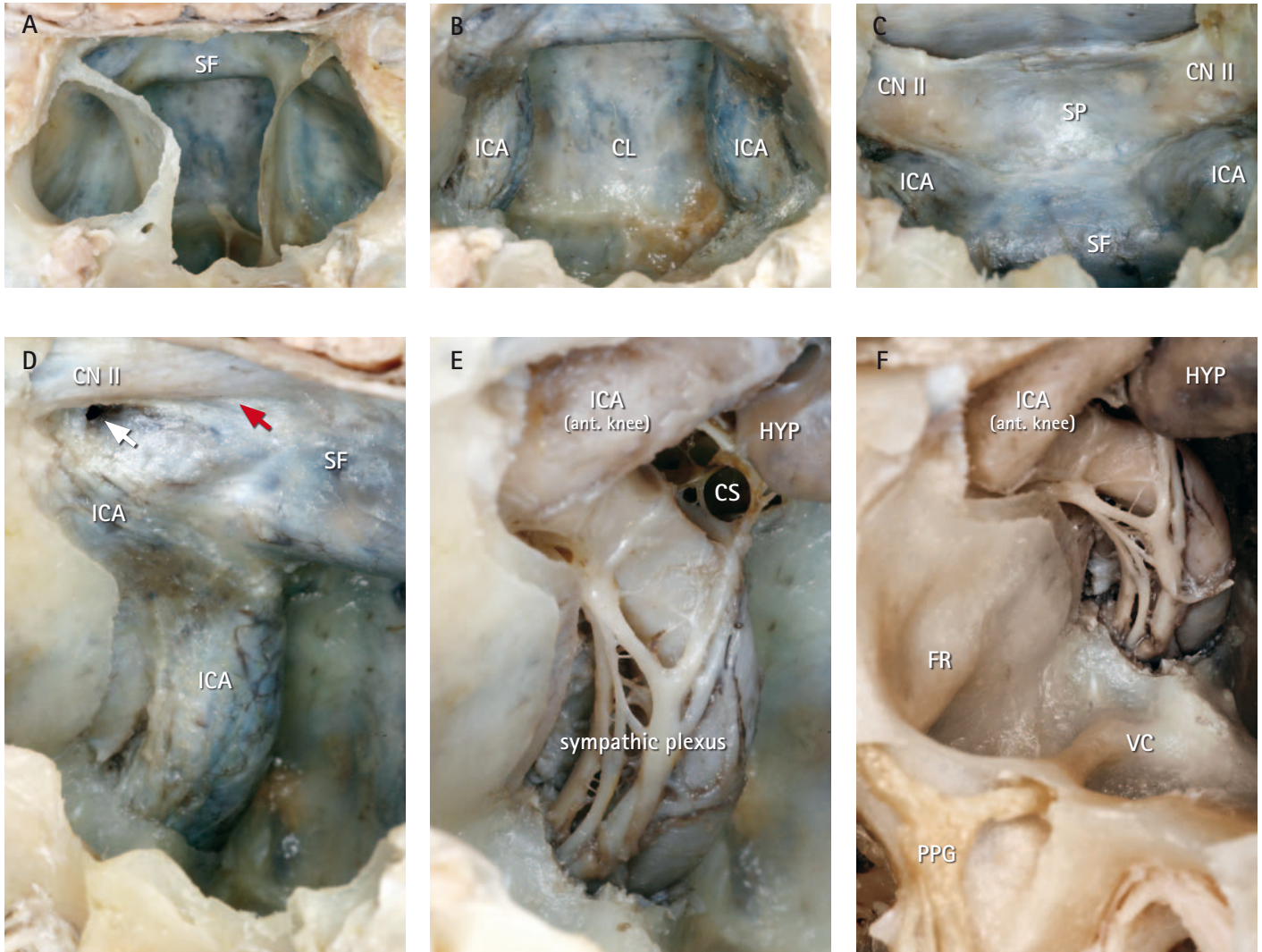


**Fig. 23** The sphenoid sinus from frontal after removal of the anterior wall. Note the paramedian septations and sellar floor (A). After resection of the bone of the posterolateral sinus wall, surrounding anatomical structures appear. Focusing inferiorly, the clival dura mater and both carotid arteries appear (B); focusing superiorly, prominences of the optic nerves can be observed. Note the special relationship between the optic and carotid prominences, sphenoid planum and sellar endosteum (C). Focusing right laterally, the course of the right internal carotid becomes visible (D). Note the intact dural covering of the optic nerve, carotid artery and pituitary gland and appearance of the lateral (white arrow) and medial (red arrow) optocarotid recess. After opening the right cavernous sinus, the internal carotid artery with the sympathetic plexus appears (E). Focusing inferolaterally, the foramen rotundum and Vidian canal appear. Note the pterygopalatine ganglion within the pterygopalatine fossa (F).



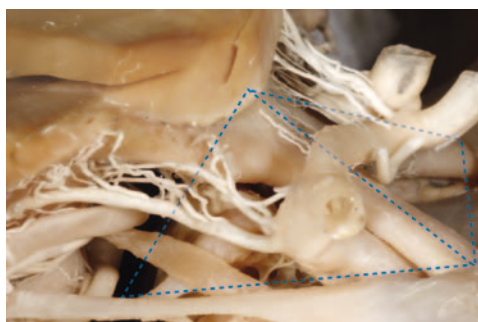
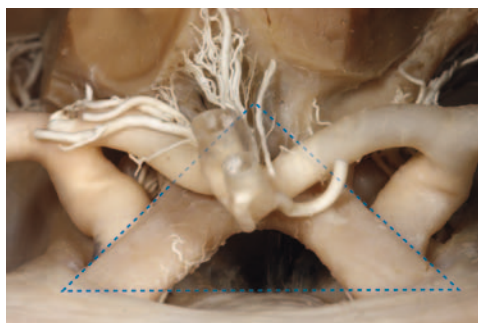


**Fig. 24** *In geometric terms, the suprasellar region can best be described as a virtual pyramid. Each of the triangular planes of the sellar pyramid is defined by certain neurovascular structures, observed from the anterior (A), anterolateral (B) and lateral direction (C). Note small perforators supplying the lamina terminalis and the optic tract.*

### The supra- and parasellar regions

In geometric terms, the supra- and parasellar regions are best described in a three-dimensional plane, as a virtual pyramid (Fig. 24). Each of the triangular planes of the sellar pyramid is defined by certain structures. The anterior plane of the pyramid is formed almost completely by the optic nerves, the chiasm and the lamina terminalis. The first segments of the anterior cerebral arteries and the anterior communicating artery are also in direct relationship to this plane. The side of the pyramid includes the optic nerve and tract, the oculomotor nerve, the ICA and its two supraclinoid branches, and the posterior communicating and anterior choroidal arteries. The posterior pyramidal plane is defined by the ventral surface of the brain stem and basilar artery with the posterior cerebral and superior cerebellar arteries. The axis of the pyramid is formed by the infundibulum and pituitary stalk. The base of the pyramid corresponds to the sella turcica with the bilateral cavernous sinus.

From a surgical point of view, the cavernous sinus can be divided into three major anatomical parts (Fig. 25). The anterior part is particularly important when dealing with a transsphenoidal exposure. The dura mater covering the inferior surface of the anterior clinoid process and the proximal dural ring of the ICA form the roof of this anterior part of the cavernous sinus. Just underneath this dural layer are the oculomotor, trochlear and ophthalmic nerves coursing towards the superior orbital fissure. The middle part of the cavernous sinus represents the real venous chamber with structures of the lateral sinus wall consisting of the oculomotor, trochlear and ophthalmic nerves and the underlying horizontal segment of the carotid artery with the abducent nerve. The posterior part involves the region of the petrous bone tip including the Dorello canal with the abducent nerve, the posterior knee of the carotid artery and the Gasserian ganglion.

The branching pattern of the ICA and arterial supply of the pituitary gland is of special surgical interest. The most prominent intracavernous branch, the meningohypophyseal trunk, takes its origin from the ICA in the posterosuperior part of the cavernous sinus and divides into three groups of smaller branches, the tentorial, clival and sellar branches. The sellar branches, also termed inferior hypophyseal arteries, supply the pituitary gland and build an important anastomosis with the supraclinoid branches of the ICA (Fig. 26).

**Fig. 25** Fixed specimen showing the neurovascular structures of the right cavernous sinus after removal of the lateral and upper sinus wall. The oculomotor, trochlear and ophthalmic nerves are retracted; note the intracavernous segment of the abducent nerve running along the internal carotid after passing the Dorello's canal below the Gruber's ligament. From a surgical point of view, the cavernous sinus can be divided into three major anatomical portions: the posterior (a), middle (b) and anterior (c) parts. The anterior part is particularly important for a transsphenoidal exposure.

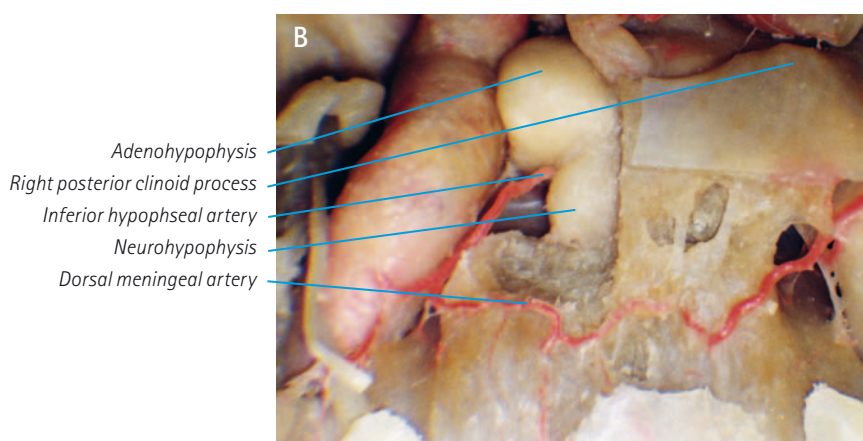
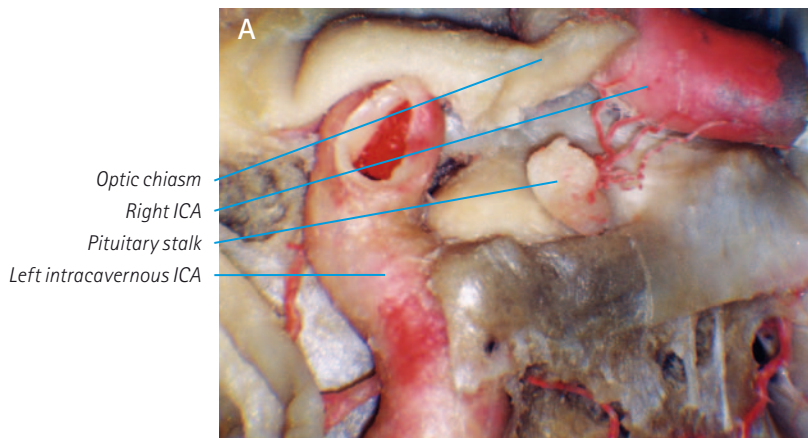
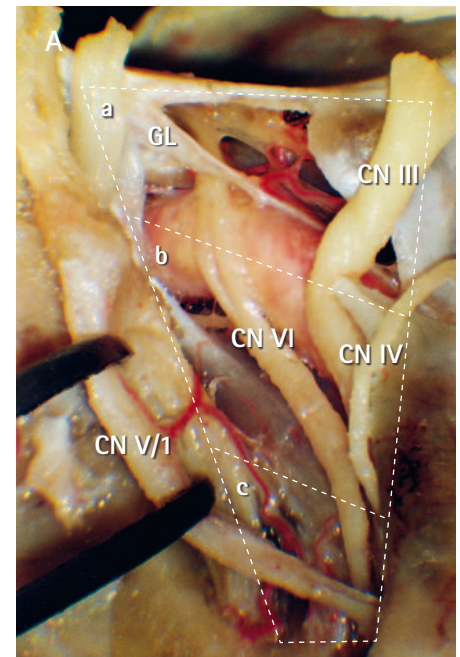
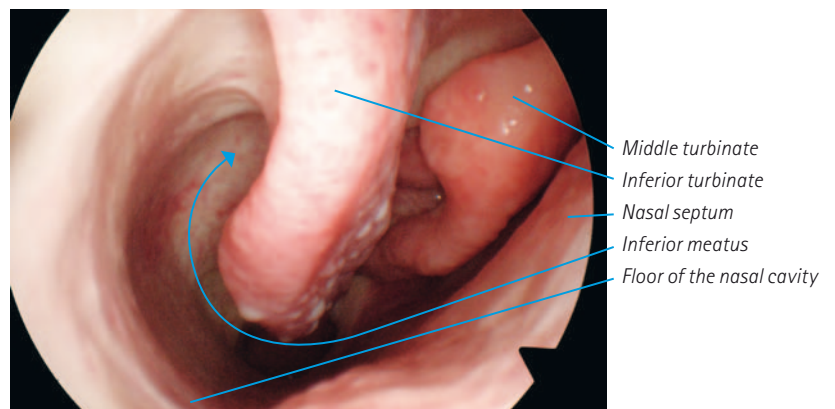


**Fig. 26** Arterial supply of the pituitary gland. Note the superior hypophyseal branches, originating from the supraclinoid carotid artery (A). After removal of the left posterior clinoid process, the inferior hypophyseal and dorsal meningeal arteries can be observed (B). Note the adeno- and neurohypophysis.

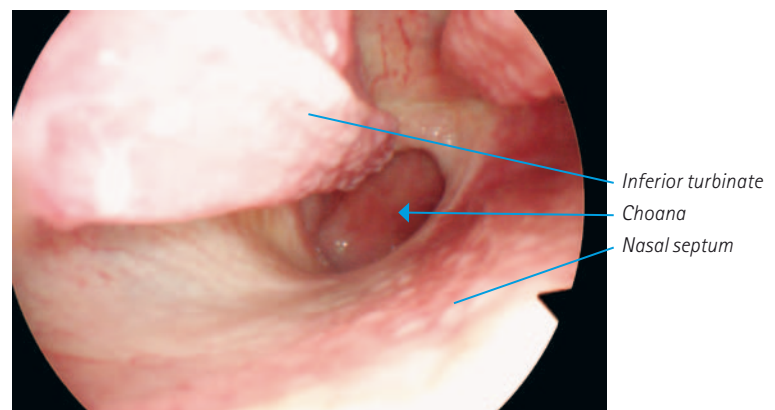
## Endoscopic anatomy of the nasal cavity and sellar region

In the following, the most important anatomical landmarks of the nasal cavity and para- suprasellar region are demonstrated in a fresh human cadaver using a 4 mm endoscope with a 30° viewing angle (Figs. 27–57).

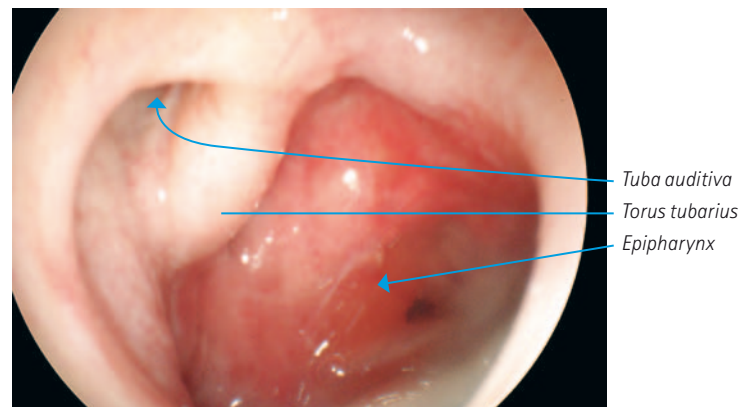
**Fig. 27** Overview of the nasal cavity. The tip of the endoscope is placed into the right nostril. Note the floor and medial wall of the cavity. The inferior turbinate and inferior meatus are clearly apparent.



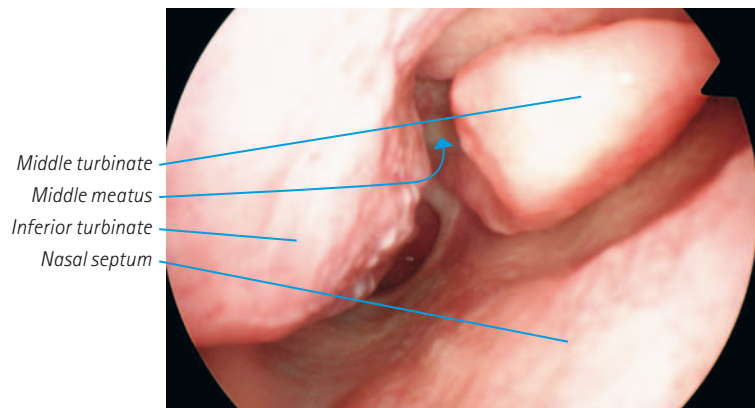
**Fig. 28** The endoscope is introduced along the inferior turbinate approaching the choanal region. Note the posterior tail of the inferior turbinate.



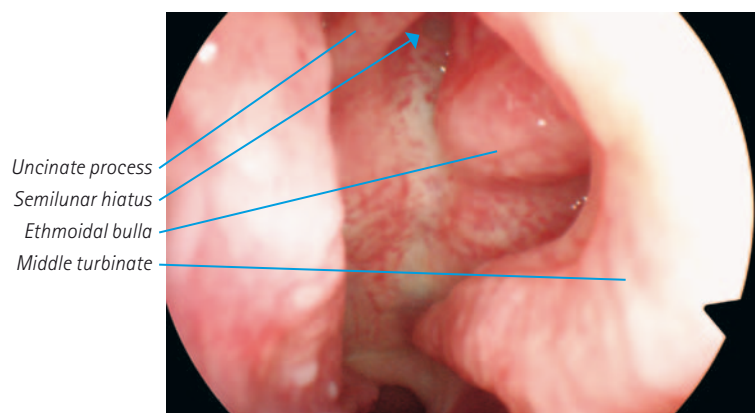
**Fig. 29** Approaching the epipharynx, the 30° endoscope is rotated to the right with visualization of the entrance of the tuba auditiva. Note the torus tubarius and the posterior wall of the pharynx.



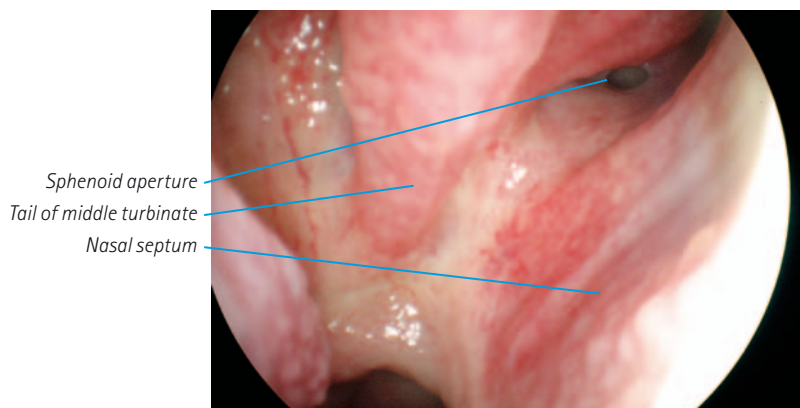




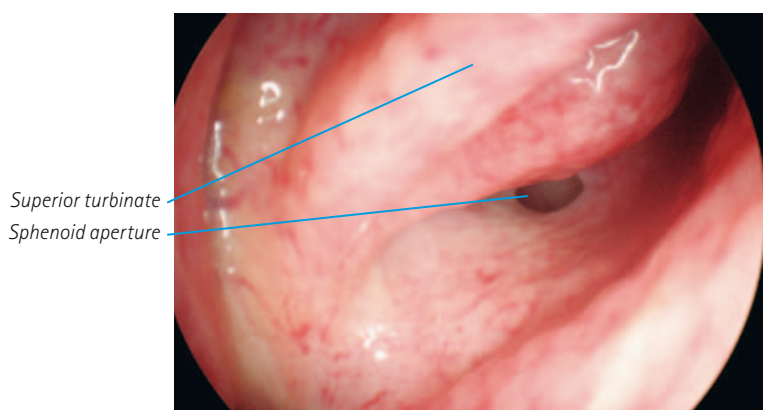
**Fig. 30** Retracting the endoscope, the head of the middle turbinate is exposed. Note the path into the middle meatus.



**Fig. 31** Using a 30° endoscope, the middle meatus is observed. Note the junction of the uncinate process with the ethmoidal process of the inferior turbinate. The semilunar hiatus appears between the uncinate process and the ethmoidal bulla, connecting the maxillar sinus with the nasal cavity.

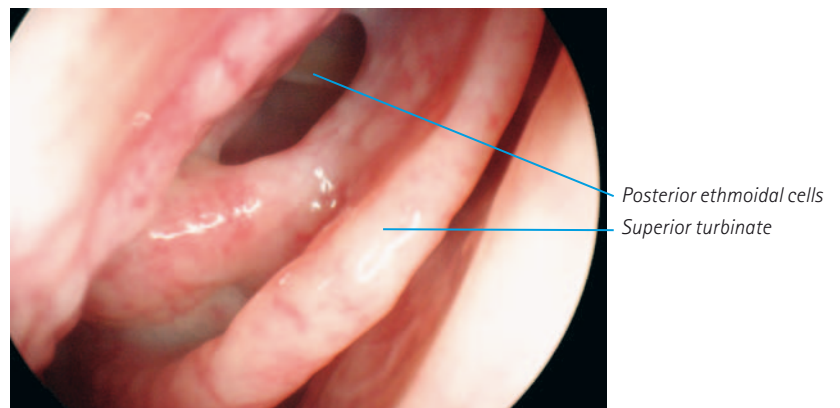


**Fig. 32** Following the inferior border of the middle turbinate, its insertion into the pterygoid bone is approached. Note the lower part of the anterior wall of the sphenoid sinus and the sphenoid aperture.

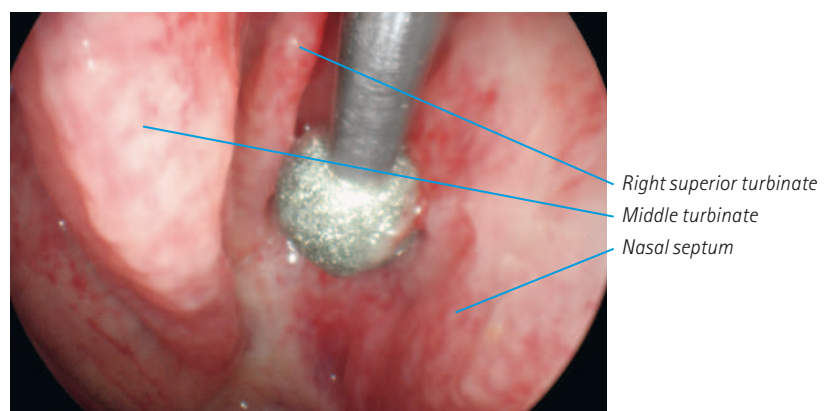


**Fig. 33** Moving upwards, the endoscope reaches the sphenoethmoidal recess. Note the superior turbinate and the entrance to the sphenoid sinus.

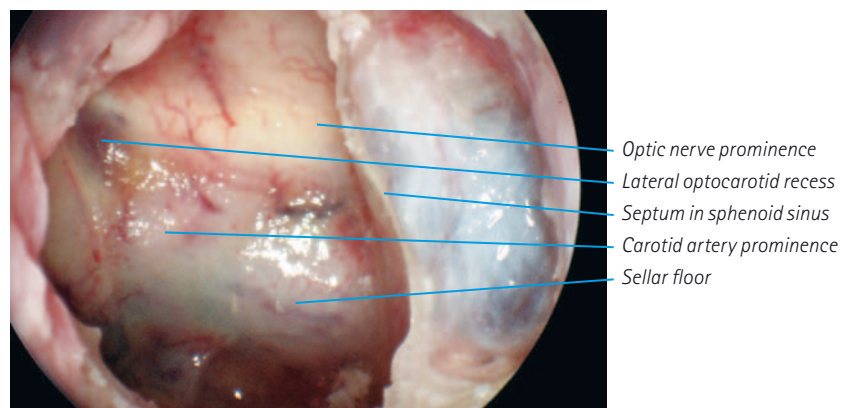
**Fig. 34** The superior turbinate is moved to medial exposing the superior meatus. Note the view into the posterior ethmoidal cells.



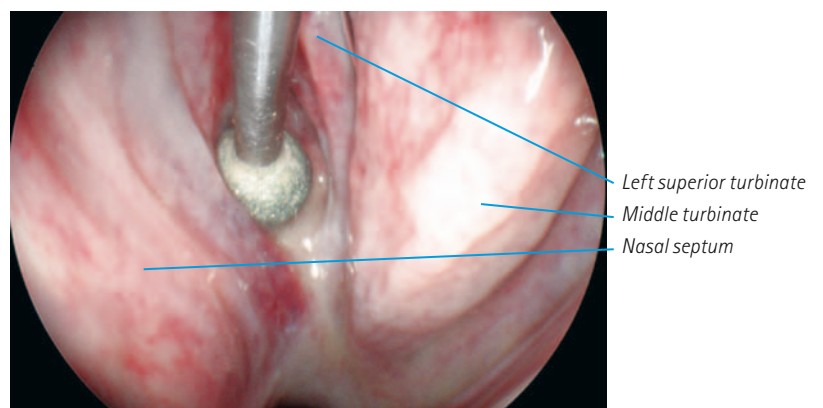
**Fig. 35** Opening the anterior wall of the sphenoid sinus with a diamond drill. Typical placement of drilling is medial from the superior turbinate just inferiorly from the sphenoidal aperture and approx. 1 cm over the choana.

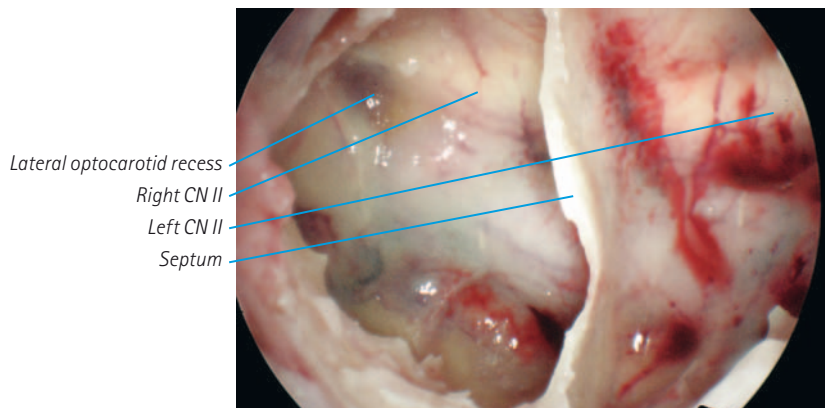


**Fig. 36** Clear view into the sphenoid sinus after drilling. Note the left paramedian septum with intact mucosa on the left side. On the right side, we gain a superb overview of the anatomical structures with direct visualization of the optic and carotid prominences, the lateral optocarotid recess and the sellar floor.

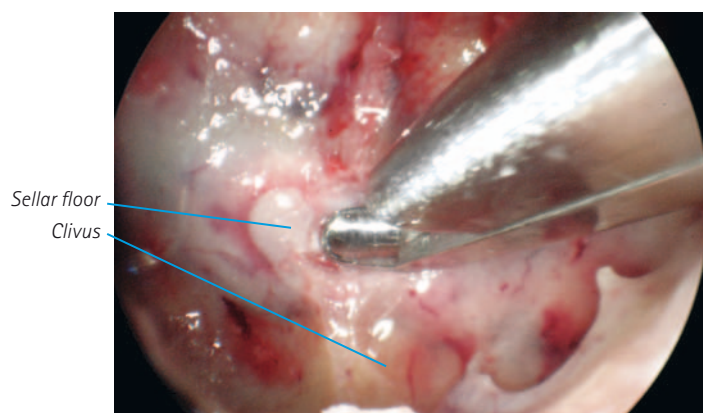


**Fig. 37** After completing the unilateral exposure, the approach is continued on the contralateral side in a similar manner allowing biportal binostril dissection within the deep-seated surgical field. Note the drill medial from the left superior turbinate.

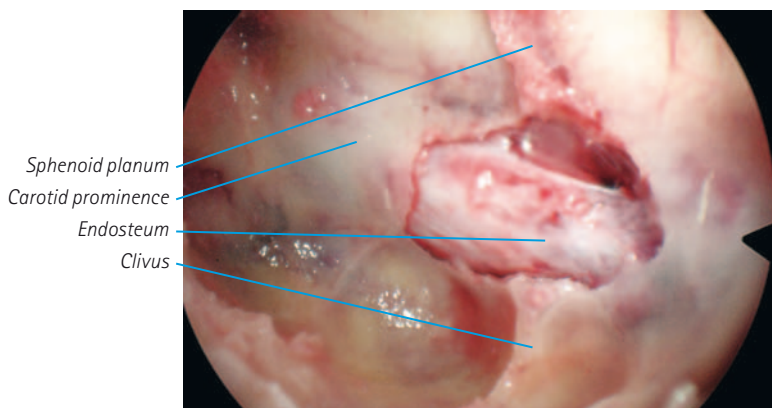




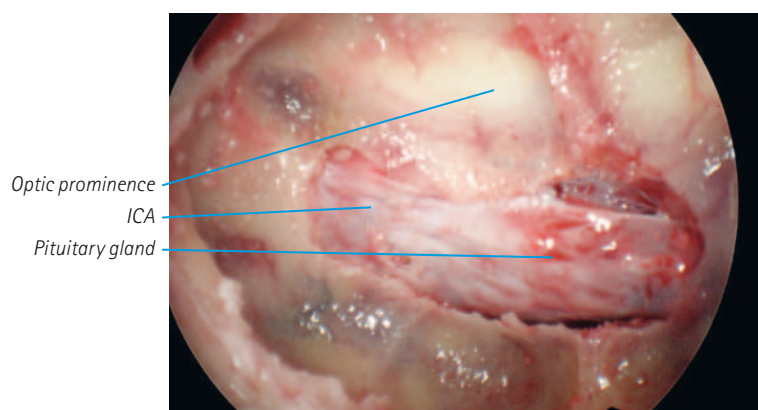
**Fig. 38** View into the sphenoid sinus from the left nostril before removal of the sphenoid septum. Note the impression of both optic nerves and the right lateral optocarotid recess.



**Fig. 39** The endoscope is placed through the right nostril, the Kerrison punch is introduced from the left to open the sellar floor. Note the perfect contra-lateral visualization without conflict between the endoscope and instrument.



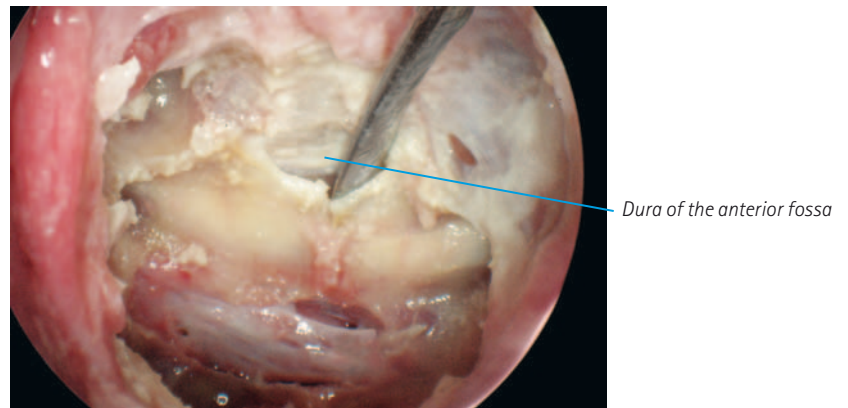
**Fig. 40** Appearance of the sellar endosteum after removal of the bony sellar floor.



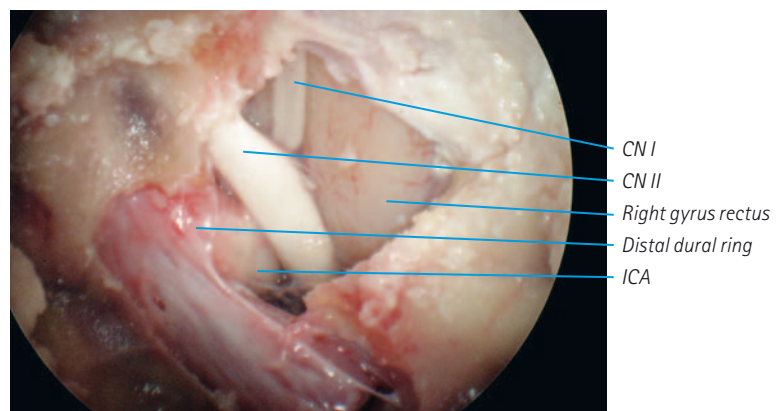
**Fig. 41** After further bony resection, the anterior knee of the right internal carotid artery is exposed. Note the optic prominence.



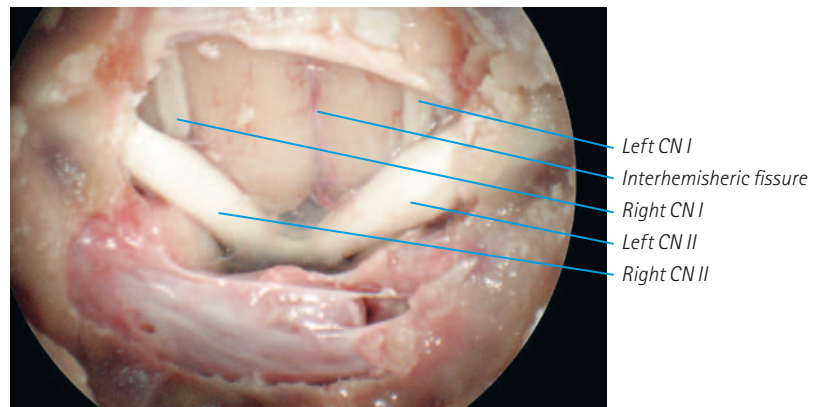
**Fig. 42** The view of the 30° endoscope is directed frontally and the sphenoid planum is opened observing the dura mater of the anterior fossa.



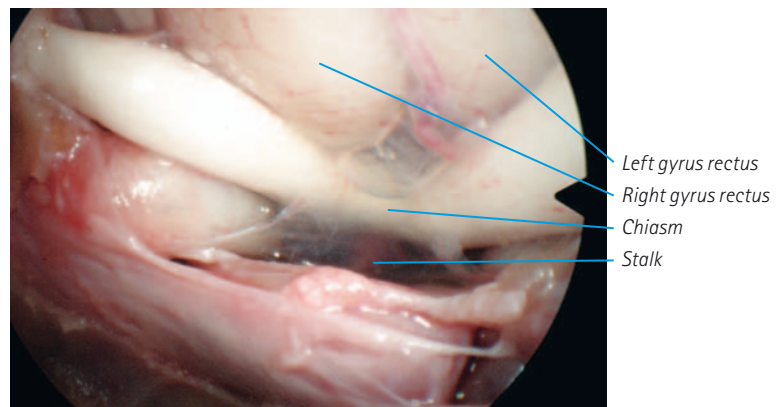
**Fig. 43** After further dissection, the anterior fossa is entered. Note the right gyrus rectus, the olfactory and optic nerves. The proximal optic canal is opened. Note the distal dural ring indicating the border between the paraclinoid and supraclinoid carotid arteries.

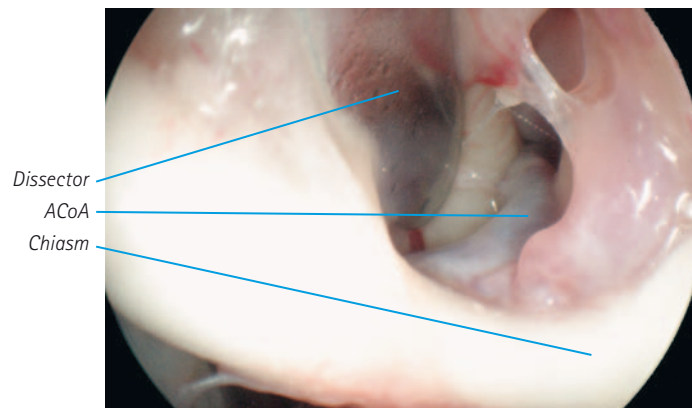


**Fig. 44** With further removal of the planum, the chiasm and both optic nerves are exposed via the special transsphenoidal route.

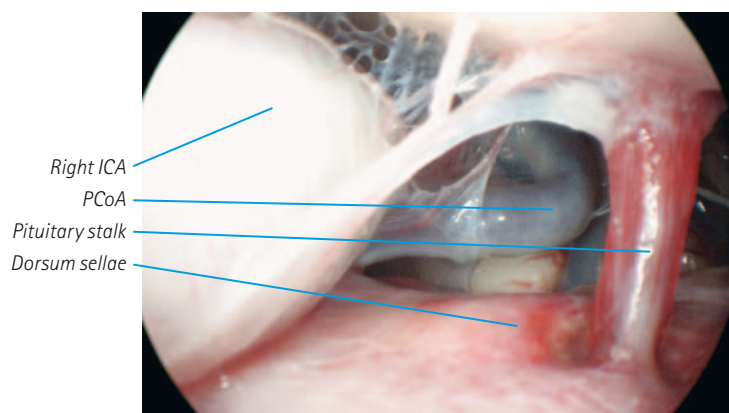


**Fig. 45** The optic chiasm in a close-up position of the endoscope. In the background, the reddish pituitary stalk can be seen.

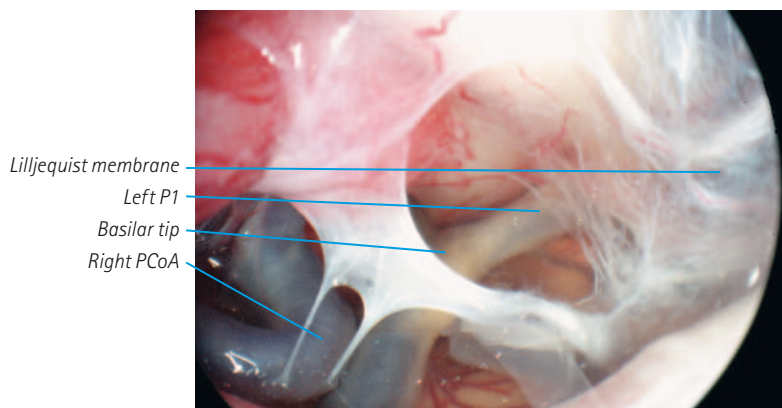




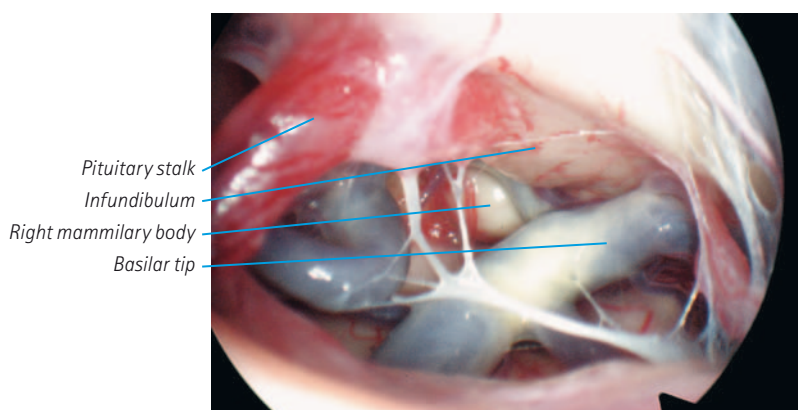
**Fig. 46** After opening the lamina terminalis cistern, the anterior communicating artery complex is approached.



**Fig. 47** The chiasma cistern is carefully opened. The deep-seated preoptine region appears through the anatomical window between the right internal carotid artery and the stalk. Note the dorsum sellae and the right posterior communicating artery in the background.



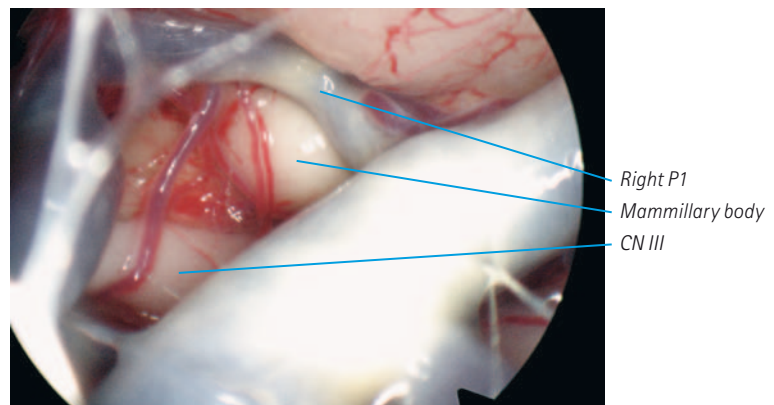
**Fig. 48** The endoscope is introduced through the left stalk – carotid gap. Note the fine remnants of the Lilljequist membrane; the basilar tip appears in the background. The left P1 segment of the posterior cerebral artery and the prominent right posterior communicating artery become visible.



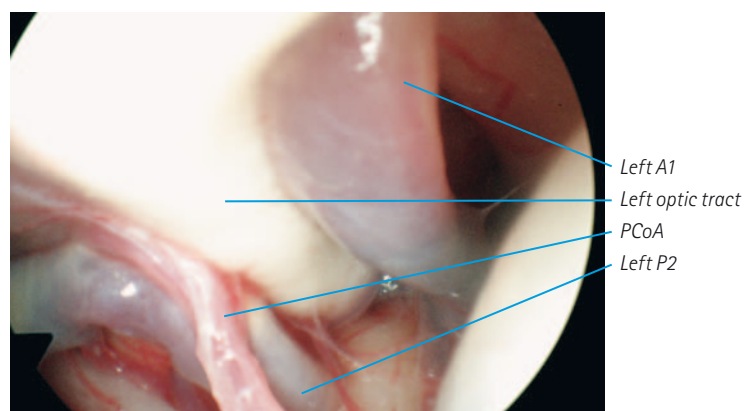
**Fig. 49** Endoscopic visualization of the distal basilar artery. Note the infundibulum and pituitary stalk.



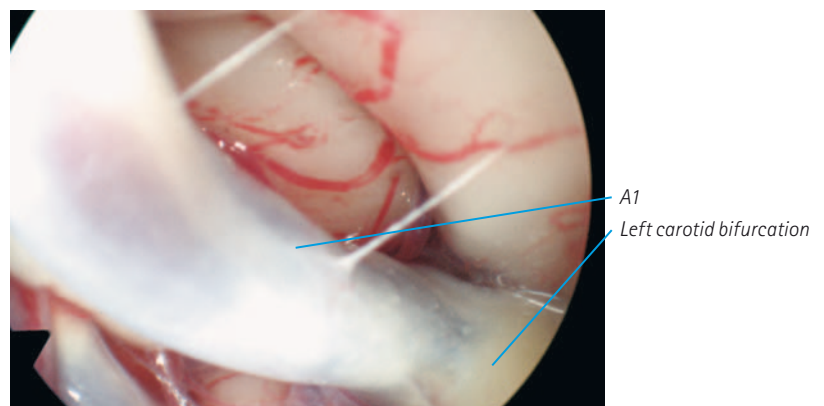
**Fig. 50** The basilar bifurcation in a close-up position. Note the hypoplastic P1 segment of the right posterior cerebral artery, right mammillary body, and the origin of the oculomotor nerve.



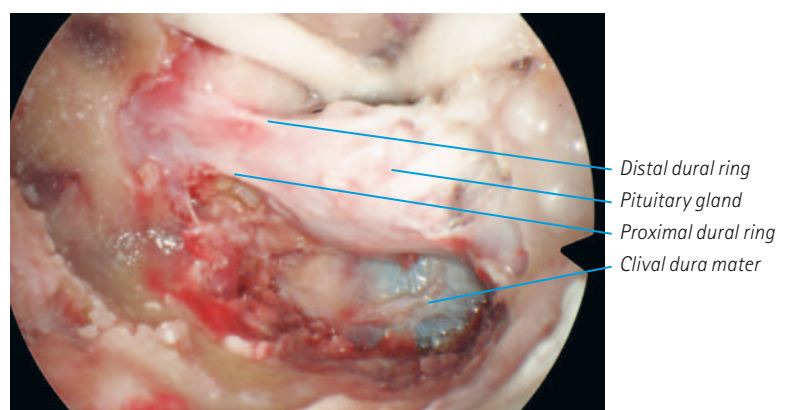
**Fig. 51** The 30° endoscope is rotated to the right and the left posterior cerebral artery is followed in a lateral direction. Note the special relationship between the left posterior communicating artery, the P2 segment, the optic tract and the A1 segment of the left anterior cerebral artery.



**Fig. 52** Following the A1 segment, the left carotid bifurcation is reached.



**Fig. 53** Retracting the endoscope, the sphenoid sinus is again exposed. Using a fine drill, the clivus is drilled basal from the pituitary gland visualizing the dura mater of the posterior fossa. Note the proximal and distal dural rings indicating the paraclinoid carotid artery.



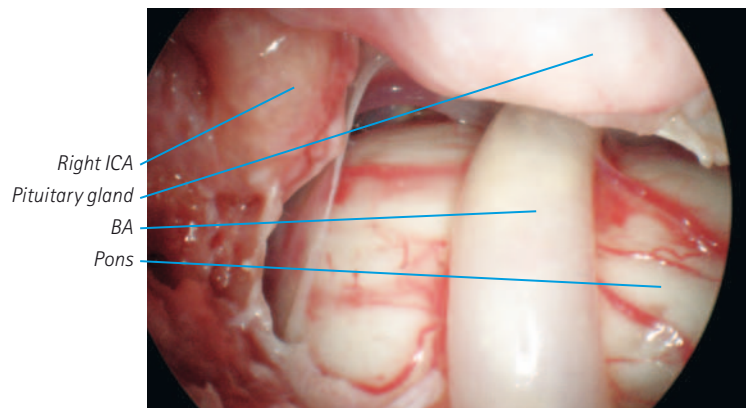


**Fig. 54** After opening the clival dura, the preoptine cistern with the basilar artery appear. Note the relation between the posterior knee of the right intracavernous internal carotid and basilar arteries.

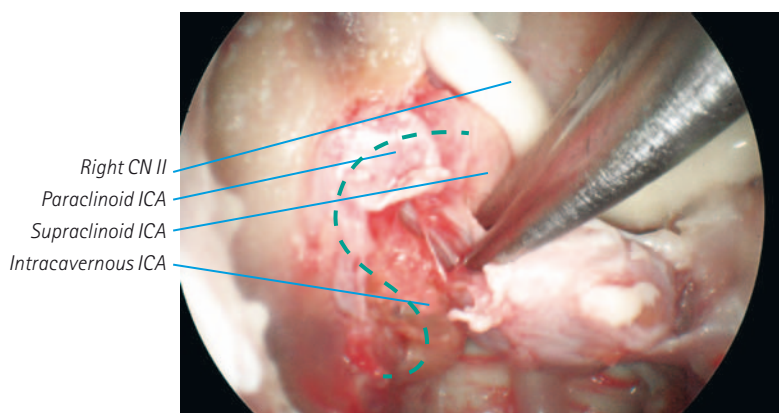


**Fig. 55** The proximal and distal dural rings are divided with microscissors allowing mobilization of the pituitary gland. Note the S-formed course of the intracavernous - paraclinoid - supraclinoid carotid artery (dashed line).

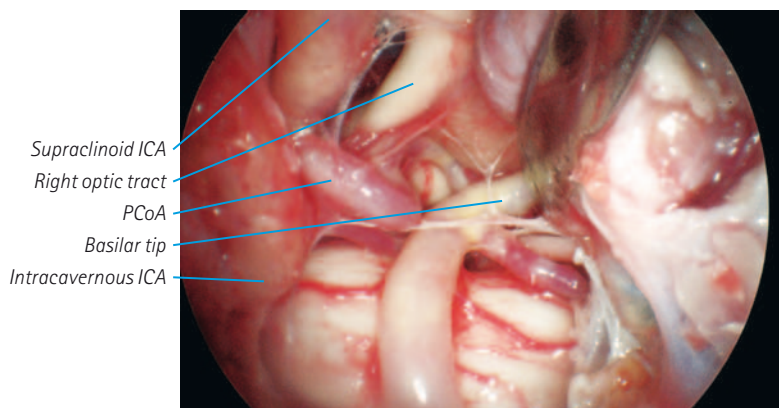


**Fig. 56** The pituitary gland is retracted with a fine microdissector allowing endoscopic investigation of the preoptine and interpeduncular regions.

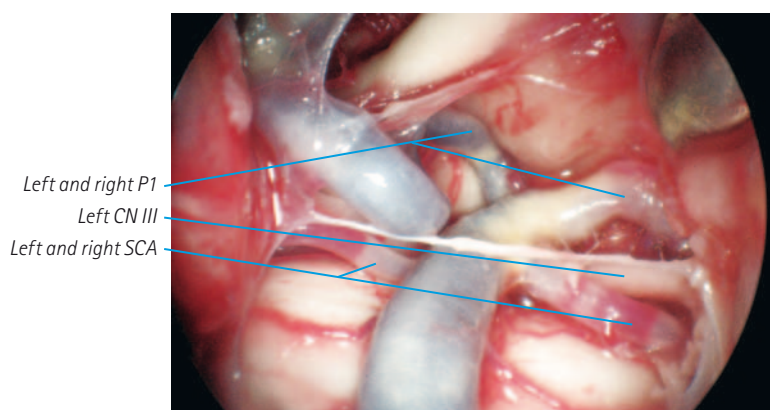


**Fig. 57** Close-up investigation of the distal basilar artery. Note the left oculomotor nerve between the posterior cerebral and superior cerebellar arteries.

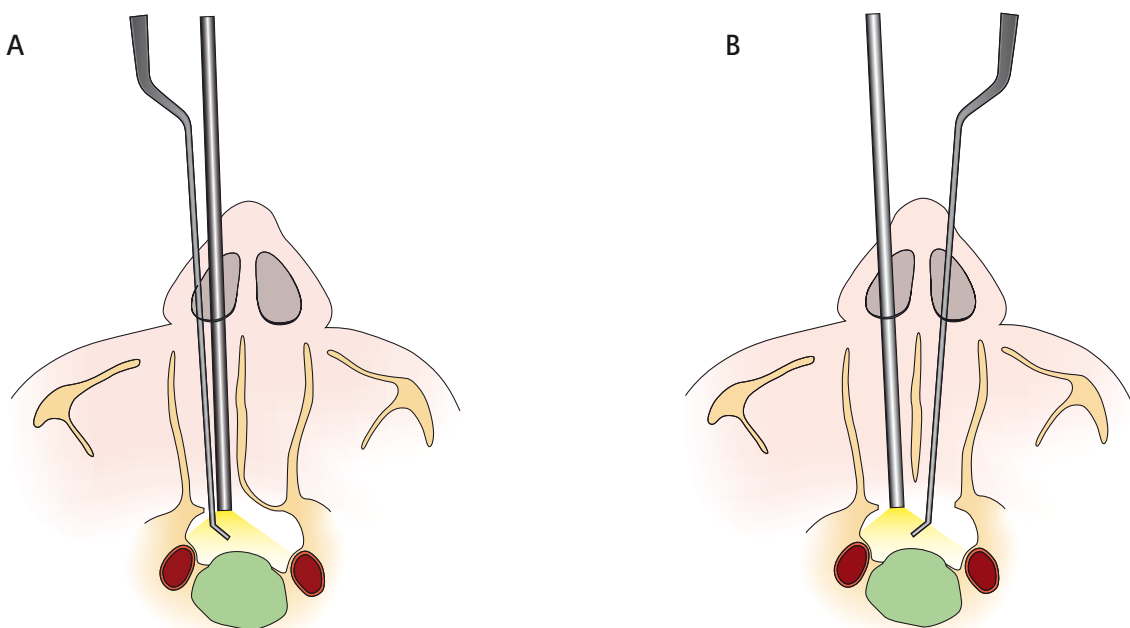
## The endonasal endoscopic approach

Most publications on endoscopic transsphenoidal surgery describe a monoportal-monostril exposure of the central skull base (Fig. 58A). These monostril approaches may cause only unilateral manipulation within the nasal cavity; however, they offer several disadvantages. The space within the nasal cavity is very narrow and restricts surgical manipulation: the tip of the endoscope disturbs the free maneuverability of instruments. Because instruments enter the field out of the line of sight of the endoscope, the nasal mucosa along the septum and middle turbinate can be severely damaged in the course of the procedure. To allow adequate dissection, a nasal speculum may be required or removal of the middle and superior turbinates may be necessary. The first causes limited surgical manipulation, the second increased surgical morbidity.

**Fig. 58** Using monoportal exposure, the space within the nasal cavity is very narrow and limits surgical manipulation. The tip of the endoscope impedes the introduction of instruments and, because of the lack of space, the nasal mucosa can be severely damaged (A). By comparison, using a biportal approach, the tip of the endoscope does not impede the surgical manipulation and the endoscope allows optimal contralateral visual control of tumor removal. Free introduction and improved maneuverability of the surgical instruments can be achieved because the endoscope is placed through the other nostril (B).

By comparison, the biportal-binostril approach offers free introduction and improved maneuverability of the surgical instruments because the endoscope is placed through the other nostril (Fig. 58B). There is no conflict between endoscope and instrument, the tip of the endoscope does not impede surgical manipulation. In addition, the contralateral positioned endoscope allows optimal visual control of tumor removal. Without using a nasal speculum, surgical manipulation is not restricted with free maneuverability of instruments.

Nevertheless, it is interesting to note here that, despite these undisputable advantages of the endoscopic biportal technique, the endoscopic method is







not in routine use everywhere and neurosurgeons are often reluctant to use it. Neurosurgeons are cautious about an endoscopic endonasal dissection because the permanent contamination of the endoscope with blood and nasal secretions hinders orientation. In addition, the para-endoscopic and biportal dissection is very unfamiliar requiring a steep learning curve that many consider unacceptable. The first frustrating steps add to the growing impatience of surgeons and prompts them to give up!

The three most important factors this novel technique are basic endoscopic experience, applied anatomical knowledge and the use of dedicated equipment. However, in our experience, if neurosurgeons perform transnasal endoscopic operations with rhinosurgical assistance, the learning curve is significantly shorter, resulting in an acceptable operating time and decreased surgical morbidity (Fig. 59). The neurosurgeons main concern is the unfamiliar and highly variegated nasal anatomy with common septal deviations, bullous turbinates, adhesions and other variations. Dealing with the nasal mucosa also represents a challenge for the neurosurgeon: for a rhinosurgeon, this is not a concern!

The productive neuro-rhinosurgical cooperation offers interdisciplinary benefits and a marked improvement in surgical results. Three- or four-hand techniques performed by a skilled team ensures that, the instruments are freely movable in the nasal cavity, thus allowing effective dissection. Certainly, effective interplay is required between the endoscopist and the surgeon: the endoscope should follow the instruments and focus dynamically on the field of interest (Fig. 60A). Alternatively, the endoscope can be fixed in a holding device should the surgeon prefer this (Fig. 60B). Note that as with microscopic surgery, adequate bimanual manipulation is essential for safe and feasible endoscopic dissection, using the freehand or even arm-based technique.

**Fig. 59** Neuro- and rhinosurgical teamwork during endoscopic skull base surgery. The procedure is initiated by the rhinosurgeon (RS), creating the endonasal approach; the cooperating neurosurgeon (NS) assists by holding the endoscope. The setup changes in the later course of the procedure, supporting free bimanual neurosurgical dissection. In our experience, this productive collaboration offers interdisciplinary benefit and a marked improvement in surgical results.



**Fig. 60A** The freehand technique supports unhindered manipulation in the field. Certainly, effective interplay is required between the endoscopist and the surgeon: the endoscope should follow the instruments and focus dynamically on the field of relevance.

**Table I. Preoperative checklist for pituitary surgery**

Endocrinology	Baseline test
	Functional pituitary test
	Optional hormonal substitution
Ophthalmology	Visual field test
Rhinology	Endoscopic nasal inspection
	Smell screening test
	Optional local steroids
Radiology	Triplanar MRI +/- contrast incl. 3D dataset
	CT with bone window for nasal cavity,
	paranasal sinuses and skull base

**Fig. 61** Three cases of large pituitary macroadenomas with similar suprasellar extension; each with very different patho-anatomical appearance however. In the first case, the sella is enlarged and the diaphragma is intact (A). In the second case, the diaphragma is ruptured with free tumor tissue in the subarachnoid spaces (B). Similarly, in the third case, the tumor is no longer encapsulated, causing severe obstructive hydrocephalus; however, the sella is not enlarged, thus making transsphenoidal removal critical (C). According to preoperative planning, cases A and B were operated transsphenoidally, case C through a transcranial supraorbital mini-craniotomy.

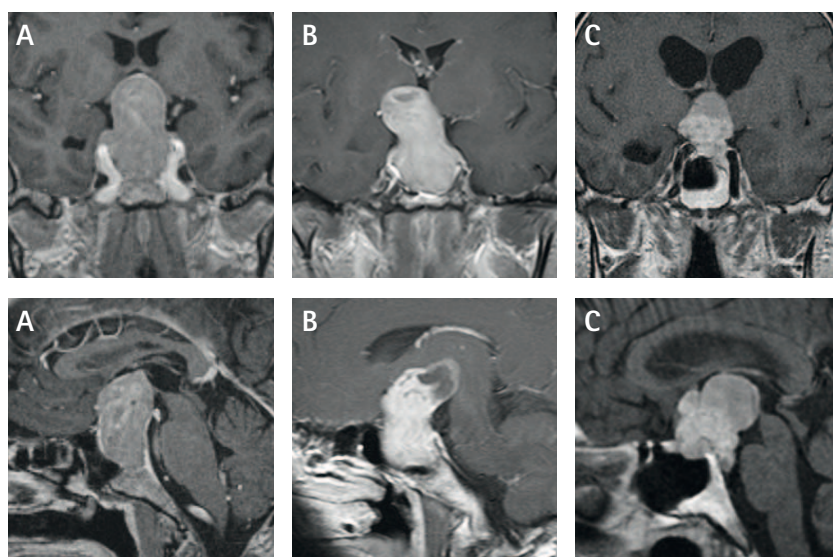


**Fig. 60B** Arm-based technique in endonasal endoscopic surgery. The endoscope is fixed in a stable holding arm, allowing feasible bimanual dissection.

### Prearrangement and planning of the procedure

Once the decision to perform surgery has been made, the patient should be fully prepared for the operation according to a general checklist (Tab. 1). Clinical prearrangement includes evaluation by a clinical endocrinologist with baseline and functional testing of the pituitary gland, ophthalmologic investigation with visual field testing, rhinologic examination with endoscopic nasal investigation and a smell screening test, in addition to detailed radiologic exploration. If necessary, hormonal substitution is administered and local nasal steroids are used ten days prior to surgery to effectively reduce inflammation of the mucosa. For planning the tailored surgical approach, a contrast enhanced MRI and CT with bone window should be performed. The triplanar MRI scans should be used to evaluate, the relationship of the tumor to the nearby neurovascular structures and subarachnoid spaces. Special attention is given to the diaphragma sellae and potential vascular incorporation of the tumor tissue due to diaphragmal rupture (Fig. 61). MR angiography provides information on the exact course of the surrounding vessels.



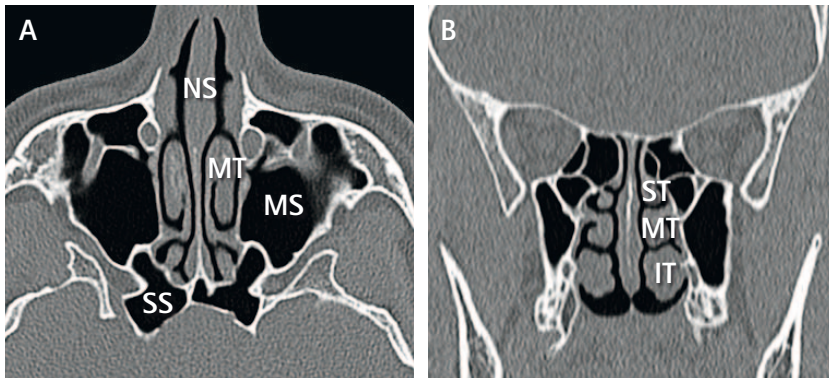


**Fig. 62** Preoperative axial spiral CT with 1 mm sections (A) and coronar reconstruction (B) showing the bony anatomy of the skull base. Careful observation of the bony skull base anatomy is essential when planning transnasal endoscopy. Special attention should be given to the nasal turbinates and the relationship between the nasal cavity and the paranasal sinuses. Within the sphenoid sinus, bony septations must be recognized precisely, giving ideal landmarks for safe orientation.

CT scan with 0.70 mm or 1 mm axial sections and coronar reconstruction with bone window are obligatory for assessment of the nasal cavity including the paranasal sinuses, sphenoid sinus and the central skull base. Here, intrasphenoid septas and the surrounding vital structures should be estimated thoroughly (Fig. 62). In selected cases, we have used three-dimensional virtual reality workstations to better understand the pathoanatomical situation (Fig. 63).

### The role of preoperative approach planning in endoscopic skull base surgery

Using modern diagnostic tools, the specific anatomy and pathology of the individual patient can be precisely visualized and anatomical pathways and surgical corridors determined for optimal surgical access (Fig. 63). Central goal in endoscopic transsphenoidal skull base surgery is not to harm the patient by creating a tailormade approach based on thorough preoperative clinical investigation and detailed planning of the procedure. By choosing the best approach to a specific lesion, surgery-related traumatisation can be dramatically reduced. This may contribute to improved surgical results with less risk of complications following the minimally invasive treatment philosophy.

### Preparation of the patient in the operating room

Today's skull base operating rooms must be large enough to accommodate the patient, the operating personnel and highly sophisticated neurosurgical equipment (Fig. 64).

Preparing the patient in the operating room is the task of the responsible surgeon: take your time for this! Before starting the operation, be sure to inspect the patient's records, MRI and CT scans again. Check that the endoscope has been prepared thoroughly by checking its optical image quality, including white balance and focusing of the camera unit. Never be tempted to start the procedure without these vital checks!

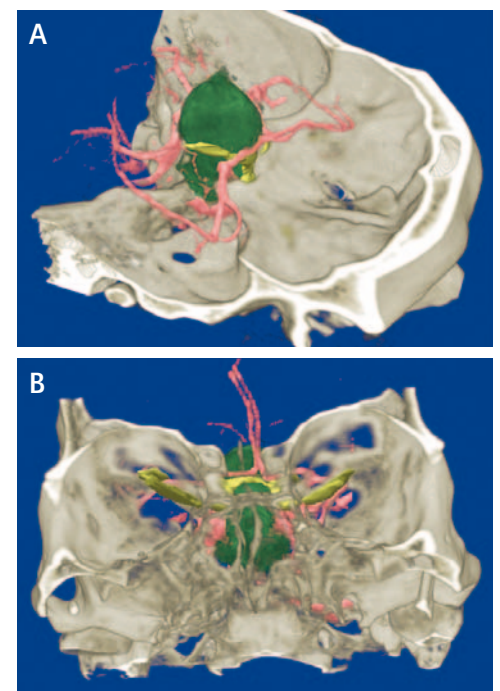


**Fig. 63** Three dimensional virtual reality representation of the large pituitary adenoma of case 61A, simulating the transcranial (A) and transsphenoidal (B) appearance (Dextroscope®, Volume Interactions, Singapore). Using modern diagnostic tools, the specific anatomy and pathology of the individual patient can be precisely analyzed to determine tailored surgical access. In this way the surgical approach can be planned and performed in a minimally invasive way. (Images courtesy of Ralf Kockro, University Hospital Zurich, Switzerland, Axel Stadie, University Hospital Mannheim, Germany, and Eicke Schwandt, Neurosurgical Department Mainz, Germany).

**Fig. 64** Highly sophisticated operating room for skull base surgery with integrated intraoperative CT and navigation devices (iCT BrainSuite®, Clinic Hirslanden Zurich). iCT offers optimal image quality in skull base surgery associated with cost-effective and user-friendly application.



**Fig. 65** Patient's positioning for image-guided transnasal endoscopic procedure. The upper part of the body is elevated slightly to avoid venous engorgement of the nasal mucosa and congestion of the deep parasellar sinusoid vessels. The head is in an elevated neutral position or rotated to some extent towards the surgeon's side to allow for efficient dissection during the procedure. The midface is disinfected with uncolored chlorhexidine solution, the para-umbilical region with iodine solution. Published with patient's permission.



**Fig. 66** If used, the navigation device should be registered after positioning the patient (BrainLAB, Feldkirchen, Germany). In endoscopic transnasal surgery we use image fusion of the CT-bone window with contrast-enhanced wT1 MRI images. We recommend navigation if conchal sella type is present, extended tumors with parasellar expansion, hormonally active microadenomas, and, especially in re-do surgeries if scarring of the sellar floor may impede intraoperative orientation. Published with patient's permission.

Following induction of general anesthesia and oral endotracheal intubation, the patient is now placed in a supine recumbent position on the operating table. The upper part of the body is raised slightly to avoid venous engorgement of the nasal mucosa and congestion of the deep parasellar sinusoid vessels (Fig. 65). The elevated head is in a neutral position or rotated to some extent towards the surgeon's side to allow for efficient dissection during the procedure.

After facultative installation of neuronavigation and intraoperative imaging (Fig. 66), the midface including the forehead is disinfected with uncolored solution. We use an aqueous chlorhexidine liquid (Merfen®) for this, the eyes are protected with cream without later draping (Figs. 67 A, 73). The nasal cavity is explored with external illumination and also disinfected carefully. Thereafter, using a Cottle dissector or nasal speculum, the nasal cavity is inspected and packing is introduced with patties soaked in 1:1000 epinephrine (Fig. 68). Note that this should be done prior to patient draping, and placed exactly in the middle meatus or between the middle turbinates and



septum to create more space by reducing mucosal inflammation (Fig. 69). A submucosal infiltration of the nasal mucosa is not recommended since this often causes a rebound effect with increased mucosal bleeding at the end of the procedure. The abdominal para-umbilical region is also routinely disinfected with an iodine solution (Betadine®) in case a fat graft is required (Fig. 67 B). After nasal packing and disinfection, taping is completed. We do not tape the eyes, so that they can regularly be examined during surgery. This guarantees control of the orbital content, including pupillomotor function (Figs. 60A, 67A, 73).

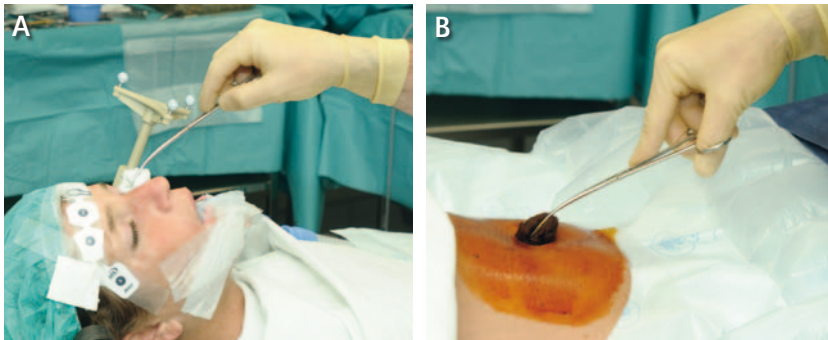


**Fig. 67** A, B After positioning, facultative installation of neuronavigation and intraoperative imaging, the midface including the forehead and periorbital region is disinfected with uncolored aqueous chlorhexidine liquid (Merfen®) solution (A, published with patient's permission). Careful disinfection of the abdominal para-umbilical region with an iodine solution (Betadine®) is used in case a fat graft is required (B).



**Fig. 68** The nasal cavity is inspected with external illumination and also disinfected carefully. Using a Cottle dissector or nasal speculum, epinephrine-soaked patties are introduced to create more space by reducing mucosal inflammation. Published with patient's permission.

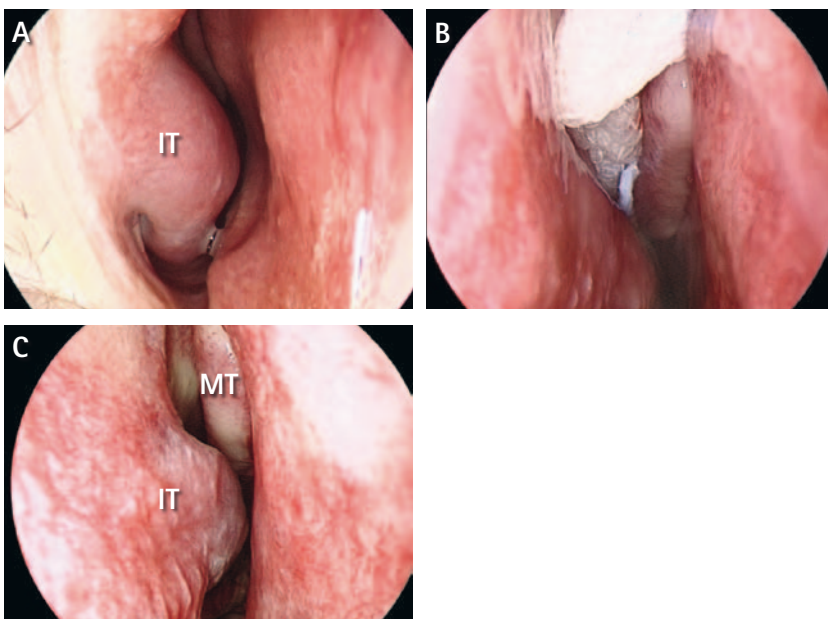


**Fig. 69** Initial endoscopic appearance of the right nasal cavity demonstrating narrow spaces (A). After exact placement of epinephrine-soaked patties (B), mucosal inflammation can be effectively reduced, thus supporting endoscopic dissection. Note unimpeded visualization of the middle turbinate (C). Dedicating the first minutes of the procedure to carefully reducing mucosal inflammation is of particular importance in avoiding later frustration because of blurred visualization of the bloody-coated endoscope. In addition, preventing mucosal damage is vital to avoid later crusting and nasal adhesions!



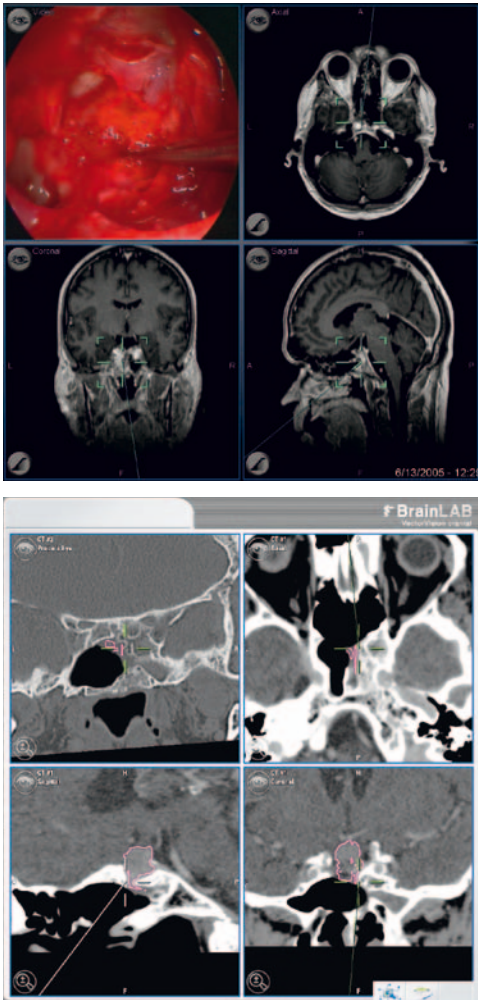


**Fig. 70** Screenshots of image-guided endoscopic transsphenoidal surgery. In the first case, the tip of the endoscope is navigated, achieving additional control in surgical orientation. Note the use of integration of video signal on the navigation panel. In the second case, an intraoperative CT scan is used, showing partial conchal sella type; previous surgery with scarring of the sellar floor necessitated the image-guided approach. Note the use of bone window and contrast assisted CT angiography; tumor tissue was marked preoperatively (BrainLAB, Feldkirchen, Germany).

### The role of navigation and intraoperative imaging

In most cases, anatomical landmarks allow safe orientation during endoscopic skull base surgery; however, in some cases, the anatomy of the nasal cavity, paranasal sinuses and the skull base is confused causing complicated orientation (Table II). The following difficulties require intraoperative navigation: If a conchal sella type is present without pneumatization of the sphenoid sinus, drilling of the skull base and opening of the sellar floor is not without severe problems. Extended tumors with parasellar, intrasphenoidal or even intranasal expansion can also cause reduced orientation because of significant loss in anatomical alignment. Hormonally active microadenomas can cause difficulties in orientation if an extensive sinusoidal bleeding occurs, and, especially in re-do surgeries, scarring of the sellar floor can impede orientation. In these cases, the intraoperative use of a navigation device is essential to avoid damage to neurovascular structures. In addition, intraoperative imaging may increase surgical safety, thus complementing the endoscope's direct visualization in hidden parts of the surgical field (Fig. 70, 71).

Table II. Indications for neuronavigation	
Conchal sella type	No anatomical landmarks
Extended tumour	Destroyed anatomical landmarks
Microadenomas	Questionable anatomical landmarks / bleeding
Re-do surgery	Confused anatomical landmarks / scarring



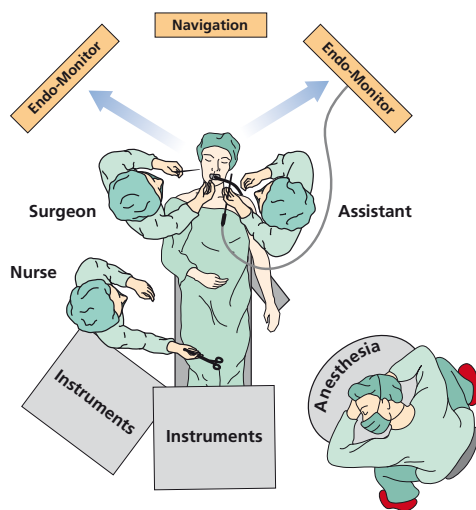
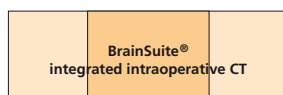
**Fig. 71** Neuronavigation-guided endoscopic skull base surgery. Note the use of the navigated endoscope for real time control during surgery.

# Surgical technique

## General hints

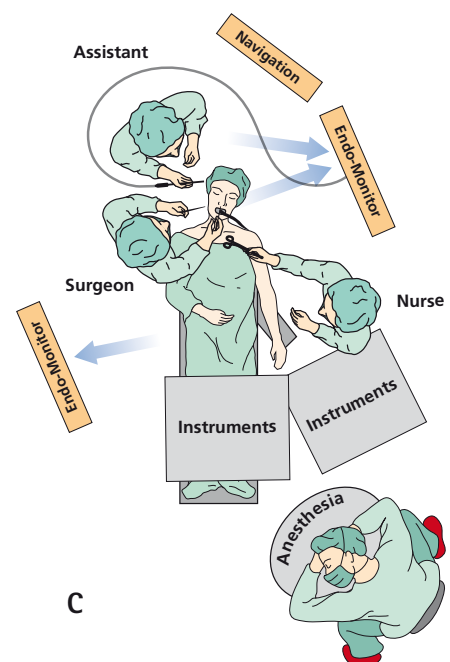
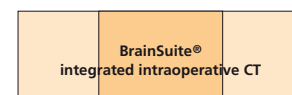
After 1) the general preparation and positioning of the patient, 2) optional installation of navigation, 3) draping and 4) final control of the endoscopic equipment, the vasoconstrictor patties are removed and the procedure can begin.

The neurosurgeon remains beside the patient, usually on the right, allowing ergonomic handling with the endoscope. The co-working surgeon is on the same or the opposite side, the scrub nurse on the right side of the surgeon. The camera equipment, monitor and light source are placed in front of the surgeon for optimal control of the procedure. Modifications of this layout are of course possible depending on the individual case and the surgeon's own practice (Fig. 72).



A

**Fig. 72A** Illustrations of possible set-ups in the operating room when performing endoscopic transsphenoidal surgery. In the face-to-face position, surgeons remain on the opposite side of the patient (A). Two separate endoscopic monitors allow for relaxed observation both for the surgeon as well as for the assistant (blue arrows).



B

**Fig. 72B,C** Photo (B) and illustration (C) showing the preferred Hirslenden set-up, utilizing the comfortable side-by-side layout. The navigation and endoscope monitors are placed opposite the operating surgeons. The scrub nurse is also on the opposite side, an additional endoscope monitor is placed for optimal control of the procedure.

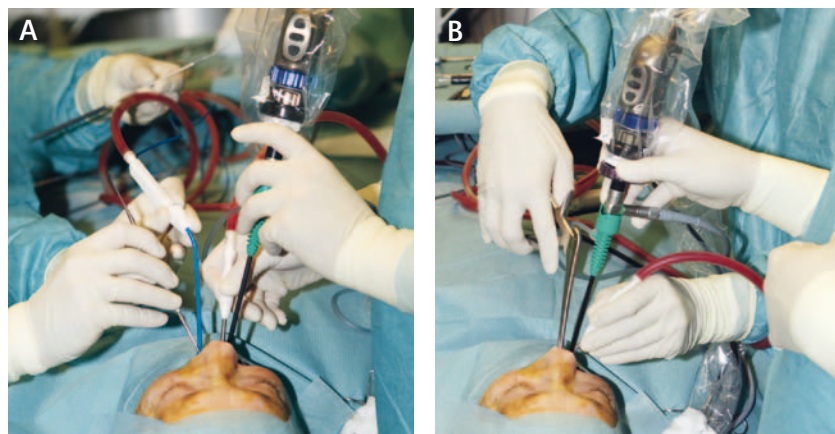


**Fig. 73** Positioning of the endoscope in the right nostril. The 12 o'clock location allows unhindered manipulation in both nostrils. Note the special draping, allowing real-time examination of the eyes during surgery. In this way, control of the orbital content including the pupillomotor function is warranted. Published with patient's permission.

The surgeon usually initiates the procedure single-handedly in the right naris, holding the endoscope in one hand, usually the left; instruments are used with the other hand. The endoscope is placed in the superior edge of the nostril in a 12 o'clock position; the instruments should be introduced inferiorly in the 6 o'clock position, thus providing more space for manipulation (Fig. 73). If necessary, the co-operating surgeon can help with the sucker, thus cleaning the field, or can hold the endoscope assisting in a three- or four-hand technique (Fig. 74). It is easier to use a 0° endoscope for most operations, which provides an overview from the central part of the surgical area. We use angled endoscopes only in the later course of the surgery, to check hidden parts of the field.

Important: do not rush in the first part of the operation! The saying "more speed, less haste" is never more true than when performing endoscopic skull base surgery. Transnasal endoscopy requires patient dissection with careful inspection of the nasal cavity, thus avoiding mucosal lacerations and unnecessary bony fractures. In addition, a controlled start gives enough time for the topical decongestant patties to work.

**Fig. 74** The four-hand technique in the face-to-face set-up with unimpeded use of the endoscope and three instruments in both nostrils (A). Side-by-side position with bimanual dissection in a single nostril (B). Published with patient's permission.



Care taken during the first 15 minutes of the procedure is a good investment as it avoids the frustration of the scope becoming coated with blood and reduces the risk of approach-related trauma of the nasal cavity. Note, that prevention of mucosal damage is essential to avoid later crusting and nasal adhesions! Stay back with the endoscope to provide more overview and reduce bloodspatter and secretions on the tip of the endoscope. Use the endoscope irrigation to clean the scope and keep the nasal mucosa moist. Note that crusted blood on the endoscope may lacerate the mucosa: clean the instruments frequently! Instruments should be introduced ahead of the endoscope to avoid blindly scuffing the anterior part of the nasal cavity. The permanent movement of the endoscope increases three-dimensional perception and supports further anatomical orientation on important landmarks.



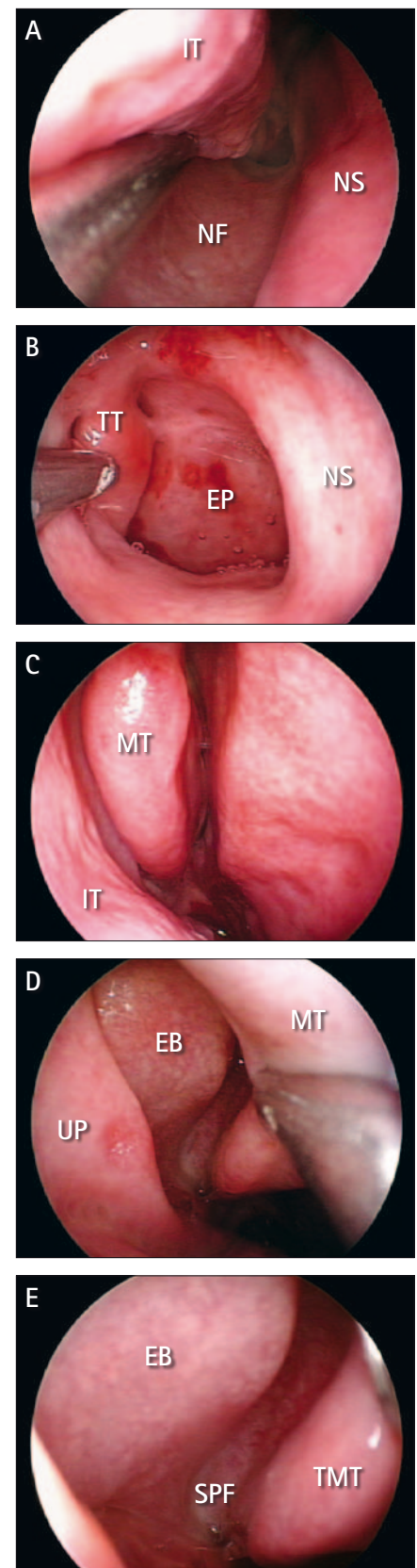
### Nasal part

At first, critical anatomical landmarks of the nasal cavity are identified. The best marker is the inferior turbinate (Fig. 75A). Below the inferior turbinate, along the inferior nasal meatus, the choana is approached checking the epipharynx with the characteristic structures of the Rosenmüller gap, torus tubarius and the Eustachian tube (Fig. 75B). Thereafter, the endoscope is moved upwards and the middle turbinate is visualized (Fig. 75C). After gentle medialization of the middle turbinate, the middle meatus is observed with the characteristic uncinete process and ethmoidal bulla (Fig. 75D). Next, the sphenopalatine foramen is recognized just medially from the tail of the middle turbinate, thus controlling the sphenopalatine artery (Fig. 75E). The middle turbinate is then pushed firmly laterally and the endoscope is introduced along its anterior inferior border, exposing the sphenothmoidal recess (Fig. 76A). Here, the anterior aperture of the sphenoid sinus can be visualized just medially from the superior turbinate (Fig. 76B).

Gentle dissection of the mucosa is of particular importance. Do not grab anything that you cannot see clearly and stop further dissection if visibility is poor! Either work on the other side or replace the vasoconstrictor patties. This effective temporary repacking can also be used to supplement, lateralization of the middle turbinate. Note that destructive fracturing of the turbinate may cause damage to the skull base and risk a subsequent CSF fistula; this should therefore be avoided at all costs. In rare circumstances, if a concha bullosa is present, partial lateral resection of the turbinate with anterior ethmoidectomy may be necessary to gain sufficient space in the nasal cavity. For this reason, surgical equipment should contain adequate nasal cutting and grasping instruments including antrum punches. We strongly advise not removing the middle turbinate routinely as it is not necessary for adequate exposure. With complete resection, postoperative difficulties such as crusting and delayed epistaxis become more prominent. In our opinion, performing middle turbinate resection in all cases casts doubt on the minimally invasive nature of the endoscopic approach as compared to the microscopic technique.

There are two different possibilities for reaching the sphenoid sinus: the medial transnasal and lateral transethmoidal approaches (Fig. 77).

**Fig. 75** Nasal part of the approach (right side). After reducing inflammation of the mucosa, the inferior turbinate and floor of the nasal cavity are exposed (A). Along the inferior meatus, the epipharynx is approached; the torus tubarius is gently lateralized, demonstrating the Rosenmüller gap (B). The endoscope is now retracted into the nasal cavity, showing the head of the middle turbinate (C). After gentle medialization of the turbinate, the middle meatus can be recognized with typical landmarks of the uncinete process and ethmoidal bulla (D). In close up, the sphenopalatine foramen can be localized, just medially from the tail of the middle turbinate (E).



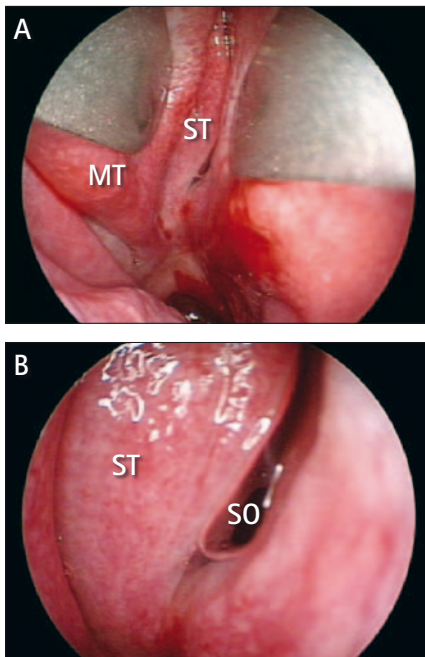


**Fig. 76** Nasal part of the approach (continuation). After controlling the sphenopalatine region, the middle turbinate is lateralized, exposing the sphenoethmoidal recess (A). The sphenoid ostium appears medially from the superior turbinate, approx. 1.5 cm above the choana (B).

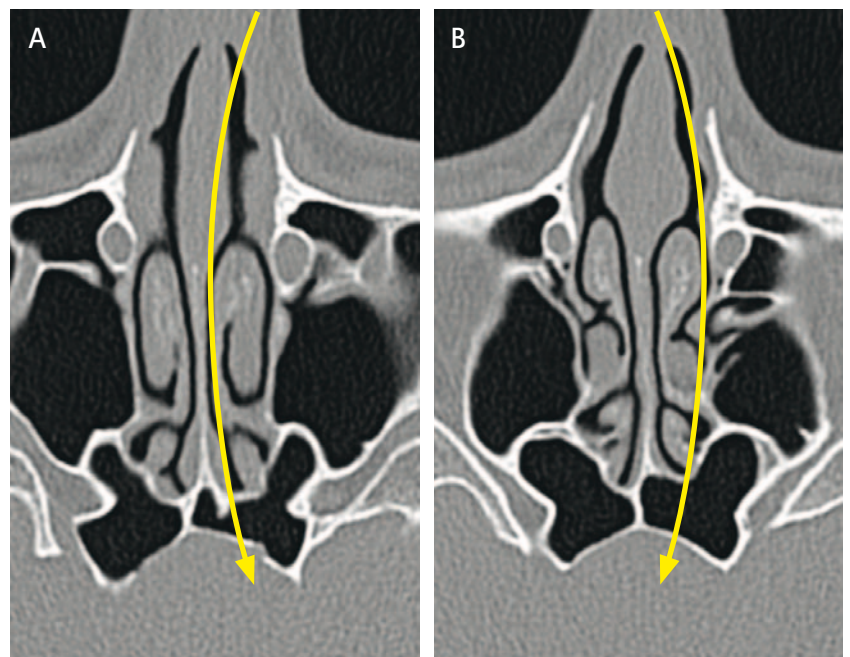


**Fig. 77** CT scans on an axial plane showing the difference between the medial transnasal (A) and lateral transtethmoidal approaches (B).

### Lateral transtethmoidal approach to the sphenoid sinus

We recommend using the transtethmoidal approach for tumors that are located laterally (Fig. 77). The aim of transtethmoidal exposure is to reach the lateral aspect of the sphenoid sinus with direct visualization of the carotid artery and optocarotid recess. Using this technique, the middle turbinate is not lateralized, but medialized, thus observing the middle meatus. Here, the uncinate process and bulla ethmoidalis are recognized. The uncinate process is incised with a curved knife (Fig. 78A), thus exposing the medial aspect of the maxillary sinus. After removing the uncinate process and ethmoid bulla with grasping instruments (Fig. 78B), the posterior ethmoid cells are approached to visualize the posterior ethmoid artery (Fig. 79A). Now, the posterior wall of the maxillary sinus, palatine bone and sphenopalatine junction are recognized (Fig. 79B,C). Here, the mucosa is dissected from the bony surface, controlling the sphenopalatine artery on the anteroinferior wall of the sphenoid sinus (Fig. 79C). The anterior wall of the sphenoid sinus is opened, entering the sinus chamber in its lateral part (Fig. 79D).

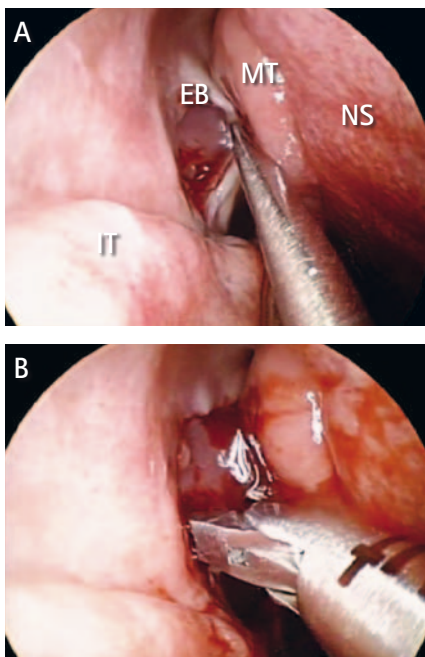


**Fig. 78** Steps of the lateral transtethmoidal approach (right side). Firstly, the middle turbinate is gently medialized, approaching the middle meatus. Here, the uncinate process is incised with a curved knife and removed with grasping instruments (A). With resection of the bulla, the ethmoid cells are opened (B).



Clear advantage of the transethmoidal technique is that the olfactory mucosa remains absolutely intact. If needed, this limited lateral approach can be extended and combined with transnasal exposure, thus creating an extended exposure of the central skull base, which is required for large tumors (Fig. 79D).

### Medial transnasal approach to the sphenoid sinus

By the commonly used medial transnasal technique, the skull base is reached in the midline (Figs. 76, 80). Exposing the sphenoethmoidal recess, the superior turbinate is identified and pushed gently to the side to expose the sphenoid aperture (Fig. 76A,B). Ensure that the mucosa in the sphenoethmoidal region remains intact, thus avoiding postoperative olfactory loss! Frequently, the ostium is covered by mucosa but it can be palpated easily with an instrument such as the suction tube. Note that in some cases a small air bubble indicates the sphenoid opening, always medial from the superior turbinate, approx. 1.5 cm above the choana. Medial and basal from the aperture, the mucosa must be coagulated to prevent bleeding from the septal artery. This coagulation must be restricted inferiorly and medially from the aperture to prevent postoperative anosmia (Fig. 80A). Note that considerable space can be gained within the sphenoethmoid recess using vasoconstrictor patties and coagulation. Thereafter, the anterior wall of the sphenoid sinus is opened with a diamond drill (Fig. 80B); for this part, a fine chisel or Kerrison punches can also be used. The endoscope is now introduced into the sphenoid sinus, allowing early recognition of vital structures of the central skull base. Care should be taken to avoid extensive coagulation and damage to the superior turbinate and upper sphenoethmoidal recess as this leads to postoperative anosmia! Thereafter, a wide anterior sphenoetomy is performed by removing the junction of the sphenoid rostrum and posterior nasal septum. At this point, the left naris is accessed and the approach is completed on the contralateral side in a similar manner. A critical stage of the nasal approach is the resection of the posterior 0.5 cm of the nasal septum. A reverse cutting antrum punch can be used effectively for this (Fig. 80C). This creates a bilateral cavity, allowing visually controlled free maneuverability of instruments in the deep surgical field without a nasal speculum. The endoscope is now introduced in the sphenoid sinus, achieving a panoramic view on the central skull base including the optic nerves, carotid arteries, sellar floor and the clivus (Fig. 80D).

### Sphenoid part

After reaching the sphenoid sinus through the medial transnasal or lateral transethmodal approach, anatomical landmarks of the central skull base can now be identified. The appearance of the main structures depends on the pneumatization of the sphenoid bones; however, in most cases, the sellar floor, clivus, sphenoid planum, optic nerves, carotid arteries, the lat-

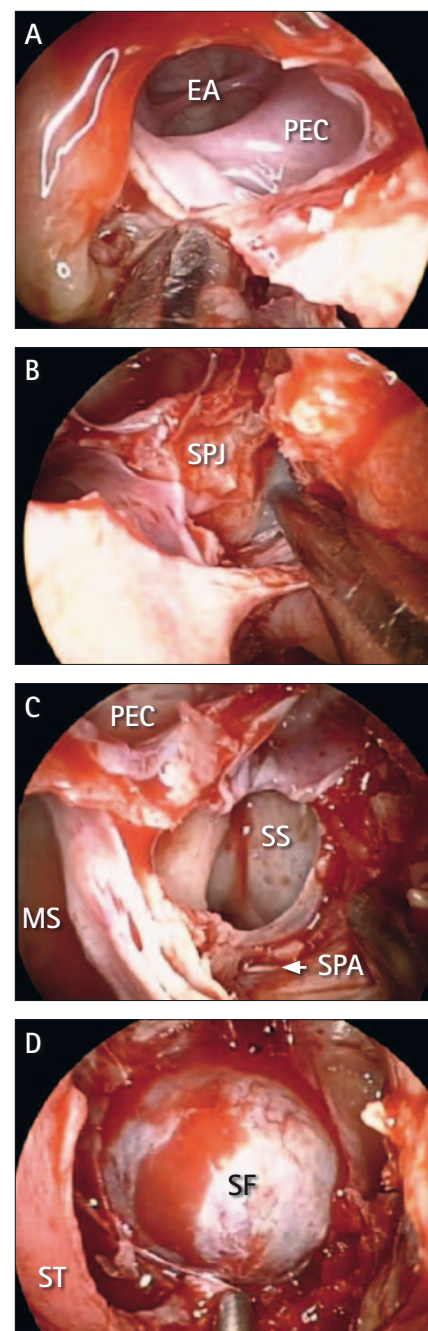


**Fig. 79** Steps of the lateral transethmoidal approach (continuation). After partial ethmoidectomy, the posterior ethmoid cells are visualized (A). Inferiorly, the sphenopalatine junction is approached (B). After removal of the important triangle- formed bony landmark, we can see into the lateral sphenoid sinus. Note its relation to the maxillary sinus and posterior ethmoid cells (C). With stepwise removal of the anterior wall of the sphenoid sinus, the central skull base can be fully visualized (D).

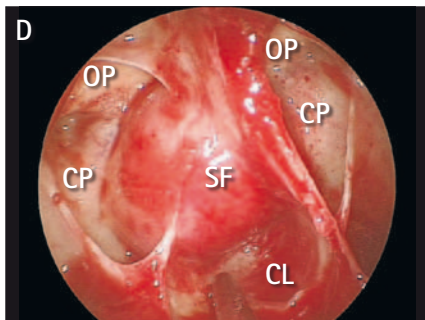
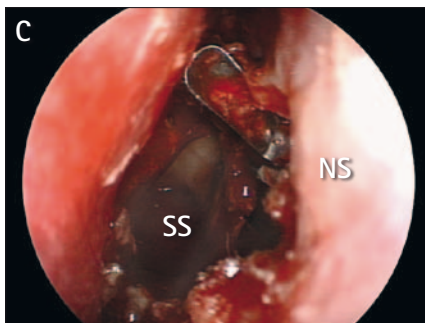
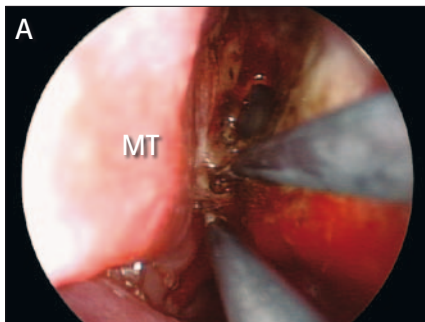


**Fig. 80** Steps of the medial transnasal approach (right side). After lateralization of the middle and superior turbinates, the sphenoid ostium appears. Inferiorly of the ostium, the mucosa is carefully coagulated, thus avoiding bleeding of the sphenopalatine artery (A). Thereafter, the ostium is enlarged with a diamond drill (B). A critical stage is the resection of the posterior 0.5 cm of the nasal septum; a reverse cutting punch can be used effectively for this (C). After anterior sphenoidotomy and posterior septectomy, the endoscope is introduced into the sphenoid sinus. Note the optic nerve and carotid prominence on both sides and the clivus. In the central field of interest, the sphenoid floor appears (D).

eral and medial optocarotid spaces can be seen allowing a perfect anatomically based point of reference (Fig. 80 D). The sphenoid septum can be removed with a diamond drill or grasping instruments should it be present and pose hindrance (Fig. 81 A). The sphenoid mucosa is separated in the central field of action; if the sinus is to be packed with an abdominal fat graft, the mucosa should be removed completely. Under secure visual control, the sellar floor is opened with a diamond drill and the opening enlarged with fine Kerrison punches. If a thin sellar floor is present, we recommend an "open door" aperture of the sella, thus making later reconstruction simple (Fig. 81 B). With the nasal cavity the biportal access, introduction and removal of instruments can be performed without hindrance and without the need for a nasal speculum. Anatomical orientation may be limited due to the shape of the conchal sella, significant intra- and parasellar tumor extension and, especially, as a result of re-do surgeries. These cases are a particular surgical challenge and careful study of pre-operative CT and MRI images should already point out eventual difficulties and the use of intraoperative neuronavigation is mandatory. After opening the sellar floor, the dura is opened with fine scissors or a microknife and the intrasellar lesion is removed with different curettes (Fig. 81 C).

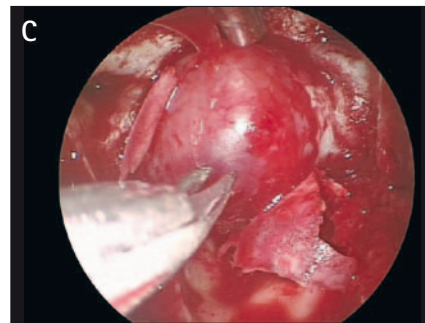
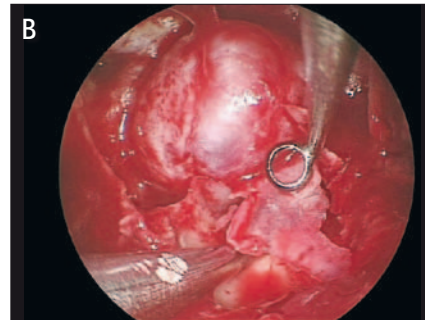
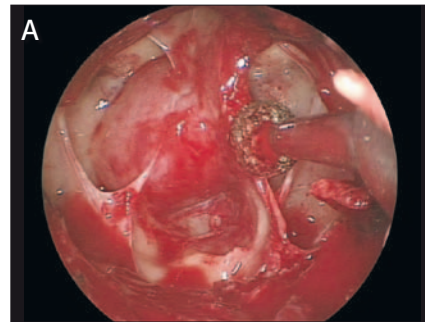


**Fig. 81** Sphenoid part of the approach. In a secure visual control, sphenoid septations are removed with a diamond drill and grasping instruments (A). The sellar floor is opened; in this case we used the "open door" technique, fracturing the thin bony sellar floor (B). After wide exposure, the sellar dura is incised with fine microscissors (C).



### Sellar part

Tumor removal is visually well controlled (Fig. 82). Principally, tumor resection should be started in the basal-clival part, then bilaterally (Fig. 82A). Using angled scopes, hidden parts of the surgical field can be detected, allowing safe resection. After partial resection of the tumor, the central and suprasellar tumor tissue should be removed, avoiding opening of the diaphragma sellae (Fig. 82B). If possible, the tumor capsule should be recognized anteriorly and followed carefully backwards without opening the diaphragma sellae (Fig. 82C). Injury of the pituitary gland can be avoided with the use of small patties. After removal of the main tumour, hidden parts can be visualized with an angled endoscope, thus controlling complete resection (Fig. 82D). If localized bleeding occurs, we use well directed bipolar coagulation with a pivot-point coagulator. In case of diffuse venous bleeding one can apply hemostatic matrix (FloSeal®), absorbable cellulose hemostatic material (Surgicel® fibrillar) or small pieces of hemocollagen sponge (Spongostan®). However, in the uneventful resection of an intrasellar tumor, we do not use intrasellar or intrasphenoidal synthetic substances and avoid packing with fat tissue. Instead, we use bone fragments for easy reconstruction of the sellar floor.

### Para- and suprasellar part

The main advantage of the pure endoscopic technique is the direct visual investigation of hidden parts of the surgical field. Compared to blind tactile control with a microscope, the endoscopic surgeon is able to see patho-anatomical details which are always hidden for microsurgical resection. The 0° endoscope is used for most of the procedure; when the anatomy is not completely visualized and hidden parts of the field need to be adequately viewed, the 30° endoscope can be used. By introducing the angled endoscope into the depth, suprasellar and intracavernous structures can be directly visualized and tumor remnants attacked (Fig. 83). In complicated cases, intraoperative imaging may increase control of tumor removal.

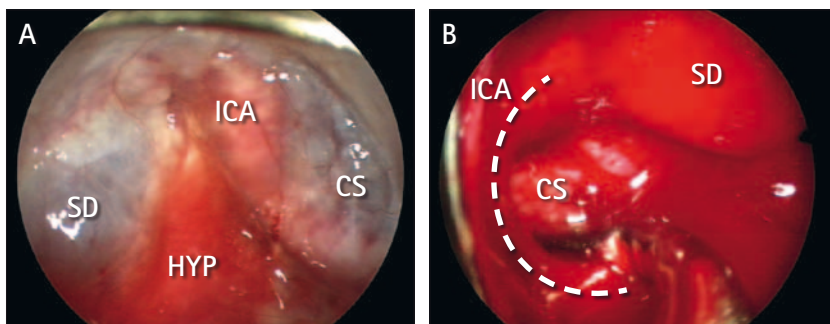


**Fig. 83** Two different cases, demonstrating the advantages of the endoscopic technique. In case A, a cystic lesion was operated. Note the sellar diaphragm, left carotid artery and medial wall of the cavernous sinus. Case B demonstrates removal of a GH-producing adenoma. Behind the well controlled anterior knee of the right carotid artery (dotted line), the final remnants of the tumor are removed.

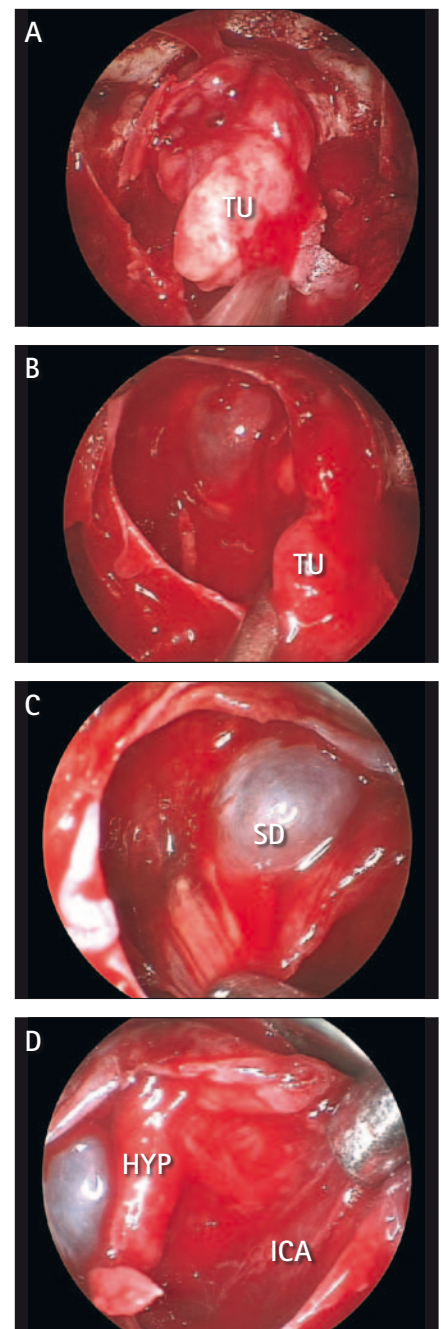


**Fig. 82** Sellar part of the approach. The tumor removal is started in the basal clival part (A). Before complete sinking of the diaphragma, bilateral intracavernous remnants should be removed under direct visual control (B). If possible, the tumor capsule should be recognized anteriorly and followed in a posterior direction (C). At the very least, laterally located parts should be checked with a 30° angled endoscope. In this case, the sellar diaphragm, pituitary gland and left internal carotid can be seen (D).

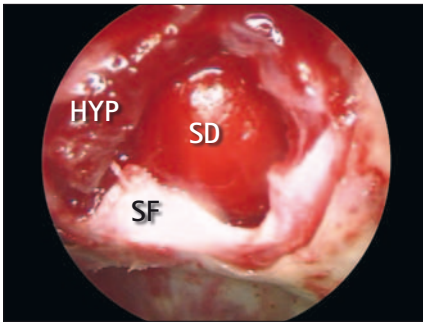


**Fig. 84** After uneventful surgery, special sellar reconstruction is not necessary.

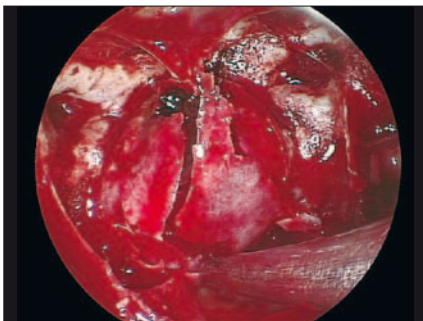


**Fig. 85** When operating on large tumors, the sellar floor should be closed thoroughly.

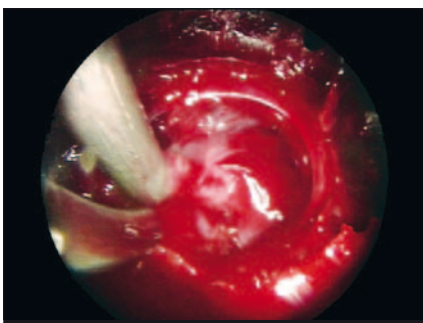


**Fig. 86** If minor CSF leakage occurs during surgery, we close the leak with Tachocomb® and pack the resection cavity with Spongostan®.

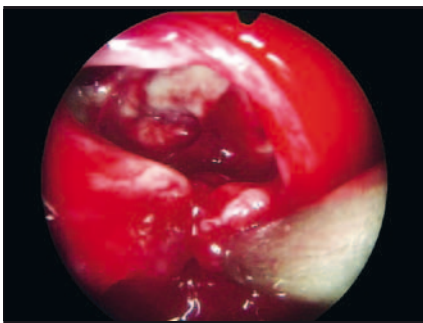


**Fig. 87** In the event of marked CSF loss, we use abdominal fat graft.

### Sellar reconstruction and closure

In uneventful surgery and if no diaphragmal opening has occurred, special sellar reconstruction is not necessary and is therefore not recommended (Fig. 84). In cases of large or giant pituitary adenomas, we repair the sellar floor with Spongostan® or bony fragments to avoid intrasphenoidal herniation of the diaphragm with potential risk of cisternal rupture and later CSF fistula (Fig. 85). If CSF leakage occurs during surgery, different closure and reconstruction techniques can be applied. In the event of minor CSF leakage, we recommend defect covering with Tachocomb® and simple packaging of the resection cavity with Spongostan® (Fig. 86). In the event of a marked diaphragmal defect and high CSF loss, we supplement the carefully placed Tachocomb® sheet with an abdominal-periumbilical fat graft soaked in fibrin glue (Fig. 87). The graft is placed into the sella, the sellar floor is ideally closed with bony fragments avoiding migration of the graft. For this purpose, a tailored, bioabsorbent material can also be used. We never push big fat grafts blindly into the sella and usually do not fill the sphenoid sinus with fat tissue.

A particular surgical challenge is, however, to close a wide dural gap especially after extended approaches for removal of large skull base tumors or intradural lesions (Fig. 88A). In such cases, careful sheet-by-sheet closure is mandatory. In our practice, the first sheet is an "inlay" fascia layer, grafted from the abdominal fascia, covering the leak site intradurally (Fig. 88B). We suggest a 5-10 mm intracranial covering of the defect; if necessary and if technically possible, the inlay may be fixed with 6-10 sutures in situ. Thereafter, a second "onlay" fascia sheet is applied (Fig. 88C). In the ideal situation, this second fascia sheet lies between the dura and the bony skull base (Fig. 108). After application of fibrin glue, fat tissue is applied as a second "onlay" graft into the sphenoid sinus to cover and replace the dural defect. We do not recommend the use of a single large fat graft but rather multiple small pieces for precise covering. If fat tissue is used within the sphenoid sinus, the sphenoid mucosa should first be completely removed. Next, a previously prepared vascularized septomucosal flap is rotated into the sinus covering the skull base (Fig. 88D). This flap is harvested during the exposure and tucked into the nasopharynx during the procedure. Following resection, the flap is positioned to cover the defect, overlapping the margins to allow contact with the bone. The preserved vascularity of the flap, supplied by a septal branch of the sphenopalatine artery, is extremely important to promote faster healing and swifter, more resistant sealing. A fat graft is not appropriate or effective on the nasal side of the flap – here Spongostan® is used and the nasal cavity is packed. Experienced teams have described the use of a complex temporoparietal fascial flap for skull base reconstruction. However, in these cases the reason for such an extensive approach-related trauma should be considered critically.



After leaving the sphenoid sinus, both nasal cavities are inspected and cleansed of clotted blood and secretions. The middle turbinates are re-medialized. We emphasize a careful "overmedialization" to prevent closure of the semilunar hiatus and subsequent chronic inflammation of the maxillary sinus. With the endonasal biportal technique without transseptal dissection, a nasal tamponade is not necessary, thus limiting breathing problems and discomfort after surgery. We only use temporary packing for 48 hours if a septonasal flap was used for an extended approach, thus stabilizing the skull base reconstruction. We never use a Foley catheter balloon for minimizing graft migration, as has been described by other groups.

Opinions vary, even among experienced practitioners, as to the necessity of lumbar drainage in the case of intraoperative CSF leakage or postoperative fistula. In the course of our early learning curve we used lumbar drainage in cases of postoperative CSF fistula; however, we now no longer use a lumbar drain on account of the potential risk of meningitis and severe pneumocephalus. Rather, we suggest re-do surgery if the fistula is persistent postoperatively and no spontaneous closure develops. Here, re-evaluation of the intraoperative videotape can be very helpful in identifying the surgical failure.

### Postoperative care

In the case of uneventful surgery, postoperative intensive care is not necessary; our patients are observed for 6 hours in the intermediate care unit. After intraoperative single-dose antibiotics, postoperative antibiotic agents are not used routinely. Perioperative hydrocortisone substitution is used in most pituitary operations; other hormonal treatment depends on the individual case.

Careful interdisciplinary treatment is essential after the operation (Tab. III). On the first daypost op, an early MRI is performed, checking for tumor resection. On the same day, the otorhinolaryngologist examines the patient. The nasal cavity is observed endoscopically with careful removal of secretion and deflation of the mucosa. The key task is to irrigate stagnant mucus and altered blood and stop it from collecting on the lining of the paranasal sinuses until ciliary function has returned. Saline nasal sprays and crème are used to prevent drying out of the nasal cavity; ideally, the patients are supervised in a douching technique of the nose before they are discharged. This ensures that patients are able to breathe through the nose, even in the early postoperative course, with significantly increased comfort. Patients are also carefully supervised by the clinical endocrinologist with daily testing of electrolyte balance and osmolality (Tab. IV). In the early postoperative course, diabetes insipidus-induced serum hypernatremia and hyper-osmolality, in the later course SIADH-induced serum hyponatremia and hypo-osmolality must be excluded. Basal hormone investigation is

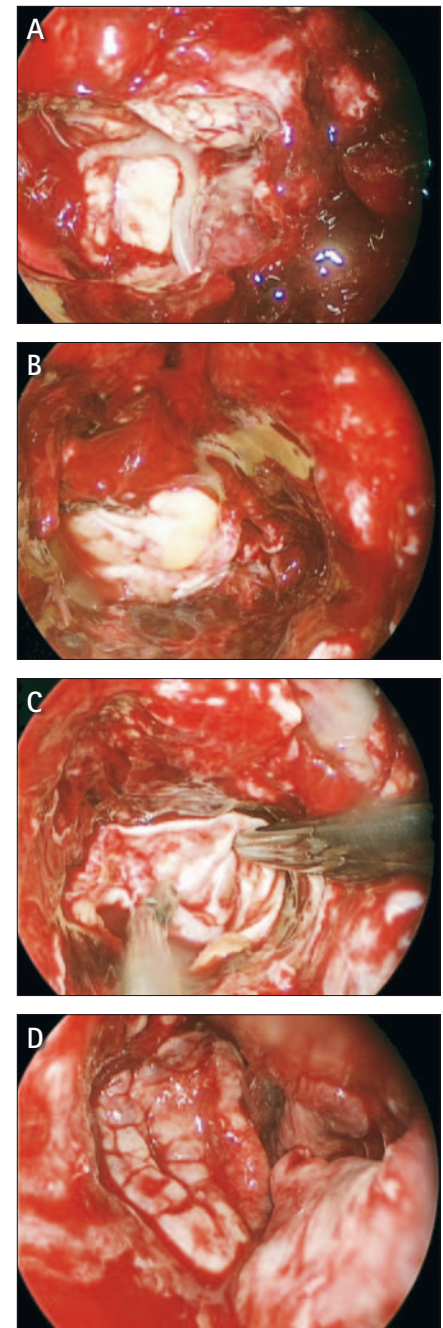


**Fig. 88** Large clival defect after removal of a skull base chordoma. Note the brain stem and basilar artery in the background (A). As a first layer of reconstruction, an inlay of fascia lata is used (B). Therefore, an onlay fascia sheet (C) and small pieces of fat tissue are applied. The previously dissected septomucosal flap is then positioned to cover the defect, overlapping the margins with contact to normal tissue.

**Table III. Interdisciplinary perioperative care of patients at Hirslanden Hospital, Zurich**

Preoperative	Day of surgery	1st POD	2nd – 3rd POD	7th POD	6th POW	3rd POM
NS, RA, RS, EC, OP	6 hours IMCU	NS, RS, RA	NS	NS, RS, EC	EC	NS, RA, RS, EC, OP

EC: endocrinology; IMCU: intermediate care unit; NS: neurosurgery; OP: ophthalmology;  
 POD: postoperative day; POM: postoperative month; POW: postoperative week; RA: radiology; RS: rhinosurgery;

**Table IV. Algorithm for endocrine clinical observation, laboratory check-ups and routine medication in pituitary surgery at Hirslanden Hospital, Zurich**

<b>Preoperative</b>	<b>L:</b>	Endocrine screening incl. baseline and functional tests Serum Na, K, Osm, Crea, BC, coagulation, GPT, GOT; Urine Na, Osm
<b>Perioperative</b>	<b>O:</b>	6 h IMCU, intake/output documentation
	<b>L:</b>	Serum Na, K, Osm, Crea, BC; Urine Na, Osm, SG
	<b>M:</b>	HC 50-100 mg i.v. during surgery, 100 mg i.v./24h postoperatively
<b>1st POD</b>	<b>O:</b>	clinical observation every 4h, intake - output documentation, weight control
	<b>L:</b>	Serum Na, K, Osm, Crea, BC; Urine Na, Osm, SG
	<b>M:</b>	HC 50 -100 mg i.v./24h
<b>2nd – 3rd POD</b>	<b>O:</b>	clinical observation 3/day, intake - output documentation, weight control
	<b>L:</b>	Serum Na, K, Osm, Crea, BC; Urine Na, Osm, SG
	<b>M:</b>	HC 10-25 mg p.o./24h
<b>3rd POD</b>	<b>routine discharge</b>	
<b>7th POD</b>	<b>L:</b>	baseline endocrine test; Serum Na, K, Osm, Crea, BC; Urine Na, Osm, SG
<b>6th POW</b>	<b>L:</b>	baseline and functional endocrine test; Serum Na, K, Osm, Crea, BC; Urine Na, Osm, SG

Abbr.: BC: blood count; Crea: Creatinine; HC: hydrocortisone; L: laboratory test; O: observation; Osm: osmolality; M: routine medication;  
 POD: postoperative day; POW: postoperative week; SG: specific gravity

performed on the 7th day and 6 weeks after surgery to verify the possible need for hormone substitution. Further monitoring with functional investigation of the pituitary gland and hormone treatment depends on the individual case.

Three months after surgery, outpatient checkups are performed, including radiological, rhinological, endocrinological, ophthalmological and surgical examinations.

## Illustrative Cases

### CASE I

#### Hormonally inactive macroadenoma

#### Approach: Combined biportal transnasal–transtethmoidal

#### Background

This 41-year-old male patient suffered from general lethargy and visual disturbances for over a year. A general physical and ophthalmological examination could not explain the cause of his discomfort. Urological exploration following fertility concerns was also without pathological findings. After a long and frustrating history, his hormonal status was investigated thoroughly and revealed a partial pituitary malfunction without hormonal excess. A subsequent MRI scan revealed a large pituitary adenoma with marked compression of the optic chiasm (Fig. 90). On the right side, the tumor ruptured the diaphragma sellae with displacement of the hypothalamus and medial basal ganglia. A revised ophthalmological examination showed severe visual field deficits (Fig. 89). Urgent treatment was indicated; surgery was performed with otorhinological assistance, an intraoperative CT was used for monitoring tumor removal.

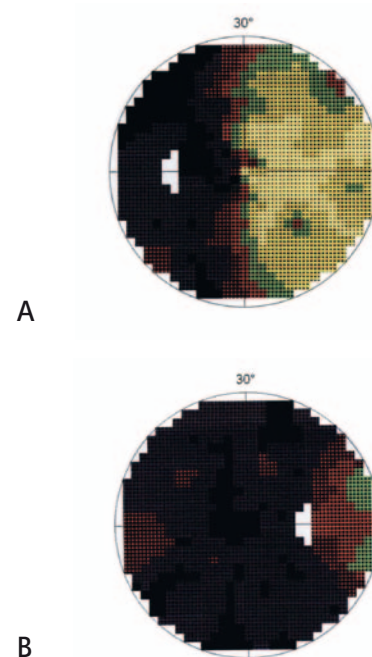
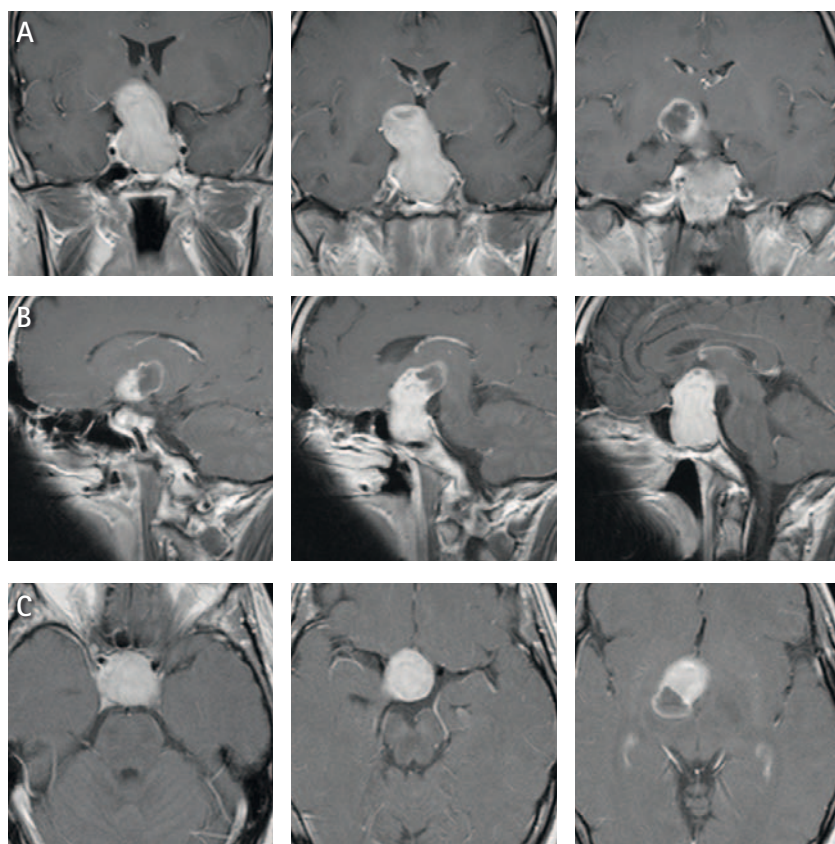


**Fig. 89** Preoperative visual field investigation showing severe deficit on the left side (A) and functional blindness on the right side (B). Courtesy of Dr. Luc Moudon and Dr. Serge Hédiguer, Lausanne.

**Fig. 90** T1 MRI scans on the coronar (A), sagittal (B) and axial (C) plane demonstrating a large pituitary adenoma. On the right side, the tumor ruptured the diaphragma sellae with displacement of the hypothalamus and medial basal ganglia.



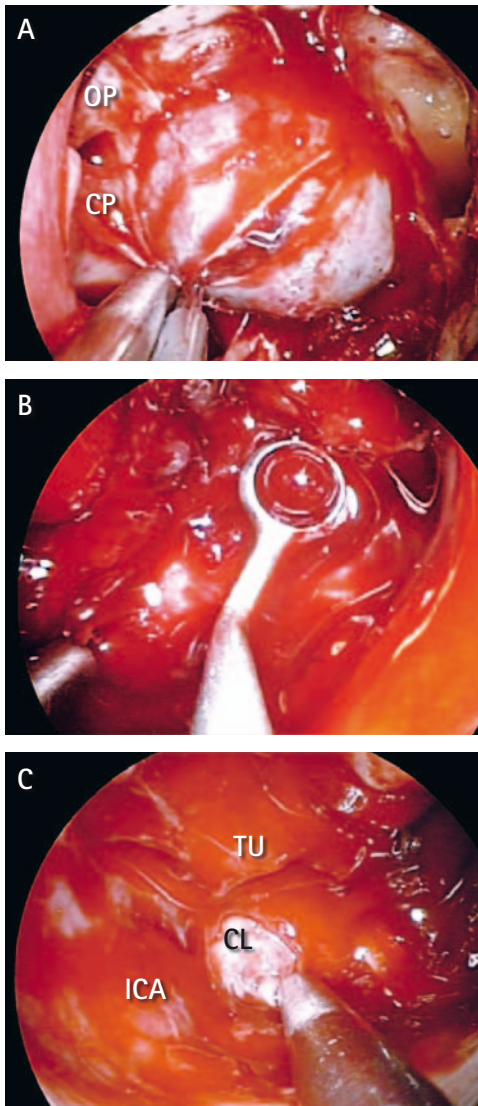


**Fig. 92** After performing a combined biportal trans-ethmoidal – transnasal approach, the bony sellar floor was carefully removed and the dura opened with a fine microknife. Note ideal visual control with bright exploration of the central skull base (A). The basal and lateral parts of the tumor were first removed, exploring the clivus and bilateral cavernous sinus (B). The medial wall of the right cavernous sinus and the pulsating ICA could be directly visualized (C). After basal tumor removal, the suprasellar part was mobilized. The diaphragm showed no spontaneous sinking; therefore iCT was performed at this stage of the operation.

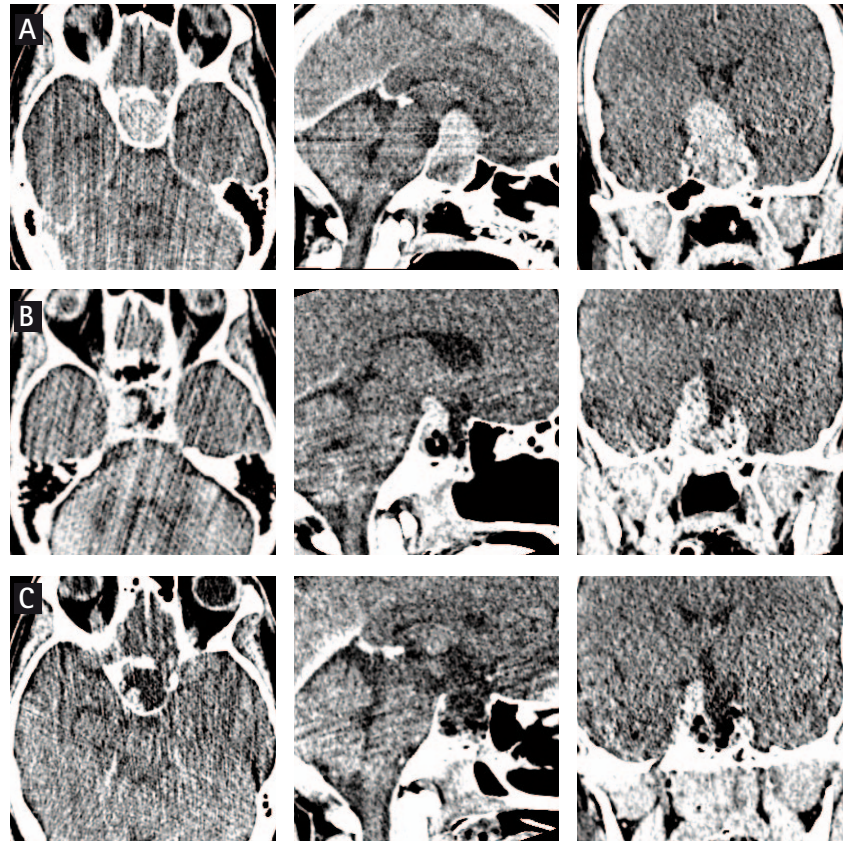


**Fig. 91** Intraoperative CT scan demonstrating tumor extension (A). After removal of the main part of the adenoma, an intraoperative CT scan was performed, showing tumor remnants in the left cavernous sinus and right suprasellar (B). After further dissection, only a tiny remnant is evident on the CT (C).

## Surgery

After positioning, a CT scan was performed showing the exact tumor location (Fig. 91 A). The sphenoid sinus was reached using a biportal technique, performing a combined transethmoidal-transnasal approach with wide exposure of the sphenoid sinus. The thin sellar floor was removed with Kerrison punches and the dura incised. The basal and lateral parts of the tumor were first removed, exploring the clivus and cavernous sinus on both sides. From the outset it was possible to visualize the carotid artery directly on the right side. After removal of the main part of the adenoma, an intra-operative CT scan was performed (Fig. 91 B). Here, successful decompression of the optic structures could be seen; however, tumor remnants were detected in the left cavernous sinus and right suprasellar. The intracavernous tumor was easy to remove; however, on the right side, in a fold of the diaphragm, a tiny remnant had to be left to avoid high-risk manipulation (Figs. 92, 93).



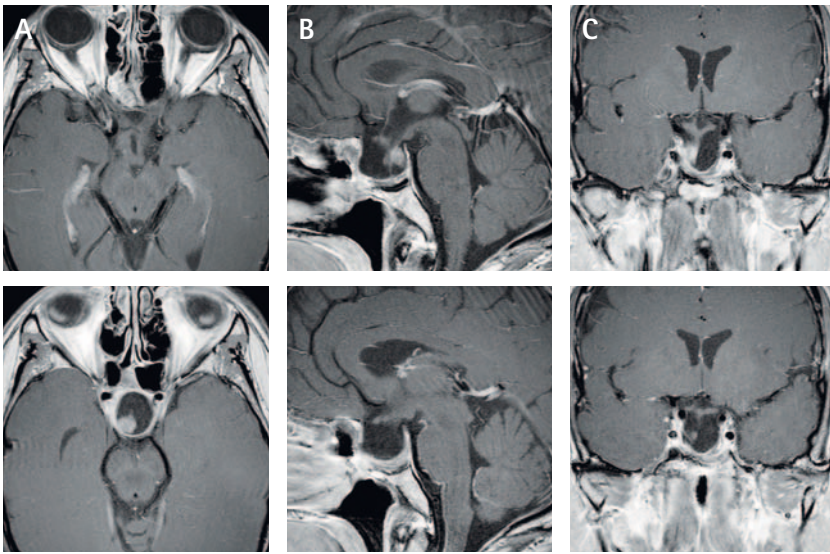


**Fig. 94** MRI scans showing an axial (A), sagittal (B) and coronar (C) view three months postoperatively, demonstrating acceptable resection with minimal residuum. Note the decompressed optic chiasm, stalk and the pituitary gland right intrasellar.

### Postoperative course

The patient made a proper recovery with marked visual improvement (Fig. 95). His hormonal dysfunction was treated medically. Three months after surgery, an MRI scan showed minimal tumor remnants with complete optic decompression (Fig. 94). At the present date, one year after surgery, "wait and see" management is recommended due to the unchanged tumor size in MRI controls and improvement both in visual and pituitary function with only gonadotrophin malfunction.

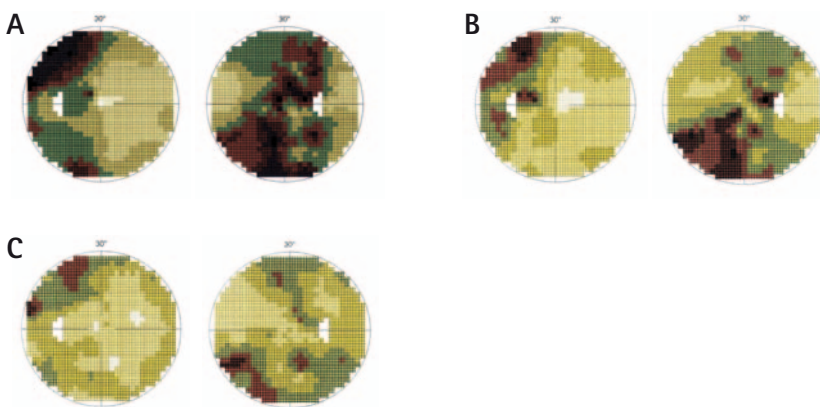


**Fig. 95** Visual field investigations 3 weeks (A), 3 months (B) and 9 months (C) after operation with marked visual improvement according to the effective optic decompression.

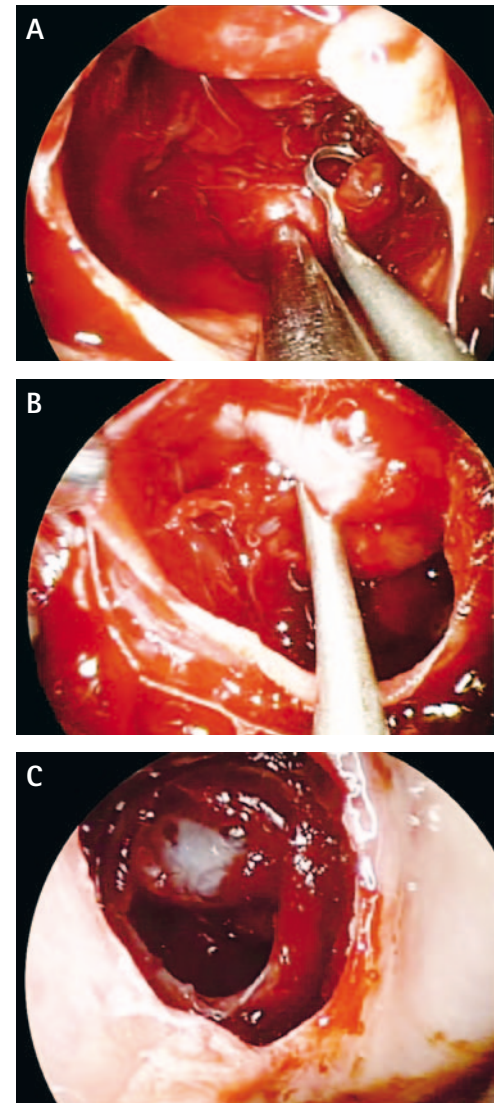


**Fig. 93** iCT revealed a tumor remnant in the left cavernous sinus and right suprasellar, therefore surgery was continued (Fig. 91B). The intracavernous part could be easily eradicated (A). However, on the right side, in a wrinkle of the diaphragm, a small remnant could not be removed, avoiding high-risk manipulation (B). Repeated CT excluded intracranial complication with effective suprasellar decompression and acceptable tumor remnant (Fig. 91C), therefore surgery was finished. Note the undamaged mucosa in the sphenoethmoidal recess and the intact diaphragm in the background (C). In this case the sellar floor was reconstructed with Tachosil® and Spongostan®, without using an abdominal fat graft.

## CASE II

### Intrasellar GH macroadenoma

#### Approach: Left-sided uninostril transthemoidal

#### Background

This 34-year-old female patient suffered from diffuse joint pain and listlessness. On diagnostic assessment, acromegalic stigmata were conspicuous. Endocrinological investigation confirmed the diagnosis with elevated GH and IGF-I level with paradox response to an oral glucose tolerance test (OGTT). Functional testing showed normal corticotrophin function but insufficiency of the gonadotrophin and thyreotrophin axis. Cardiological investigation excluded a cardiomegaly by normal action of the heart.

MRI of the brain showed a left intrasellar macroadenoma with displacement of the pituitary gland to posterior and right lateral without invasion of the cavernous sinus (Fig. 96). On account of the increasing symptoms and MRI scan, indication for surgery was given.

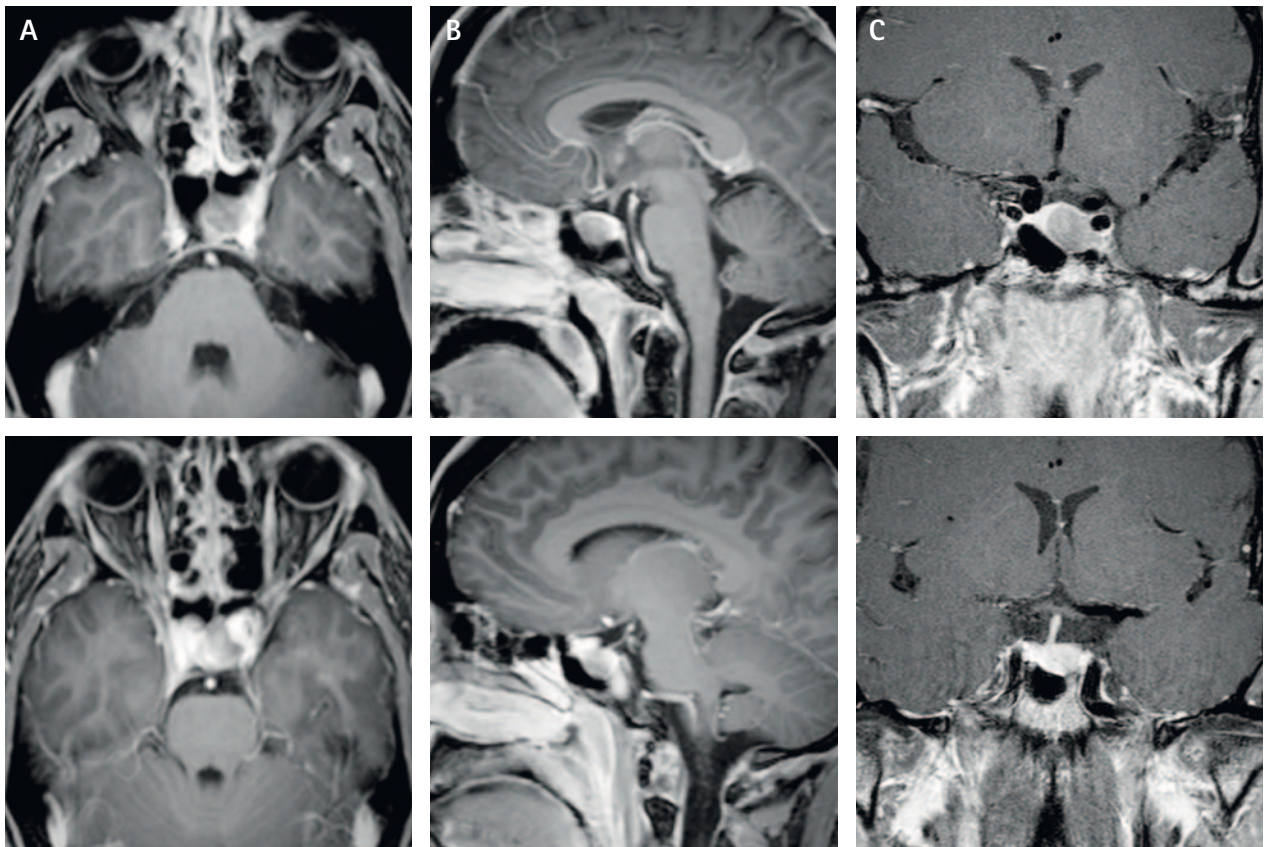


**Fig. 96** Contrast enhanced T1w MRI on the axial (A), sagittal (B) and coronar (C) plane showing a left intrasellar macroadenoma with compression of the pituitary gland and displacement of the stalk. The medial wall of the cavernous sinus is compressed; however, no cavernous invasion can be seen in the coronar view.



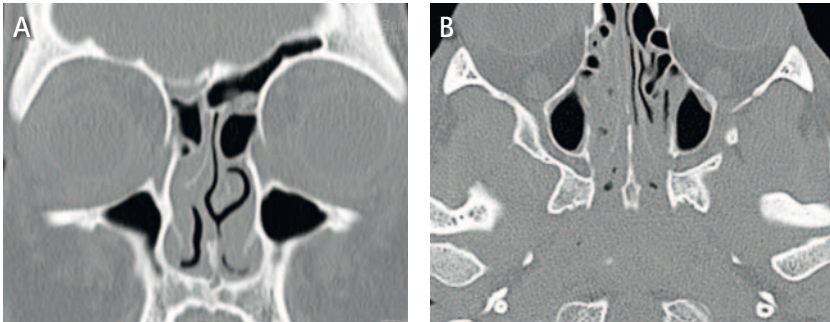


**Fig. 97** Bone CT scans in coronar (A) and axial (B) view showing severe mucosal inflammation, thus making elective transnasal surgery impossible. Note the septal deviation.

Preoperative CT showed a slight septal deviation to the right and a severe inflammation of the mucosa when suffering with a bad cold (Fig. 97). In this situation surgery was cancelled. Nevertheless, after strong antibiotics and local nasal steroids, the patient's condition improved and the elective surgery could be performed in a neuro-rhinological cooperation.

### Surgery

Due to the septal deviation, endoscopic inspection of the nose revealed asymmetric nasal cavities. Therefore, we performed a unilateral transthemoidal approach to the sphenoid sinus, thus achieving sufficient exposure of the central skull base. The sellar floor was opened with a diamond drill, the tumor was immediately visible. The tumor capsule was then recognized in the anterior sella and followed backwards with gentle dissection. The pituitary gland could be clearly identified and protected using cottonoid patties. The tumor could be removed in toto without CSF leakage or injury to the hypophysis (Fig. 98).

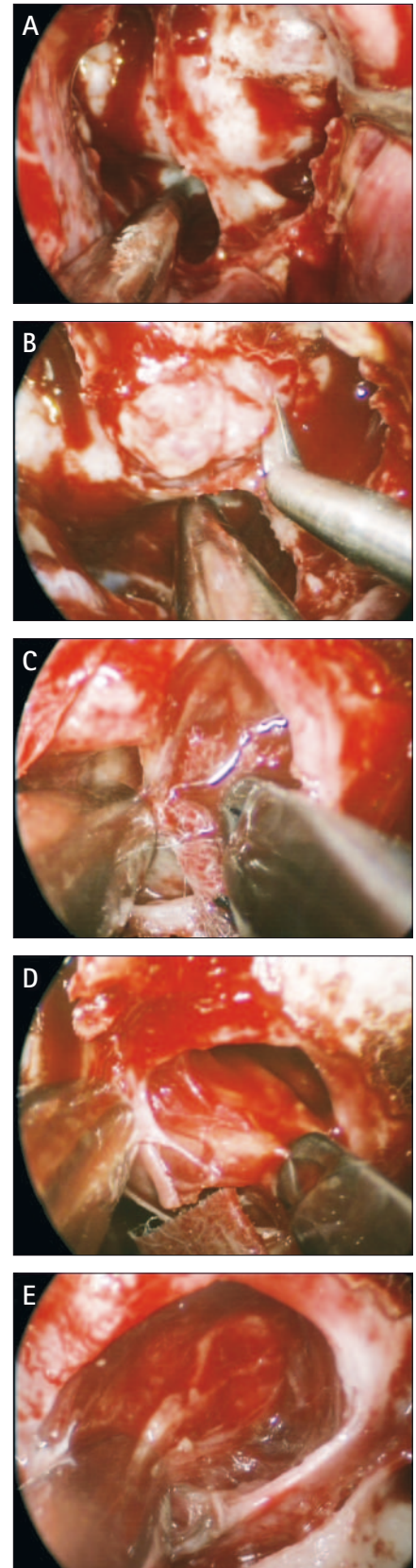


**Fig. 98** After conservative treatment with antibiotics and nasal steroids, transnasal surgery was uneventful. Due to the septal deviation, the left nasal cavity offered more space for dissection. Therefore, the central skull base was approached via a unilateral transthemoidal approach (A). The sellar floor was opened and the whitish tumor tissue mobilized (B). The tumor capsule could be defined using sensitive patties (C), thus allowing complete capsular resection (D). At the end of surgery, the medial wall of the left cavernous sinus was visualized with 30° endoscope (E). Note the reddish tissue of the pituitary gland; in this case, no special reconstruction was performed.

### Postoperative course

The patient made an uneventful recovery. Six weeks after surgery, hormonal investigation showed no residual activity with normal response in OGTT and unchanged pituitary function. Nasal airflow improved as a result of the normal GH-level and atraumatic surgical technique. No visual disturbances occurred. Three months later, MRI revealed complete tumor resection with cosmetic improvement to the patient (Fig. 99).

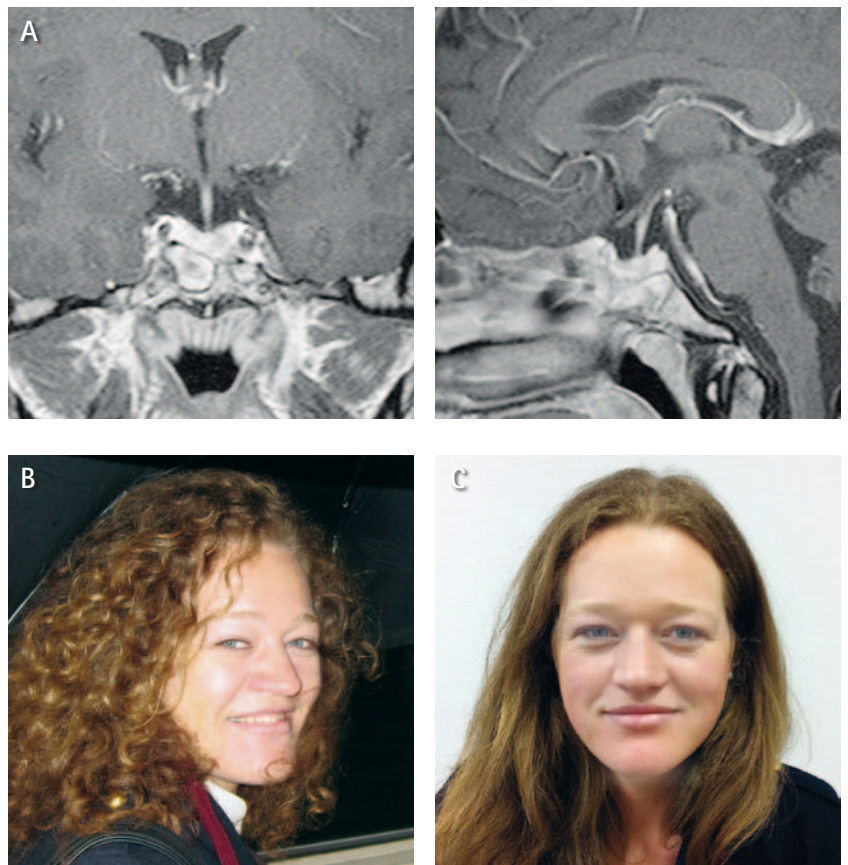


**Fig. 99** MRI three months after surgery without evidence of residual tumor (A). Note the patient's photograph before (B) and three months after successful treatment (C), published with patient's permission.

### CASE III

#### Recurrent ACTH microadenoma

#### Approach: Binostril transnasal

##### Background

This 51-year-old female suffered from Cushing disease caused by an ACTH-producing microadenoma (Fig. 101). Initial surgery was performed in an external hospital using the traditional microsurgical technique. Postoperative hormonal assessment revealed unchanged ACTH secretion; there was no other hormonal or visual deficit. An MRI scan showed a residual intrasellar tumor, located posteriorly and on the right side (Fig. 100). Due to a partial conchal sella type and previously performed operation, re-do surgery was planned with the intraoperative use of neuronavigation (Fig. 102).

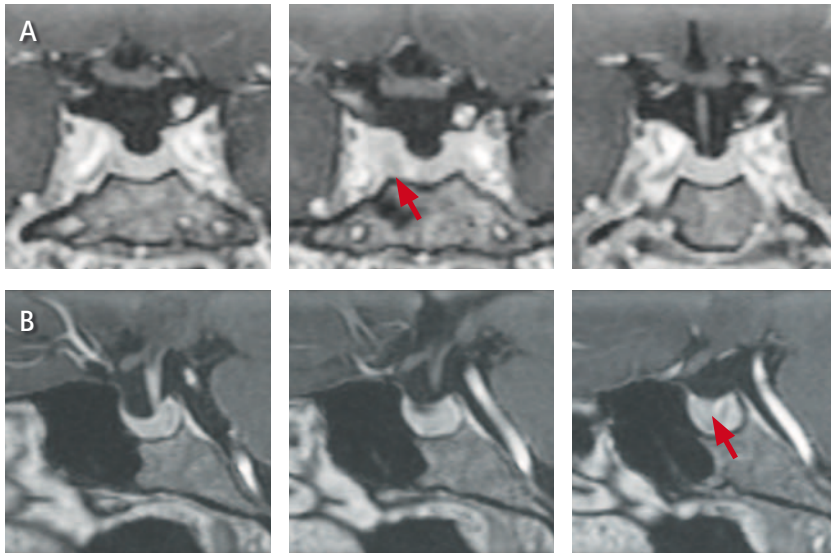


**Fig. 100** T1w MRI after gadolinium in coronar (A) and sagittal (B) view with assumed residual tumor right intrasellar (arrow).



**Fig. 101** Patient's photograph with signs of Cushing disease. Published with patient's permission.

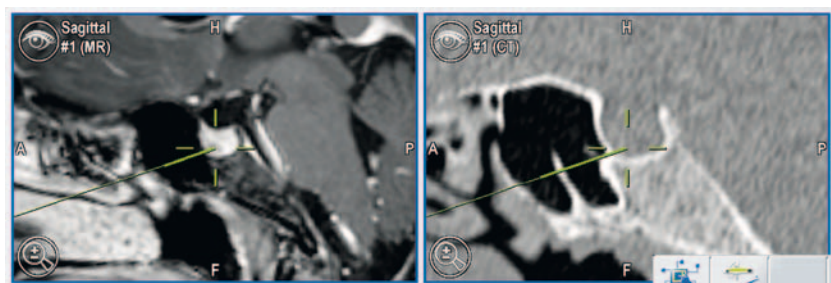
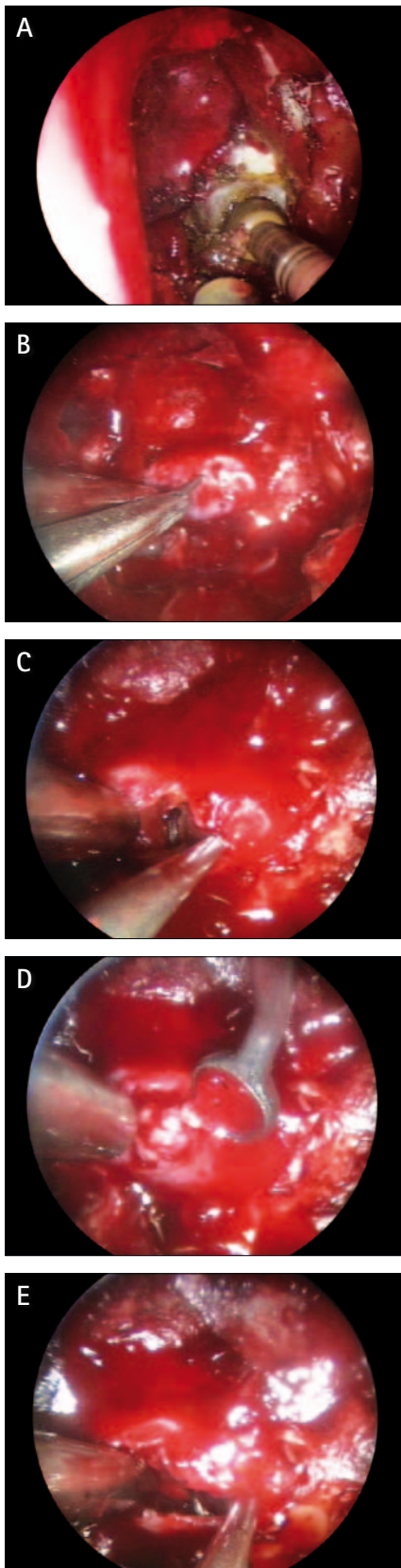


**Fig. 102** The use of neuronavigation was obligatory in this case. Note the exact localization of the right intrasellar residual tumor.





### Surgery

A marked septal perforation could be seen, which resulted from the previous surgery. The anterior wall of the sphenoid sinus was opened on the right side; the left sphenoethmoidal recess was not destroyed, allowing anatomical orientation in the nasal cavity. The sphenoid sinus, however, showed marked adhesions and scarring of the sellar floor, which complicated the endoscopic orientation. After completion of the binostril approach, the scarred floor of the sella was re-opened with a diamond drill using a navigation-guided technique. Neuronavigation was essential for a precisely targeted approach. After sufficient opening, the pituitary gland was reached and the tumor tissue identified on the right side. A small remnant behind the gland could also be removed successfully (Fig. 103).

**Fig. 103** Despite perfect endoscopic visualization of the central skull base, anatomical orientation was impossible, thus making navigation-guided opening of the sellar floor obligatory (A). After sufficient opening, the dura was opened with fine scissors (B) and the pituitary gland gently mobilized to the left (C). On the right side, it was possible to successfully localize (D) and completely remove (E) the tumor.

### Postoperative course

The patient made an uneventful recovery with no nasal airflow problems. Postoperative MRI and hormonal investigation showed no evidence of residual tumor with normal pituitary function (Fig. 104). No visual disturbances occurred.

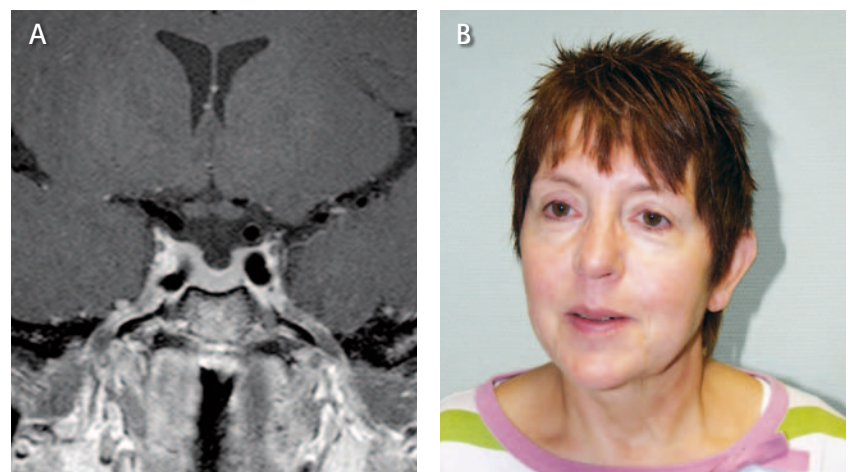


**Fig. 104** Contrast enhanced T1w scan in coronar view reveals no tumor remnant (A). Patient's photo one year after surgery shows obvious changes resulting from to the successful surgery (B, published with patient's permission).

## CASE IV

### Intra- and suprasellar macroadenoma

#### Approach: Combined transcranial – transnasal surgery

Main surgeon: André Grotenhuis, M.D., Ph.D.

#### Background

This 17-year-old female patient presented with decreased visual acuity and a bitemporal hemianopia, more on the right side. Endocrinologically there was a high IGF-1 level with mild symptoms of acromegaly. An MRI scan showed an enlarged sella with a macroadenoma with suprasellar extension that clearly showed a no longer encapsulated part on the right side, encasing the right anterior cerebral artery (Fig. 105). Because of the hormonal activity, the objective of the planned surgery was complete resection of the tumor. However, it was considered that it would be more hazardous to try to remove that part using only a transnasal approach, so we decided to combine that approach with a supraorbital craniotomy and to do that simultaneously during the same surgical procedure (Fig. 106).

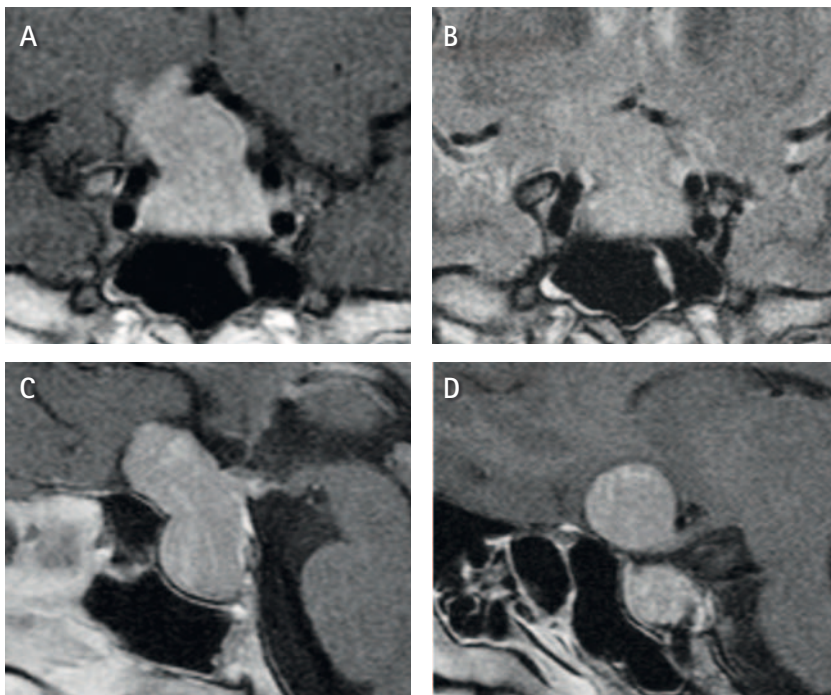
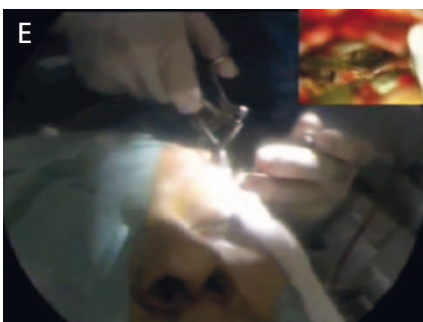
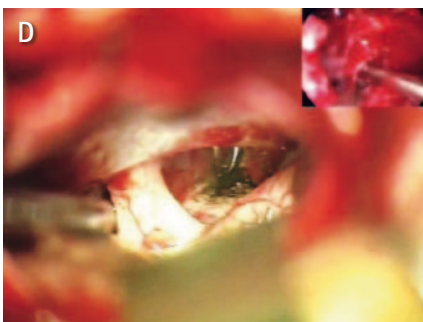
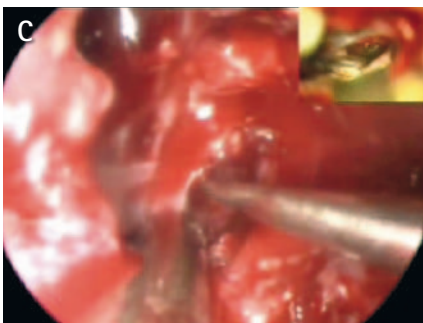
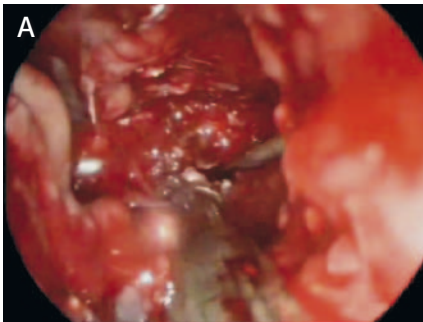


**Fig. 105** MRI scans in a coronar (A,B) and sagittal (C,D) view demonstrating an enlarged sellar floor caused by a GH-macroadenoma with suprasellar extension. Note that the tumor is no longer encapsulated, encasing the right anterior cerebral artery (A,B).



**Fig. 106** Intraoperative set up, performing simultaneous transcranial-transnasal surgery.



## Surgery

The procedure commenced with the nasal portion. After preparation of both nostrils, the ostia were interconnected to a wide bilateral sphenotomy by removing part of the vomer. The sella was opened using a high-speed drill, the dura was incised and a rather more firm grayish adenoma was removed.

Subsequently, a right supraorbital craniotomy was performed. After eye-brow skin incision, a frontolateral bone flap was created measuring 2.5 x 2 cm. The dura was opened curvilinear, exposing the suprasellar cisterns. The adenoma had pushed the optic nerves and chiasm upwards and backwards and, as expected, a non-capsulated part of the adenoma was found here which fully encased the right anterior cerebral artery. Under endoscope-assisted microscopic vision, this part of the tumor could be dissected safely.

Then, working simultaneously transnasally and transcranially, the remaining part of the adenoma, including the whole capsule, was removed completely. The remaining normal part of the pituitary gland could be clearly identified. The sella was filled with an umbilical fat pad soaked in fibrin glue. The sellar floor was then closed with some Spongostan® followed by thorough rinsing from above. No fluid could be detected by endoscopic inspection from below. After closure of the supraorbital craniotomy, the endoscope was retracted out of the sphenoid sinus; no nasal tamponade and no lumbar drain were used (Fig. 107).

**Figs. 107** The combined operation started with the nasal part and the grayish adenoma was partially removed (A). Then, a right supraorbital craniotomy was performed, approaching the optic nerve and suprasellar region (B). As expected, the non-capsulated part of the adenoma was found here which fully encased the right anterior cerebral artery. Note the picture-in-picture mode, showing the simultaneously performed procedure through the transnasal (C) and transcranial approaches (D, E).



### Postoperative course

The postoperative course was uneventful and no CSF leakage occurred. On the second postoperative day, the MRI scan showed removal of the adenoma and the fat tissue in place (Fig. 108 A). Endocrinologically, the IGF-1 level normalized with all other pituitary functions intact. An MRI scan 3 months later showed the pituitary stalk to be in a midline position and normal appearance of the hypophysis with proper re-pneumatization of the sphenoid sinus (Fig. 108 B, C, D).

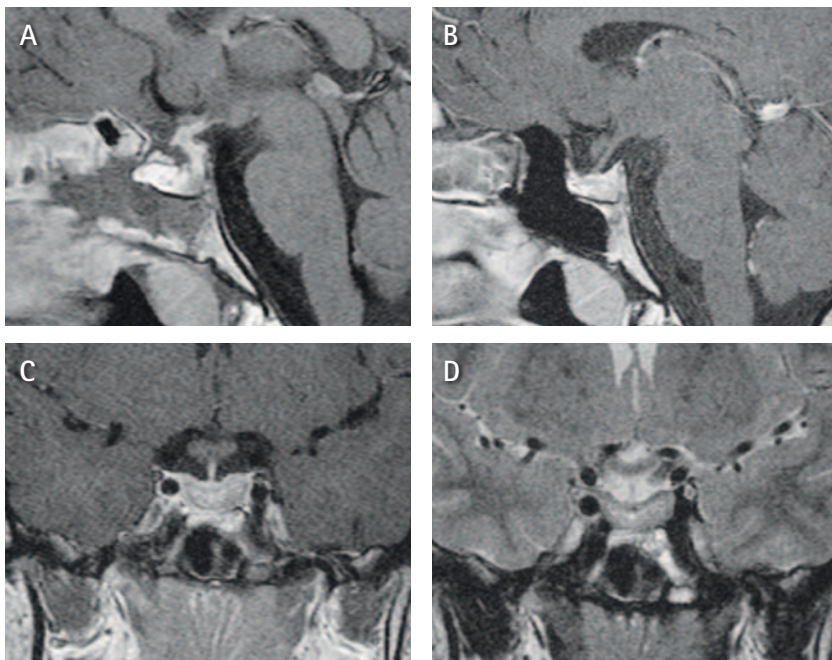


**Fig. 108** T1w MRI scans in sagittal view two days (A) and three months (B) after surgery. Contrast assisted T1w (C) and T2w (D) MRI scans in coronar view show the pituitary gland to be in a normal midline position.

---

## TRanssphenoidal ENDoscopy: the TREND-setting equipment

Considering recent publications on transsphenoidal surgery, it is clear: TRanssphenoidal ENDoscopy is TREND-setting! However, this endoscopic technique is not in routine use everywhere and neurosurgeons are often reluctant to use it. The cause of this aversion is the steep learning curve. Permanent contamination of the endoscope with blood and nasal secretions causes difficult orientation and, without a nasal speculum, endonasal dissection is a mystery to neurosurgeons. In addition, para-endoscopic and biportal dissection is very unfamiliar.

As described previously, prerequisites for transsphenoidal endoscopy include basic endoscopic experience and anatomical studies in the laboratory. In addition, fruitful co-operation with an otorhinological surgeon experienced in endoscopy may lessen the initial frustration. It is, however, an undisputable fact that the best endoscopic equipment also shortens the difficult learning phase. The endoscope for transsphenoidal skull base surgery must combine brilliant optics with practical and user-friendly application during surgery.

To meet these requirements, the TREND transsphenoidal endoscope was developed through the international co-operation of experienced endoscopic neurosurgeons, to offer the following features:

1. Superior optical quality for optimal visualization
2. An optimal suction-irrigation device for effective cleaning of the scope
3. Ergonomic handling for relaxed application
4. Sufficient endoscope length for trouble-free application during extended approaches
5. Connection to a holding device for possible fixation
6. Connection to a navigation device for safe orientation of the endoscope
7. Highly sophisticated additional endoscope equipment for user-friendly operation
8. Dedicated surgical instruments for effective para-endoscopic dissection

1. The TREND endoscope has been meticulously developed to achieve exceptional image quality. The high-quality endoscope with a 4 mm diameter offers an undisturbed, true color and highly realistic view of structures. For unproblematic visualization of hidden parts of the surgical field, a variable application of 0° and 30° endoscopes is available (Figs. 109, 110).

2. In transsphenoidal surgery, most endoscopes do not provide adequate suction and irrigation near to the tip of the instrument. However, when us-



**Fig. 109** Photograph showing the Aesculap TREND pituitary endoscope with a 4 mm diameter offering an undisturbed, true color and highly realistic view of structures. For direct visualization of hidden parts of the surgical field, a variable application of 0° and 30° endoscopes is available. For approaching deep-seated lesions, an effective length of the endoscope has been defined. Note specially created surgical instruments for transnasal use, allowing unimpeded, safe and effective endoscopic transnasal surgery.



**Fig. 110** Photographs demonstrating the ergonomic grasping part of the endoscope. An efficient suction-irrigation device is incorporated where the valve is controlled simply with the index finger. In addition, the grasping part offers a quick connection of the endoscope to a holding arm and navigation device.



---

ing a pure endoscopic approach without a nasal speculum, the endoscope is permanently contaminated with blood and mucosal secretions, which limits the surgeon's view. Continuous removal and introduction of the endoscope invokes additional damage to the nasal mucosa. Based on experience in transnasal surgery, the TREND endoscope was developed with an effective irrigation and suction device. Continuous suction avoids fogging of the endoscope in the warm, wet nasal cavity and immediately removes vapor and smoke. The intermittent irrigation can be effectively controlled with the index finger, offering useful additional cleaning of the optics and flushing of the surgical field (Figs. 110, 111). An essential and undisputable advantage of the TREND equipment!

3. Difficulties in the learning curve of transsphenoidal endoscopy are also caused by an additional problem, namely by inefficient endoscope systems. Uncomfortable handling causes uncontrolled and rough movements within the sensitive surgical field and, in addition, is tiring for the surgeon. The TREND endoscope effectively compensates for this drawback through its human-engineered grasping part. The surgeon holds the TREND endoscope as a fine microinstrument allowing precise manipulation. The efficient suction-irrigation device is also incorporated within the grasping part where the valve is controlled simply with the index finger. Moreover, the unique construction and perfect balance of the TREND endoscope provide a less tiring tool for the neurosurgeon (Fig. 111). In addition, the grasping part offers a quick connection of the endoscope to a holding arm (Figs. 112, 114).

4. The newly developed TREND endoscope should be able to meet the demands of extended skull base approaches. For approaching deep-seated lesions, an effective length of the endoscope has been defined: it is not too long to ensure efficient handling, but is long enough to be able to reach targets of the skull base and intradural space.

5. Bimanual, two-handed dissection forms the foundation of microneurosurgery and is also essential for transsphenoidal endoneurosurgery, especially during complicated skull base surgery. For this reason, after completing the biportal-binostril approach, the TREND endoscope can be easily fixed in a special holding arm: the endoscope placed through the other nostril does not disturb surgical dissection (Figs. 112, 114). Alternatively, the three- or four-handed technique can be used with a co-operating surgeon, thus also allowing trouble-free dissection (Fig. 113).



**Fig. 111** Intraoperative use of the TREND endoscope. Note the ergonomic grasping part; the surgeon holds the endoscope as a fine microinstrument, allowing precise manipulation with perfect intraoperative balance.



**Fig. 112** After creating the transnasal approach, the endoscope can be connected to a holding device. In this way, tumor removal can be performed bi-manually.



**Fig. 113** The ergonomic endoscope design allows fruitful assistance of the cooperating surgeon, by permitting the three- or four-handed technique. In this case, surgeons stay face-to-face, allowing effective interplay. Advantage of the free hand technique is, that the scope can follow the instruments and focus dynamically on the field of interest. This continuous manipulation of the endoscope offers an additional feeling of three-dimensionality, thus making surgery safer particularly during the endoscopic learning curve.

---

6. As discussed above, anatomical landmarks allow safe orientation during endoscopic endonasal surgery. Additional, but not essential, employment of a C-arm may provide further verification for an exact and delicate dissection; it can be helpful especially during the learning curve. In some cases, however, the intranasal anatomy is confused, causing complicated orientation. Typical situations include a conchal sella (problematic orientation), extended tumors with parasellar, intrasphenoidal or even intranasal expansion (no anatomical alignment), hormonal active microadenomas (extensive sinusoidal bleeding), and re-do surgeries (scarring of the sellar floor). In these cases, the intraoperative use of a navigation device is recommended and frequently essential to avoid damage to neurovascular structures. The special construction of the TREND endoscope allows easy and uncomplicated connection to several navigation systems: the tip of the endoscope can then be steered with safe control of the surgical approach (Figs. 71, 111, 112, 113).

7. A highly sophisticated endoscope also needs related equipment. Recently, the intraoperative use of full high definition (HD) image quality has opened a new area in endoscopic neurosurgery with an increased range of indications in minimally invasive neurosurgery. The image quality of the full-HD camera and monitor system is markedly superior to that of a standard one- or three-chip camera unit and provides a five times higher optical resolution. This superior quality is particularly important in delicate situations, namely the differentiation of subtle structures and where scope vision is blurred. A typical situation in transsphenoidal surgery is to differentiate the pituitary gland from tumor tissue in a bloody surgical field. The enormous optical resolution of HD cameras needs optimal illumination of the field: high power xenon sources with cold light and ideal light cables are important for this reason. An effective recording system is also an important part of the equipment for documentation of the procedure, which is useful for scientific evaluation and teaching purposes. An ideal solution is a digital video system allowing user-friendly and rapid recording.

8. Surgical dissection along the endoscope requires special expertise and, for this reason, surgical instruments should also offer dedicated features. Slender transnasal microinstruments have been specially created to allow unimpeded introduction of the tool through the narrow nasal cavity (Figs. 109, 112, 113). These tube-shaft designed instruments and special curettes can be used in a much reduced operating corridor enabling safe manipulation within the limited surgical passage and clear visualization of the surgical field. A specially designed bipolar forceps completes the equipment: by additional forced closing, its knob reopens the tip of the scissors. In several cases, the use of these specially designed instruments is obligatory when operating through biportal approaches.





**Fig. 114** *Easy and user-friendly connection of the endoscope to the holding device. A pneumatic arm was used here.*

**Fig. 115** The robustly fixed endoscope (A) is now placed in the left nostril (B) and the operation is continued through the right nasal cavity. The fixed endoscope does not disturb surgical dissection; note unlimited manipulation, using dedicated microinstruments.



---

## Abbreviations

BA	basilar artery
BT	Bertini's turbinate (concha sphenoidalis)
CL	clivus
CN I	olfactory nerve
CN II	optic nerve
CN III	oculomotor nerve
CN IV	trochlear nerve
CN V/1	ophthalmic nerve
CN VI	abducent nerve
CP	carotid prominence
CS	cavernous sinus
EA	ethmoid artery
EB	ethmoid bulla
EP	epipharynx
FR	foramen rotundum
GL	Grubert's ligament
HYP	pituitary gland
ICA	internal carotid artery
IT	inferior turbinate
MS	maxillary sinus
MT	middle turbinate
NF	floor of the nasal cavity
NS	nasal septum
OC	oral cavity
OP	optic prominence
PCoA	posterior communicating artery
PEC	posterior ethmoid cells
PPG	pterygonalpalatine ganglion
SA	septal artery
SD	sellar diaphragm
SF	sellar floor
SO	sphenoid ostium
SOF	superior orbital fissure
SP	sphenoid planum
SPA	sphenopalatine artery
SPF	sphenopalatine foramen
SPJ	sphenopalatine junction
SS	sphenoid sinus
ST	superior turbinate
TA	tuba auditiva
TMT	tail of middle turbinate
TT	torus tubarius
TU	tumor
UP	uncinate process
VC	Vidian's pterygoid canal





# MINOP® TREND

## TRansnasal ENDoscopic System





■ ■ When looking at recent publications on transsphenoidal surgery, it will be clear that **TR**ans-sphenoidal **END**oscopy is TREND-setting! However, this endoscopic technique is not in routine use everywhere and neurosurgeons are often reluctant to use it: One is often cautious about an endoscopic endonasal dissection because the permanent contamination of the endoscope with blood and nasal secretions hinders orientation. In addition, the para-endoscopic and biportal dissection is very unfamiliar requiring an unacceptably steep learning curve.

Nevertheless, endoscopic visualization and para-endoscopic dissection without using the surgical microscope offers several undisputable advantages. Advantages in visualization increases light intensity in the deep-seated surgical field and clearly displays patho-anatomical details. In addition, the extended viewing angle of endoscopes enables surgeons to observe hidden parts of the surgical field. The major benefit in surgical dissection is the unhindered approach to these clearly visible structures: Without using a nasal speculum, surgical manipulation is not impeded and the instruments are freely mobile. In addition, a pure endoscopic technique avoids the need for rhinoseptal submucosal dissection providing a direct

and quicker approach to the sphenoid sinus. This method avoids the need for postoperative nasal packing, thus causing less pain and discomfort after surgery, providing better nasal airflow and a shorter hospital stay.

Pre-conditions of transsphenoidal endoscopy are the basic endoscopic experience and anatomical studies in the laboratory; however, it is indispensable to use a dedicated endoscopic system to further shorten the learning phase. The endoscope for transsphenoidal skull base surgery must provide a brilliant image quality with true colors, high contrast and highly realistic images. This simplifies the differentiation between healthy or pathological structures. It is essential to have an effective cleaning function in order to free the endoscope lens from fog, blood or mucosal secretions. The endoscope must offer a highly ergonomic design and sufficient working length for extended approaches. For selected cases, it is also necessary to connect the endoscope to a navigation system or a holding device. ■ ■

André Grotenhuis, Robert Reisch



# MINOP® TREND

## TRansnasal ENDoscopic System

### MINOP® TREND

#### FH615

**Handle with irrigation button**  
for FH610R and FH611R  
Ergonomic grasping part



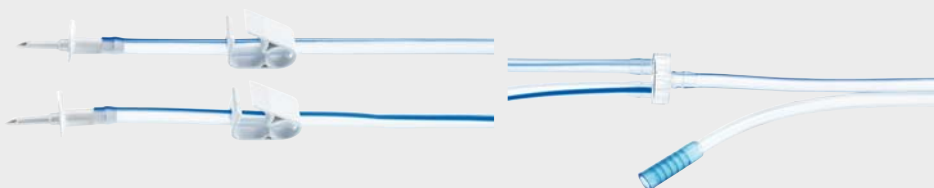
#### RT099R

**Adapter** for Aesculap  
holding arm



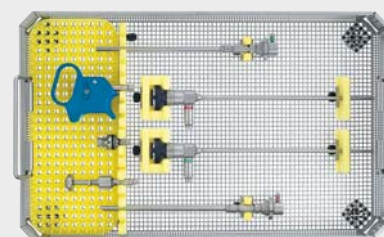
#### FH605SU

**Suction and irrigation tube,**  
sterile, 4.5 m, 2 puncture needles,  
for MINOP® TREND handle FH615  
and FH610R/FH611R,  
Package of 10 tubes



#### FF357R

**Storage tray** with silicone  
padding and lid for all  
MINOP® TREND components



#### JK740

**container body 3/4**  
with base perforation  
(L/W/H 470/274/90)

#### JK789

**container lid 3/4**  
blue



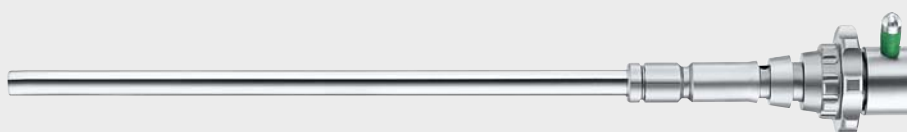
#### FH610R

##### Suction and irrigation trocar

for 0° endoscope PE487A

Diameter: 4.5 / 6.0 mm

Working length: 120 mm



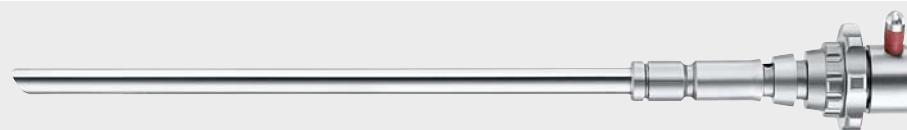
#### FH611R

##### Suction and irrigation trocar

for 30° endoscope PE507A

Diameter: 4.5 / 6.0 mm

Working length: 120 mm



#### PE487A

##### Endoscope,

0° viewing angle,

shaft diameter 4.0 mm



#### PE507A

##### Endoscope,

30° viewing angle,

shaft diameter 4.0 mm



# MINOP® TREND

## TRansnasal ENDoscopic System

### TREND – Currettes and Dissectors

#### FA041R-FA068R

Working length  
130 mm, 5 1/8"

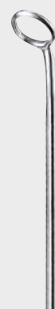
Total length  
280 mm, 11"



NICOLA

#### FA041R

Curette  
diam. 6.5 mm  
45° vertical angled  
long neck



NICOLA

#### FA042R

Curette  
diam. 6.5 mm  
45° horizontal  
angled, short  
neck



HARDY

#### FA043R

Enucleator  
left cutting



HARDY

#### FA044R

Enucleator  
right cutting



HARDY

#### FA045R

Curette  
diam. 4.0 mm  
90° left angled  
long neck



HARDY

#### FA046R

Curette  
diam. 4.0 mm  
90° left angled  
short neck



HARDY

#### FA047R

Curette  
diam. 4.0 mm  
90° right angled  
long neck



HARDY

#### FA060R

Curette  
diam. 4.0 mm  
90° right angled  
short neck





HARDY

**FA061R**

Curette  
diam. 4.0 mm

45° left  
horizontal angled  
short neck



HARDY

**FA062R**

Curette  
diam. 4.0 mm

45° right  
horizontal angled  
short neck



HARDY

**FA063R**

Curette  
diam 6.0 mm

90° left angled  
long neck



HARDY

**FA064R**

Curette  
diam. 6.0 mm

90° left angled  
short neck



HARDY

**FA065R**

Curette  
diam. 6.0 mm

90° right angled  
long neck



HARDY

**FA066R**

Curette  
diam. 6.0 mm

90° right angled  
short neck



REULEN-  
LANDOLT

**FA067R**

Micro Hook  
diam. 1.7 mm



REULEN-  
LANDOLT

**FA068R**

Dissector  
diam. 2.0 mm

blunt

# MINOP<sup>®</sup> TREND

## TRansnasal ENDoscopic System

### TREND – Currettes and Dissectors



#### FA030R-FA040R

Working length:  
140 mm, 5 1/2"

Total length:  
265 mm, 10 1/2"

Straight design with  
ergonomic grasping  
part and semi-sharp  
tips

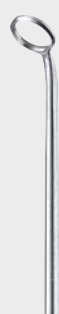


NICOLA

**FA030R**

Curette  
diam. 6.5 mm

45° vertical  
angled, long neck



NICOLA

**FA031R**

Curette  
diam. 6.5 mm

45° horizontal  
angled, short neck



HARDY

**FA032R**

Enucleator

left cutting

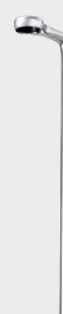


HARDY

**FA033R**

Enucleator

right cutting



HARDY

**FA034R**

Curette  
diam. 4.0 mm

90° angled  
long neck



HARDY

**FA035R**

Curette  
diam. 4.0 mm

90° angled  
short neck



HARDY

**FA036R**

Curette  
diam. 4.0 mm

45° angled  
short neck

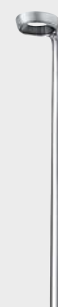


HARDY

**FA037R**

Curette  
diam. 6.0 mm

90° angled  
long neck

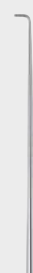


HARDY

**FA038R**

Curette  
diam. 6.0 mm

90° angled  
short neck



LANDOLT-  
REULEN

**FA039R**

Micro Hook  
diam. 1.7 mm



LANDOLT-  
REULEN

**FA040R**

Dissector  
diam. 2.0 mm

blunt

## Nasal Specula

**OK090R**

**Nasal specula for  
protective mobilization  
of the turbinates**

Length 135 mm, 5 1/4"  
90 x 7 mm





# MINOP<sup>®</sup> TREND

## TRansnasal ENDoscopic System

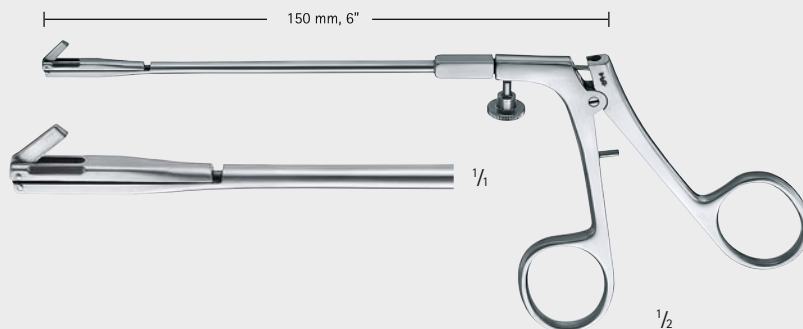
### Pituitary Instruments

FA076R

**Backwards cutting  
antrum punch,**

Rotating sheath 360°,  
Working length: 120 mm, 4 3/4"

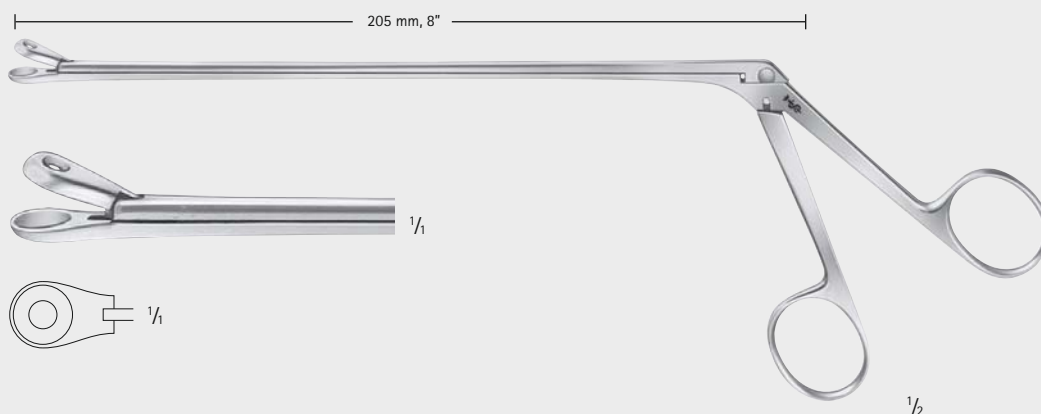
For removal of posterior  
nasal septum



### LANDOLT

FF345R

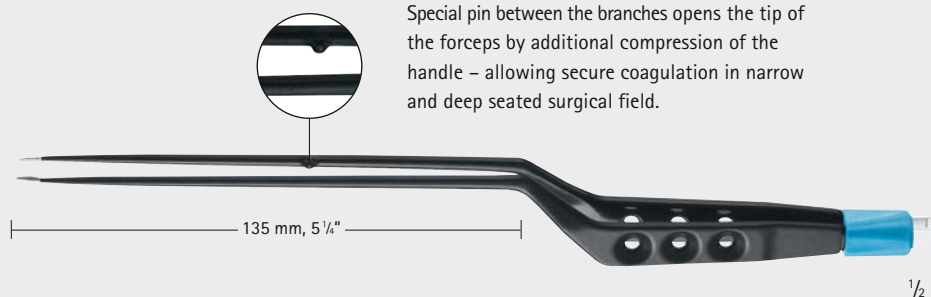
Tumor grasping forceps,  
blunt  
Diam. 9.0 mm



#### GK801R

**Bipolar coagulation forceps**  
with slender jaws and higher  
spring tension

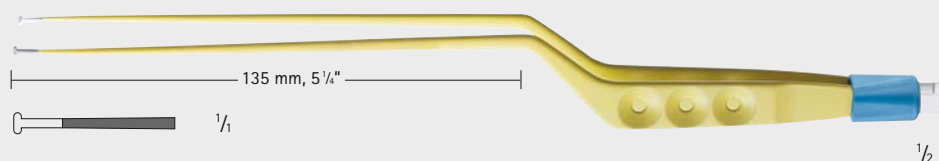
Total length 255 mm, 10"  
Working length 135 mm, 5 1/4"



#### GK800R

**T-coagulation forceps**  
with blunt, t-shaped tips

Total length 255 mm, 10"  
Working length 135 mm, 5 1/4"



#### FM158R

**Bayonet grasping forceps**  
straight tip

Total length 240 mm, 9 1/2"  
Working length 120 mm, 4 3/4"



#### FM156R

Jaw 0.5 mm

#### FM157R

Jaw 0.9 mm

**Bayonet micro grasping**  
forceps straight tip

Working length 120 mm, 4 3/4"  
Total length 245 mm, 9 3/4"



# MINOP<sup>®</sup> TREND

## TRansnasal ENDoscopic System

### Pituitary Scissors

165 mm, 6 1/2"

FAHLBUSCH

**FD220R**

1/1 Micro scissors, extra delicate pattern, curved on flat, horizontal cutting

NICOLA

**FD222R**

1/1 Forceps, scoop-shaped, diam. 2.5 mm

YASARGIL-NICOLA

**FD224R**

1/1 Grasping forceps with long conical jaw

NICOLA

**FD226R**

1/1 Micro scissors, straight, diam. 2.5 mm

**FD220R-FD226R**

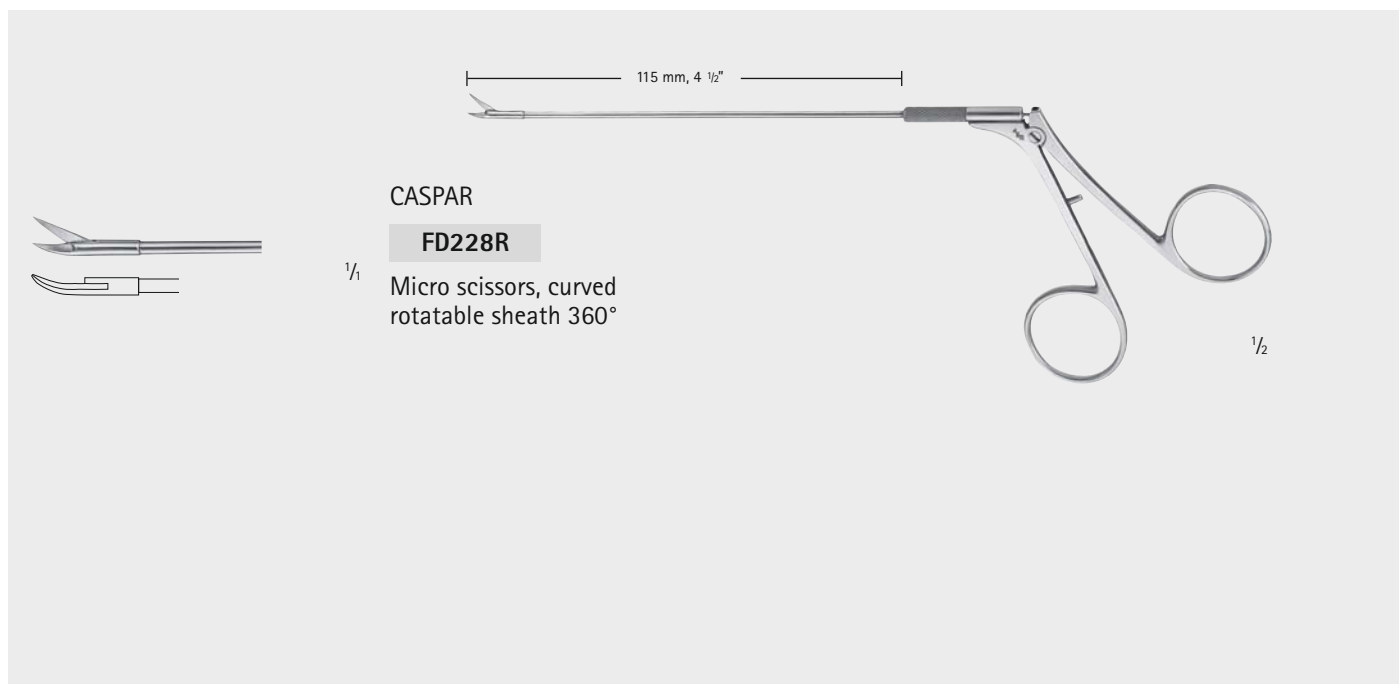
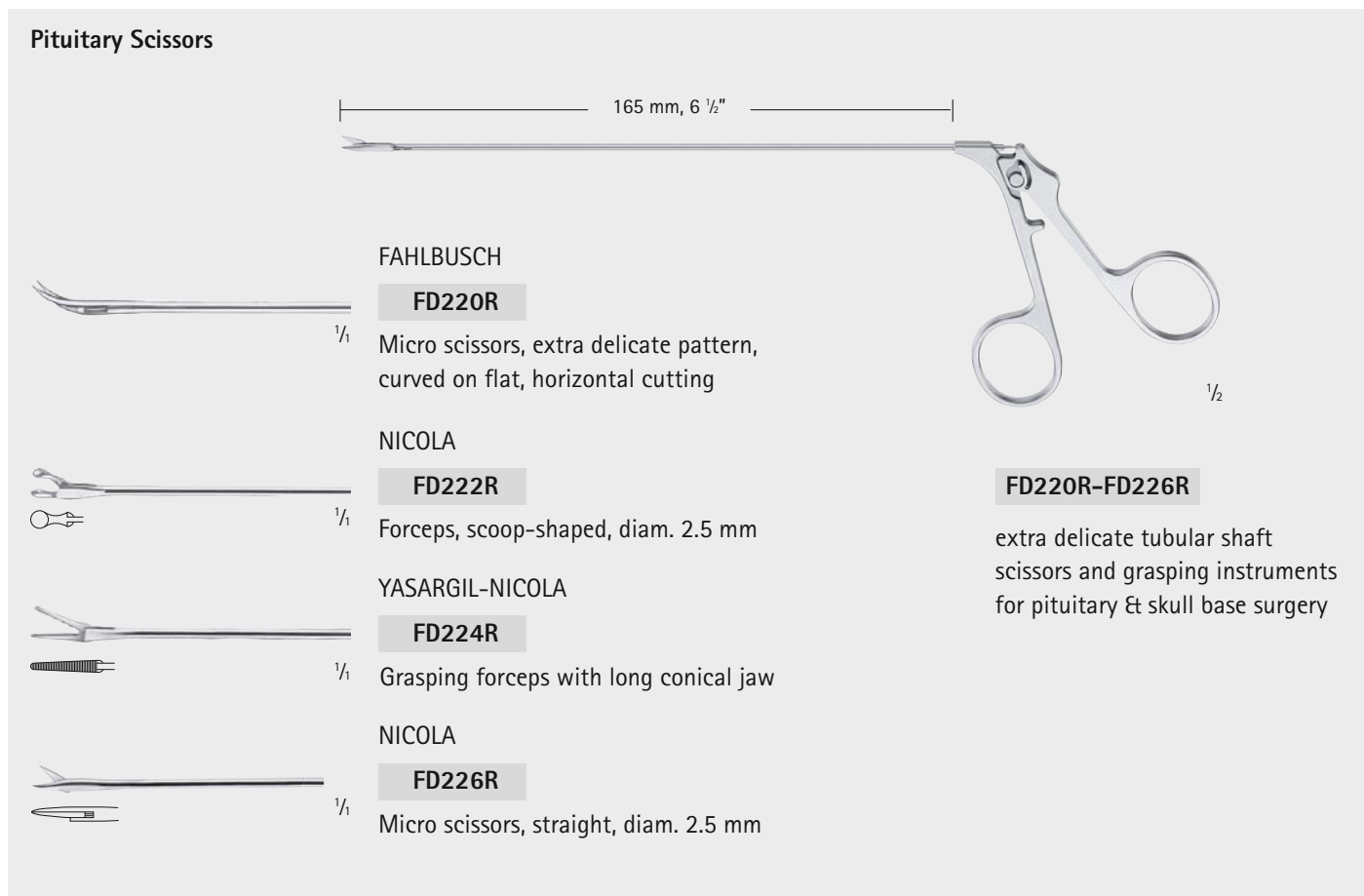
extra delicate tubular shaft scissors and grasping instruments for pituitary & skull base surgery

115 mm, 4 1/2"

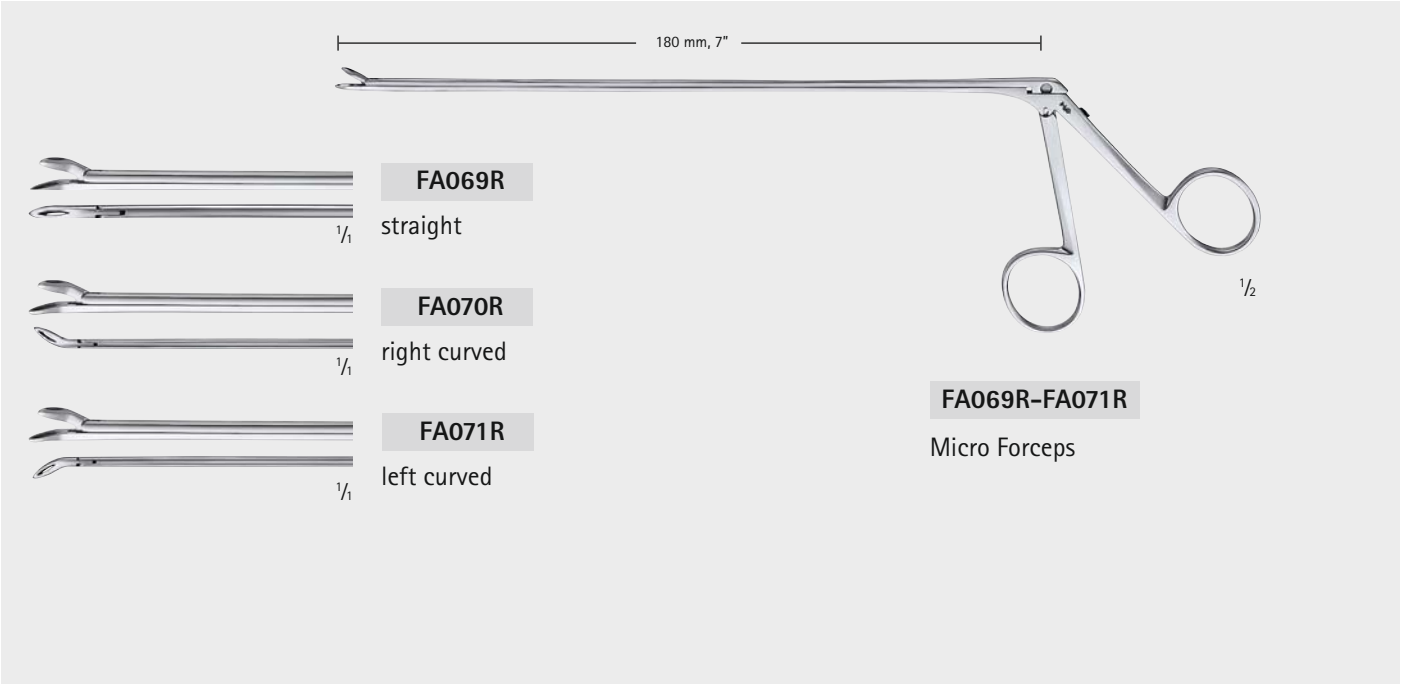
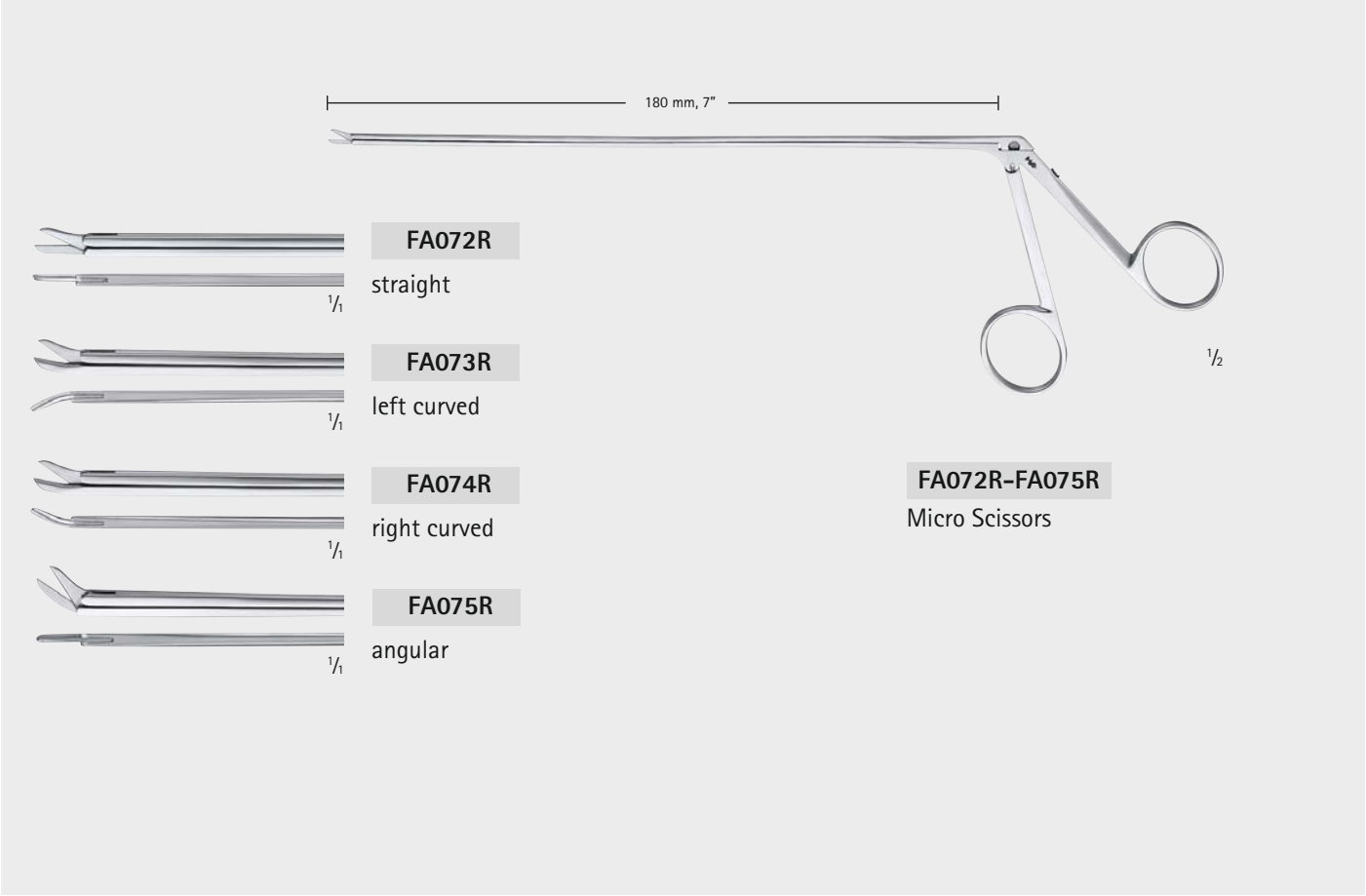
CASPAR

**FD228R**

1/1 Micro scissors, curved rotatable sheath 360°





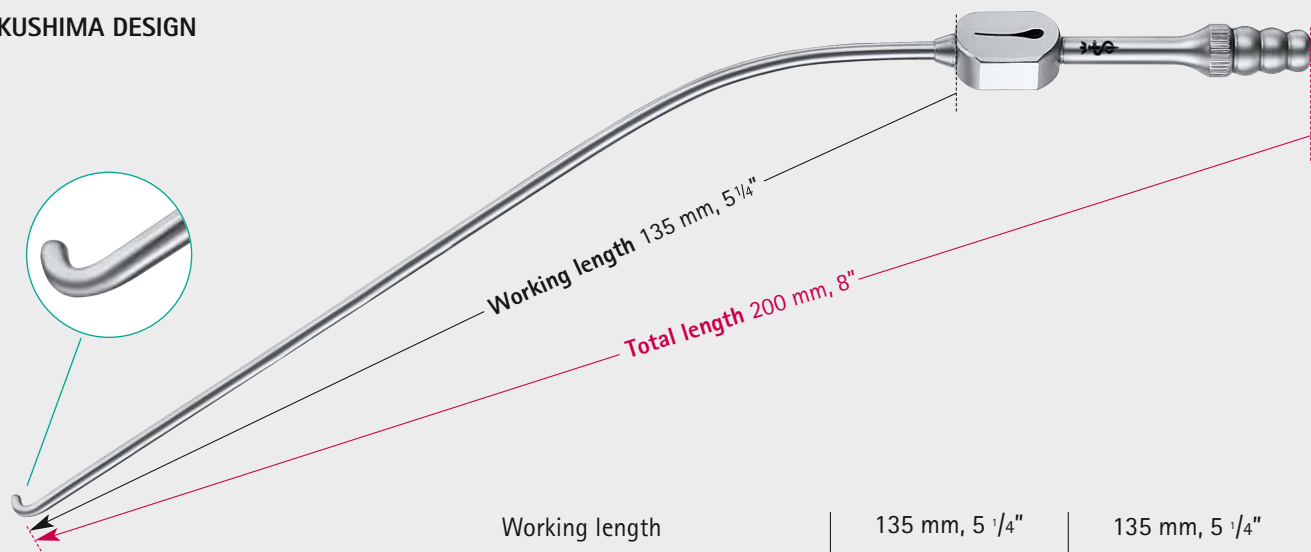


# MINOP® TREND

## TRansnasal ENDoscopic System

### Curved Micro Suction Instruments

Suction cannulas  
Curved suction instruments  
FUKUSHIMA DESIGN



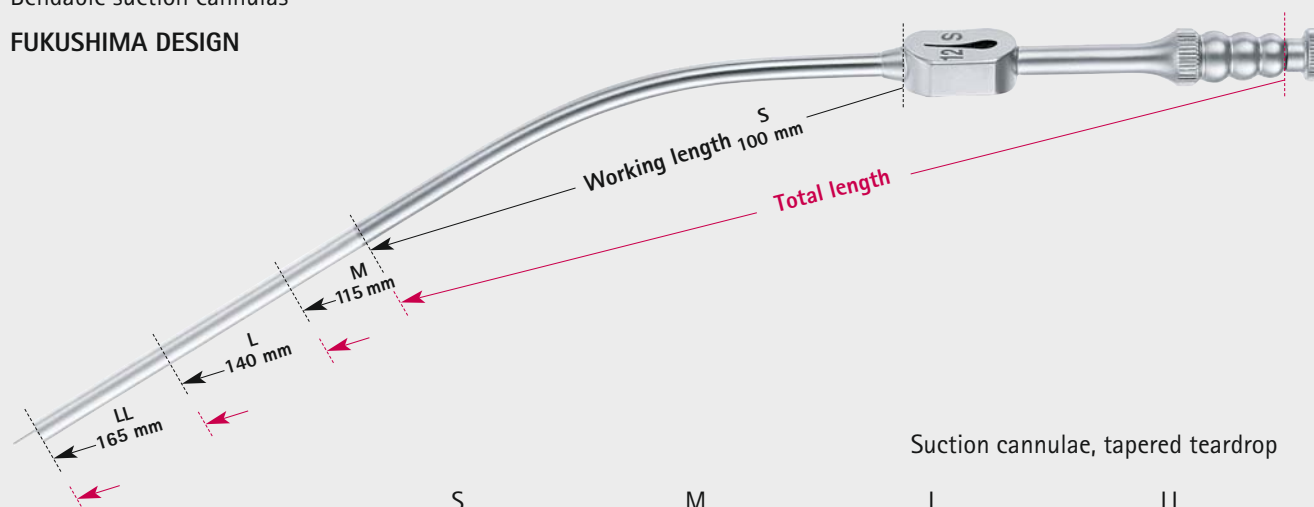
Working length	135 mm, 5 1/4"	135 mm, 5 1/4"
Total length	200 mm, 8"	200 mm, 8"
Outer diameter	2.7 mm	2.7 mm
Inner diameter	2.0 mm	2.0 mm
Angled tip	Right angled tip	Left angled tip
	GF431R	GF432R

## Micro Suction Instruments

### Suction Cannulas

Bendable suction cannulas

#### FUKUSHIMA DESIGN



Suction cannulae, tapered teardrop




	S	M	L	LL
Working length	100 mm, 4"	115 mm, 4 1/2"	140 mm, 5 1/2"	165 mm, 6 1/2"
Total length	165 mm, 6 1/2"	180 mm, 7"	205 mm, 8"	230 mm, 9"
Outer diameter				
3 Fr ○ 1.0 mm	GF401R	GF391R	GF411R	GF421R
4 Fr ○ 1.4 mm	GF402R	GF392R	GF412R	GF422R
5 Fr ○ 1.7 mm	GF403R	GF393R	GF413R	GF423R
6 Fr ○ 2.0 mm	GF404R	GF394R	GF414R	GF424R
7 Fr ○ 2.3 mm	GF405R	GF395R	GF415R	GF425R
8 Fr ○ 2.7 mm	GF406R	GF396R	GF416R	GF426R
9 Fr ○ 3.0 mm	GF407R	GF397R	GF417R	GF427R
10 Fr ○ 3.3 mm	GF408R	GF398R	GF418R	GF428R
12 Fr ○ 4.0 mm	GF409R	GF399R	GF419R	GF429R

# MINOP® TREND



## TRansnasal ENDoscopic System

### Kerrison Bone Punches

#### Jaw position 130°, upward opening

								
Length	Width	Footplate	Non detachable, without ejector	Detachable	Ejector	NOIR®, detachable	Ejector	Jaw opening
180 mm, 7"	1.0 mm	thin	FF771R	FK906R	-	FK906B	-	8 mm
	1.5 mm	thin	FF645R	FK923R	-	FK923B	-	9 mm
	2.0 mm	thin	FF772R	FK907R	✓	FK907B	✓	9 mm
	2.5 mm	thin	FF646R	FK924R	✓	FK924B	✓	10 mm
	3.0 mm	thin	FF773R	FK908R	✓	FK908B	✓	10 mm
	4.0 mm	thin	FF769R	FK909R	✓	FK909B	✓	12 mm

#### Jaw position 130°, downward opening

								
Length	Width	Footplate	Non detachable, without ejector	Detachable	Ejector	Jaw opening		
180 mm, 7"	1.0 mm	thin	FF781R	FK936R	-	8 mm		
	2.0 mm	thin	FF782R	FK937R	✓	9 mm		
	3.0 mm	thin	FF783R	FK938R	✓	10 mm		



Kerrison Bayonet Bone Punches

Jaw position 130°, upward opening

Length	Width	Working length	Article No.	Jaw opening
240 mm, 7"	2.0 mm	170 mm	FF496R	10 mm
	3.0 mm	170 mm	FF497R	10 mm
	4.0 mm	170 mm	FF498R	10 mm
	5.0 mm	170 mm	FF499R	10 mm



# Aesculap® Holding Devices

## M-TRAC – Mechanical Holding Arm

### FF168R

#### M-TRAC

- Flexible holding device with mechanical fixation
- Assembly: flexible holding arm with integrated fixation bar
- Total length: 107 cm
- Length of fixation bar: 46 cm
- Diameter of fixation bar: 20 mm
- Total weight: 0,7 kg
- Holding force: 4 kg
- Easy mechanical fixation by clamping handle
- Small, flexible joints for fine positioning
- Autoclavable 134°C, 5 minutes
- Full range of accessories/adapters for connecting Aesculap endoscopes, trocars and instruments
- Holding Arm fits into regular Standard 1/1 Container



**FF280R**

Flexible fixing element with ball joint suitable for RT040R and FF168R



**RT090R**

Flexible fixing element with sprocket suitable for RT040R and FF168R



**FF151R**

Rigid fixation element suitable for RT040R and FF168R

## UNITRAC – Pneumatic Holding Arm

### RT040R

#### UNITRAC®

- Single handed use
- Fast sterile set-up in the OR
- Universal retraction and holding system with special accessories for neuroendoscopy
- Simple to assemble onto the OR table railing
- Integrated safety systems prevent collapse of holding arm if OR compressed air supply is interrupted
- Direct connection to OR compressed air supply
- Diameter of fixation bar: 20 mm
- To be used with JG901



### JG901

Sterile drape for coverage of the Unitrac® arms, single-use product, package of 50 pcs.

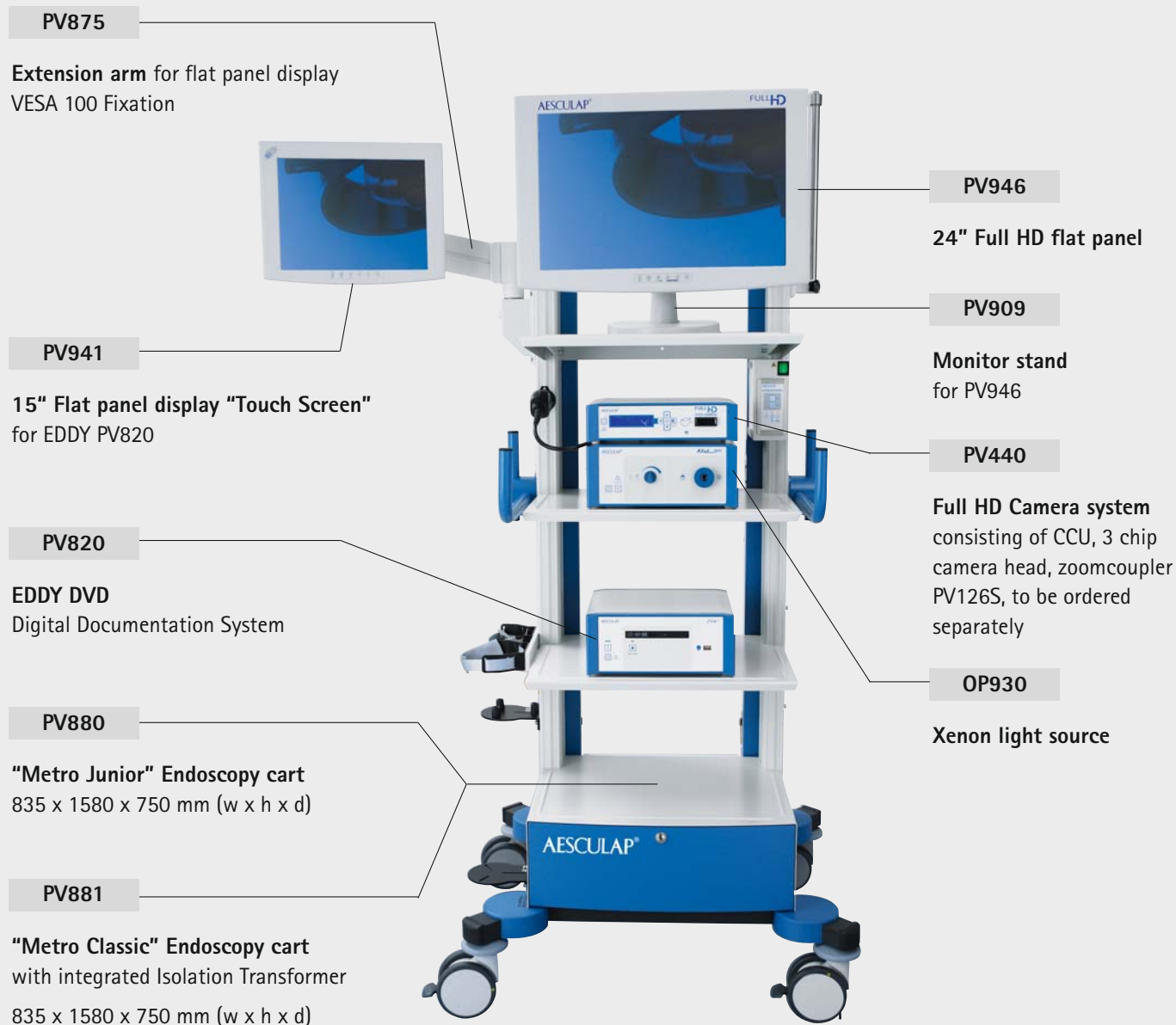


### RT020R

Quick connect adapter for use with sterile drape JG901 allows the change of instruments after draping with JG901

# Aesculap® Visual Equipment

## Neuroendoscopy Tower with FULL HD Camera and Touch Screen





#### OP923

**Full HD Light cable,**  
autoclavable, diam. 4.8 mm,  
length 250 cm



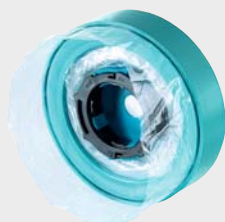
#### JG904

**Sterile Camera drape,**  
disposable, ring design,  
package of 25



#### JG908SU

**Closed sterile Camera drape,**  
15 cm diam. the optic can  
be changed under sterile  
conditions during surgery,  
package of 10



# Aesculap Power Systems

## microspeed uni – Electric High Speed Motor System

### System components:



**GD670**

microspeed uni  
control unit



**GD675**

microspeed uni XS  
high speed motor



**GD668**

foot control  
– single pedal



For more information about  
microspeed uni equipment and  
accessories, please ask your local  
Aesculap sales representative or  
see brochure no. 028302

## HiLAN XS – Pneumatic High Speed Motor System



**GA740R**

HiLAN XS  
high speed motor



**GA521**

Foot Pedal

**GA513R**

Motor hose (3 m)



**GA464R**

Supply hose (3 m)  
wall connection  
Aesculap Dräger

**GA468R**

Supply hose (3 m)  
wall connection Schrader

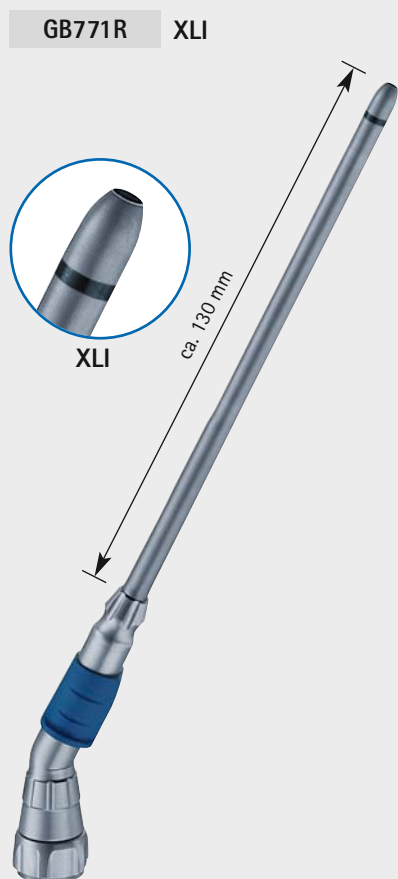
**GA461R**

Supply hose (3 m)  
wall connection DIN



For more information about  
Hilan XS equipment and accessories,  
please ask your local Aesculap sales  
representative or see brochure no.  
026002

## Highspeed Tools for microspeed uni and HiLAN XS



### Rosen burrs

Ø 2.3



GE704R

Ø 3.1



GE706R

Ø 4.0



GE707R

Ø 5.0



GE708R

Ø 6.0



GE709R

### Diamond burrs

Ø 2.3



GE714R

Ø 3.1



GE716R

Ø 4.0



GE717R

Ø 5.0



GE718R

Ø 6.0



GE719R

### Neuro cutter

Ø 3.1



GE702R

### Barrel burrs soft cut

Ø 4.0



GE711R

Ø 5.0



GE729R

Ø 6.0



GE712R

### Twist drill

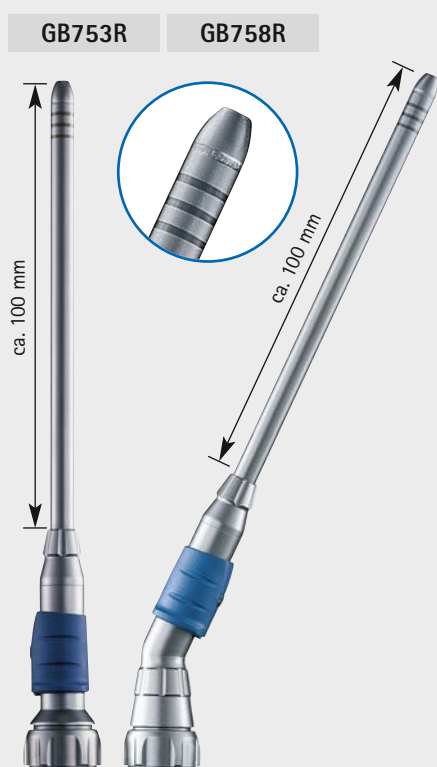
Ø 1.5



GE700SU

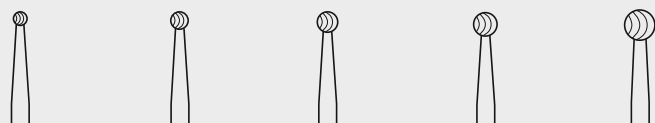
# Aesculap Power Systems

## Highspeed Tools for microspeed uni and HiLAN XS



### Rosen burrs

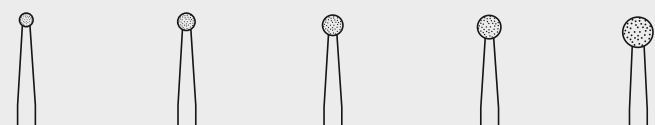
Ø 1.8 Ø 2.3 Ø 2.7 Ø 3.1 Ø 4.0



GE603R GE604R GE605R GE606R GE607R

### Diamond burrs

Ø 1.8 Ø 2.3 Ø 2.7

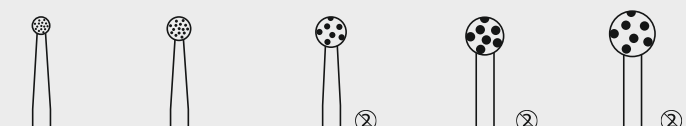


GE613R GE614R GE615R GE616R GE617R

### Diamond burrs coarse

### Extra coarse

Ø 2.3 Ø 3.1 Ø 4.5 Ø 6.0

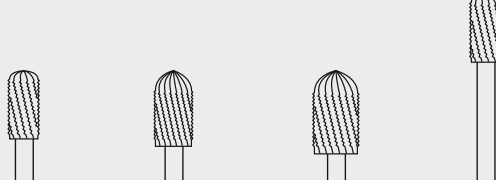


GE624R GE625R GE656SU GE657SU GE658SU

### Barrel burrs

#### soft cut

Ø 4.0 Ø 5.0 Ø 6.0 Ø 4.0



GE648R GE649R GE650R GE645R



Ø 5.0



GE608R

Ø 6.0



GE609R

Ø 6.0



GE618R



GE619R

#### Neuro cutters

Ø 1.8



GE631R

Ø 2.3



GE634R

Ø 3.1



GE635R

Ø 3.1



GE653R

#### Neuro cutters

Diamond coarse

Ø 3.1



GE654R

Ø 3.1



GE655R

Ø 4.0



GE639R

#### Barrel burrs standard

Ø 4.0



GE644R

Ø 6.0



GE646R

#### Tungsten carbide

Rosen burrs

Ø 4.0



GE607TC-SU

Ø 5.0



GE608TC-SU

Neuro cutter

Ø 3.1



GE635TC-SU

# Aesculap Academy Neuroendoscopy Courses



## Horizons of Knowledge. Competence to Master the Future.

Innovative developments in the field of medical technology, sophisticated new treatment methods, increasingly more stringent requirements for hospital and quality management and, last but not least, a healthy interest in acquiring new knowledge have given rise to an enormous and ever-increasing demand for further and advanced training.

The Aesculap Academy enjoys a world-wide reputation as a leading forum for medical training and answers the demands of physicians and medical staff in OR, anaesthesia, ward, outpatient care and hospital management. The course program comprises a wide range of hands-on workshops, management seminars and international symposia.

Aesculap Academy courses are of premium quality and are accredited by the respective medical societies and international medical organizations. A scientific advisory board guarantees the selection of speakers and topics.

All of our courses are conducted by pioneering neurosurgeons who will address the theoretical knowledge of neuroendoscopy, cranial endoscopic anatomy, and clinical applications of neuroendoscopy. Each course includes extensive hands-on sessions or possibly live surgeries. Course attendees will benefit from discussions and analysis of real cases together with expert colleagues from all over the world. The training facilities of the Aesculap Academy in Berlin and Tuttlingen are traditional and spectacular locations for "sharing expertise".

Competence to master the future – keep yourself fit for the future and ask for the latest course programme offerings, e.g.

- "Basic" Neuroendoscopy Course
- "Advanced" Neuroendoscopy Course
- "Applied" Neuroendoscopy Course

Visit our website and register for one of the next neuroendoscopy courses –

[www.aesculap-neuro.com](http://www.aesculap-neuro.com) or [www.aesculap-academy.com](http://www.aesculap-academy.com)  
or contact your local B. Braun Aesculap representative.



[www.aesculap-neuro.com](http://www.aesculap-neuro.com) or  
[www.aesculap-academy.com](http://www.aesculap-academy.com)

■ ■ Pre-requisites of intracranial neuroendoscopy are valuable and user-friendly endoscopic equipment. However, despite of availability of dedicated systems, the endoscopic technique is not in routine use everywhere and neurosurgeons are often hesitant to use it. The cause of the aversion is often the steep learning curve. The goal of our Neuroendoscopy Courses is to facilitate the initial steps, thus giving a comprehensive overview in contemporary endoscopic techniques, including intraventricular, transcranial and transnasal applications. Didactic lectures by international experts give the necessary theoretical basis. Extensive hands-on laboratory allow basic anatomical studies and offer practical experience with endoscopes. Illustrative live surgeries show clinical application, giving advantageous tips in the every-day application of neuroendoscopy. ■ ■

Programm



### Basic Intracranial Neuroendoscopy

a basic hands-on training course for endoscopic neurosurgery

Programm



### Advanced Intracranial Neuroendoscopy

a comprehensive hands-on course on minimally invasive and endoscopic neurosurgery

Programm



### Applied Intracranial Neuroendoscopy

a clinical observer course on minimally invasive and endoscopic neurosurgery

#### "Basic" Neuroendoscopy Course

The objective of the course "Basic Intracranial Neuroendoscopy" is to offer a comprehensive overview on endoscopic techniques in intracranial neurosurgery. Didactic lectures, extensive hands-on laboratory and illustrative live-surgeries are especially designed for newcomers in the field of neuroendoscopy, giving excellent theoretical and practical basis. Manuals and digital documentation of your own laboratory exercise provide an additional positive impact on your learning.

#### "Advanced" Neuroendoscopy Course

"Advanced Intracranial Neuroendoscopy" is designed for neurosurgeons with basic experience in neuroendoscopic techniques. The didactic lectures address the preoperative surgical planning as well as distinguished endoscopic techniques for cranial neurosurgery. Extended hands-on dissections and illustrative live surgeries demonstrate clinical applications in the daily routine offering important tips and tricks as well as valuable instructions for everyday use. The course is offered in two complementary parts. However, please note, that the both parts can be booked separately as well as in combination.

**Part I** (Endoscope-assisted Neurosurgery) concentrates on minimally invasive transcranial keyhole approaches and endoscope-assisted techniques dealing in a comprehensive way with the supra-orbital, subtemporal and retrosigmoidal exposure.

**Part II** (Endoscopic Transsphenoidal Surgery) deals with endoscopic techniques to treat sellar and parasellar lesions via the transsphenoidal route. Special attention will be given to extended skull base surgery.

#### "Applied" Neuroendoscopy Course

The course "Applied Intracranial Neuroendoscopy" offers a clinically oriented comprehensive overview on contemporary techniques in cranial endoscopic neurosurgery. Dedicated lectures, extensive case discussions and live surgeries will offer important tips and tricks providing valuable instructions for your everyday use. This event is a well recommended adjunct to the hands-on courses on "Basic Intracranial Neuroendoscopy" and "Advanced Intracranial Neuroendoscopy" in Berlin and Tuttlingen. In addition, you will have the opportunity to look behind the scenes of the headquarters and manufacturing plant of B. Braun Aesculap in Tuttlingen. Forming aneurysm clips yourself, experiencing how micro instruments are manually fabricated and visiting the famous Surgery Museum Asclepios are impressive parts of the course.



André Grotenhuis  
Nijmegen, Netherlands



Nikolai Hopf  
Stuttgart, Germany



Peter Nakaji  
Phoenix, USA



Robert Reisch  
Zurich, Switzerland



Mark Souweidane  
New York, USA

# Aesculap Neurosurgery Product Brochures

## ■ Neuroendoscopic Equipment



... for cranial and spinal neuroendoscopy.

## ■ Aesculap Neurosurgery Main Catalogue



... with all neurosurgery products.

## ■ Visual Equipment



... imaging and accessories for minimal  
invasive surgery.



For more information see  
Brochure C35502



For more information see  
Brochure C20102



For more information see  
Brochure C46702



## ■ Aesculap Power Systems

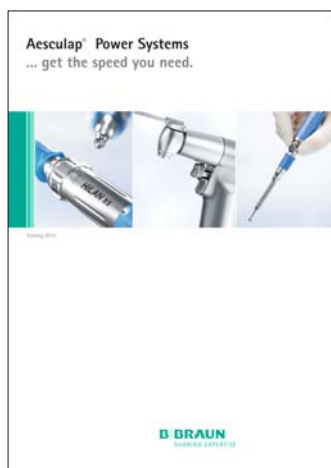


... Aesculap is a pioneer in surgical power systems.

## ■ Aesculap Power Systems Burrs & Blades



... Here it is... the Aesculap tools catalogue.



For more information see  
Brochure 022711



For more information see  
Brochure 017599

# Index

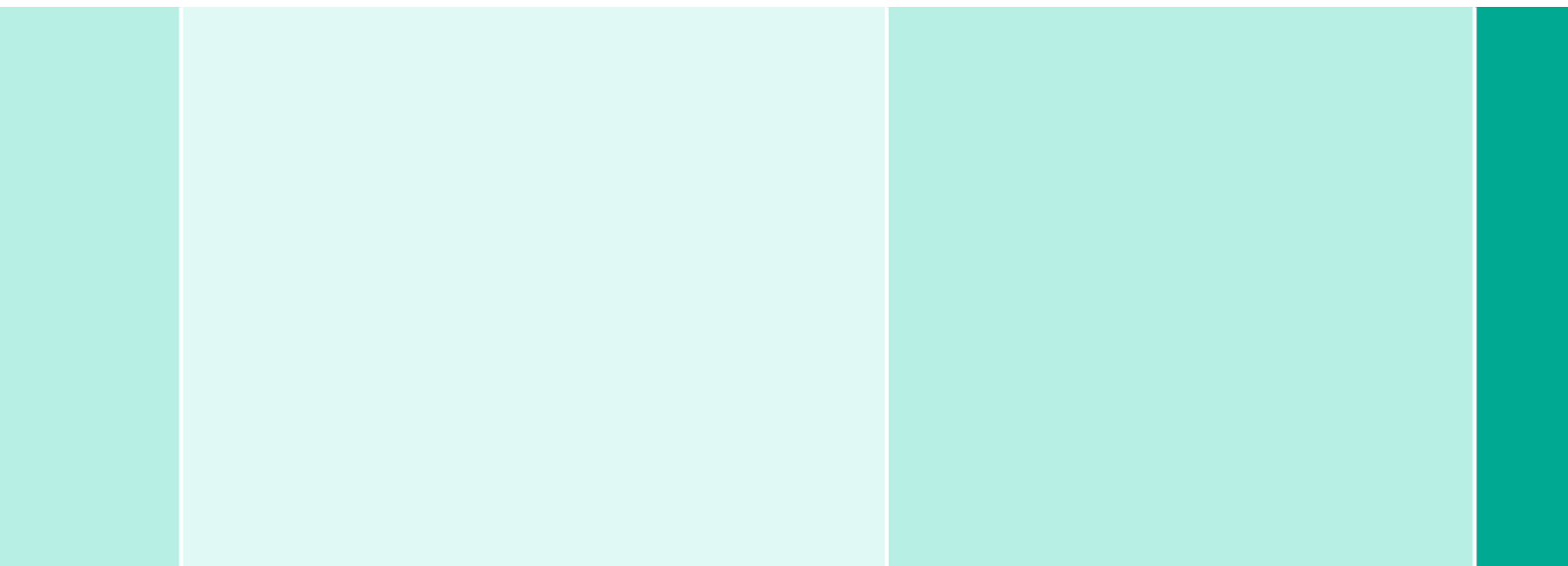
Art.-No.	Page	Art.-No.	Page	Art.-No.	Page
FA030R	72	FD220R	76	FK923B	80
FA031R	72	FD222R	76	FK923R	80
FA032R	72	FD224R	76	FK924B	80
FA033R	72	FD226R	76	FK924R	80
FA034R	72	FD228R	76	FK936R	80
FA035R	72	FF151R	82	FK937R	80
FA036R	72	FF168R	82	FK938R	80
FA037R	72	FF280R	82	FM156R	75
FA038R	72	FF345R	74	FM157R	75
FA039R	72	FF357R	68	FM158R	75
FA040R	72	FF496R	81		
FA041R	70	FF497R	81	GA461R	86
FA042R	70	FF498R	81	GA464R	86
FA043R	70	FF499R	81	GA468R	86
FA044R	70	FF645R	80	GA513R	86
FA045R	70	FF646R	80	GA521	86
FA046R	70	FF769R	80	GA740R	86
FA047R	70	FF771R	80	GB753R	88
FA060R	70	FF772R	80	GB758R	88
FA061R	71	FF773R	80	GB771R	87
FA062R	71	FF781R	80	GD668	86
FA063R	71	FF782R	80	GD670	86
FA064R	71	FF783R	80	GD675	86
FA065R	71	FH605SU	68	GE603R	88
FA066R	71	FH610R	69	GE604R	88
FA067R	71	FH611R	69	GE605R	88
FA068R	71	FH615	68	GE606R	88
FA069R	77	FK906B	80	GE607R	88
FA070R	77	FK906R	80	GE607TC-SU	89
FA071R	77	FK907B	80	GE608R	89
FA072R	77	FK907R	80	GE608TC-SU	89
FA073R	77	FK908B	80	GE609R	89
FA074R	77	FK908R	80	GE613R	88
FA075R	77	FK909B	80	GE614R	88
FA076R	74	FK909R	80	GE615R	88

Art.-No.	Page	Art.-No.	Page	Art.-No.	Page
GE616R	88	GE718R	87	GF426R	79
GE617R	88	GE719R	87	GF427R	79
GE618R	89	GE729R	87	GF428R	79
GE619R	89	GF391R	79	GF429R	79
GE624R	88	GF392R	79	GF431R	78
GE625R	88	GF393R	79	GF432R	78
GE631R	89	GF394R	79	GK800R	75
GE634R	89	GF395R	79	GK801R	75
GE635R	89	GF396R	79		
GE635TC-SU	89	GF397R	79	JG901	83
GE639R	89	GF398R	79	JG904	85
GE644R	89	GF399R	79	JG908SU	85
GE645R	88	GF401R	79	JK740	68
GE646R	89	GF402R	79	JK789	68
GE648R	88	GF403R	79		
GE649R	88	GF404R	79	OK090R	73
GE650R	88	GF405R	79	OP923	85
GE653R	89	GF406R	79	OP930	84
GE654R	89	GF407R	79		
GE655R	89	GF408R	79	PE487A	69
GE656SU	88	GF409R	79	PE507A	69
GE657SU	88	GF411R	79	PV440	84
GE658SU	88	GF412R	79	PV820	84
GE700SU	87	GF413R	79	PV875	84
GE702R	87	GF414R	79	PV880	84
GE704R	87	GF415R	79	PV881	84
GE706R	87	GF416R	79	PV909	84
GE707R	87	GF417R	79	PV941	84
GE708R	87	GF418R	79	PV946	84
GE709R	87	GF419R	79		
GE711R	87	GF421R	79	RT020R	83
GE712R	87	GF422R	79	RT040R	83
GE714R	87	GF423R	79	RT090R	82
GE716R	87	GF424R	79	RT099R	68
GE717R	87	GF425R	79		









ISBN 978-3-00-025156-6

Aesculap AG | Am Aesculap-Platz | 78532 Tuttlingen | Germany  
Phone +49 (0) 74 61 95-0 | Fax +49 (0) 74 61 95-26 00 | [www.aesculap.com](http://www.aesculap.com)

Aesculap – a B. Braun company

The main product trademark 'Aesculap' and the product trademarks 'Minop' and 'Unitrac' are registered marks of Aesculap AG.

Subject to technical changes. All rights reserved. This brochure may only be used for the exclusive purpose of obtaining information about our products. Reproduction in any form partial or otherwise is not permitted.

Brochure No. C26402

0511/1.0/1